1-1-2012

Evaluation of the Role of Oxidative Stress, Inflammation and Apoptosis in the Pulmonary and the Hepatic Toxicity Induced by Cerium Oxide Nanoparticles Following Intratracheal Instillation in Male Sprague-Dawley Rats

Siva Krishna Nalabotu
sivaknalabotu@gmail.com

Recommended Citation

EVALUATION OF THE ROLE OF OXIDATIVE STRESS, INFLAMMATION AND APOPTOSIS IN THE PULMONARY AND THE HEPATIC TOXICITY INDUCED BY CERIUM OXIDE NANOPARTICLES FOLLOWING INTRATRACHEAL INSTILLATION IN MALE SPRAGUE-DAWLEY RATS

A Dissertation submitted to the Graduate College of

Marshall University

In partial fulfillment of the requirements for the degree of

Doctor of Philosophy in Biomedical Sciences

by

Siva Krishna Nalabotu, DVM, M.S.

Approved by

Eric R. Blough, Ph.D., Committee Chairperson

Todd L. Green, Ph.D.

Monica A. Valentovic, Ph.D.

Gary O. Rankin, Ph.D.

Robert O. Harris, Ph.D.

Department of Pharmacology, Physiology and Toxicology

Joan C Edwards School of Medicine

Marshall University, Huntington, WV

May 2012

ACKNOWLEDGMENTS

I would like to take this opportunity to thank one and all who have given scientific, financial, technical, spiritual and psychological support to realize this dissertation. I would like to thank everyone who helped me to reach this far in my personal and professional life.

First of all, I would like to express my deepest gratitude to my advisor Dr. Eric R. Blough who always helped me to make my journey at Marshall University very smooth. Dr. Blough gave me confidence that he is there to help me at each and every phase of this dissertation. I am not sure many graduate students are given the opportunity to develop their own individuality and self-sufficiency by being allowed to work with such independence. I strongly believe that the work experience I got under his guidance is most valuable. Dr. Blough has been very helpful and easily accessible with a single knock on his office door to discuss at length about my research. Often times, it surprises me that he used to keep his work aside to discuss about my research and I would never forget warm support and affection he showed towards me and my research. Thank you very much Eric, for believing in me and guiding me to become strong in personal and professional life.

I would like to thank Dr. Monica Valentovic, who has been very supportive in my class and research work. Dr. Valentovic always tried to solve the problems that I had with my research work. Thank you very much Dr. Valentovic, for the help and support that you gave me to work with my research and sponsoring me to attend the Society of Toxicology Annual Meetings.

I would like to thank my other committee members Dr. Todd Green, Dr. Gary Rankin, and Dr. Robert Harris for their critical thinking on my research, valuable comments and

DEDICATION

To my parents Venkateswarlu Nallabothu and Sailaja Kumari for their hard work, intelligence

and vision in realizing their dream of giving good education to my family

TABLE OF CONTENTS

LIST OF FIGURES

LIST OF TABLES

ABSTRACT

EVALUATION OF THE ROLE OF OXIDATIVE STRESS, INFLAMMATION AND APOPTOSIS IN THE PULMONARY AND THE HEPATIC TOXICITY INDUCED BY CERIUM OXIDE NANOPARTICLES FOLLOWING INTRATRACHEAL INSTILLATION IN MALE SPRAGUE-DAWLEY RATS

By

Siva Krishna Nalabotu

The field of nanotechnology is rapidly progressing with potential applications in the automobile, healthcare, electronics, cosmetics, textiles, information technology, and environmental sectors. Nanomaterials are engineered structures with at least one dimension of 100 nanometers or less. With increased applications of nanotechnology, there are increased chances of exposure to manufactured nanomaterials. Recent reports on the toxicity of engineered nanomaterials have given scientific and regulatory agencies concerns over the safety of nanomaterials. Specifically, the Organization for Economic Co-operation and Development (OECD) has identified fourteen high priority nanomaterials for study. Cerium oxide (CeO_2) nanoparticles are one among the high priority group. Recent data suggest that CeO_2 nanoparticles may be toxic to lung cell lines *in vitro* and lung tissues *in vivo*. Other work has proposed that oxidative stress may play an important role in the toxicity; however, the exact mechanism of the toxicity, has to our knowledge, not been investigated. Similarly, it is not clear whether CeO_2 nanoparticles exhibit systemic toxicity. Here, we investigate whether pulmonary exposure to CeO_2 nanoparticles is associated with oxidative stress, inflammation and apoptosis in the lungs and liver of adult male Sprague-Dawley rats.

Our data suggest that the intratracheal instillation of CeO_2 nanoparticles can cause an increased lung weight to body weight ratio. Changes in lung weights were associated with the accumulation of cerium in the lungs, elevations in serum inflammatory markers, an increased Bax to Bcl-2 ratio, elevated caspase-3 protein levels, increased phosphorylation of p38-MAPK and diminished phosphorylation of ERK1/2-MAPK.

Our findings from the study evaluating the possible translocation of CeO_2 nanoparticles from the lungs to the liver suggest that CeO_2 nanoparticle exposure was associated with increased liver ceria levels, elevations in serum alanine transaminase levels, reduced albumin levels, a diminished sodium-potassium ratio and decreased serum triglyceride levels. Consistent with these data, rats exposed to CeO_2 nanoparticles also exhibited reductions in liver weight and dose dependent hydropic degeneration, hepatocyte enlargement, sinusoidal dilatation and the accumulation of granular material in the hepatocytes.

In a follow-up study, we next examined if CeO_2 deposition in the liver is characterized by increased oxidative stress and apoptosis. Our data demonstrate that increased cerium in the liver is associated with increased oxidative stress and apoptosis as assessed from hydroethidium staining, the analysis of lipid peroxidation, and TUNEL staining. In addition, increased cerium concentration in the liver was associated with an increased Bax to Bcl-2 ratio, elevated caspase-9 and elevated caspase-3 protein levels.

Taken together, these data suggest that exposure to CeO_2 nanoparticles is associated with increased oxidative stress and cellular apoptosis in the lungs. It is also evident that CeO_2 nanoparticles can translocate to liver and induce hepatic damage. The hepatic damage induced by CeO_2 nanoparticles is associated with increased oxidative stress and apoptosis in the liver.

Chapter 1

Introduction

Nanotechnology can be defined as the design, synthesis, and application of materials and devices whose size and shape have been engineered at the nanoscale (1-100 nm). Particles with at least one dimension smaller than 100 nm and potentially as small as atomic and molecular length scales (~0.2 nm) are termed nanoparticles [1, 2]. Given a very high surface area to volume ratio, nanomaterials have different physical and chemical properties when compared with their bulk counterparts and have been proposed to exhibit tremendous applications in several sectors [2]. At the nanoscale, quantum effects start to dominate which can result in different electric, magnetic and conductive properties than that observed in traditional materials [3]. Because of these special properties, nanomaterials have been proposed to be of use in the biomedical sector for applications in imaging, diagnosis and as therapeutic agents [4]. It is estimated that there are almost 800 nanoproducts available in the market that have been manufactured by 322 companies across the world [5].

With the growing incorporation of nanomaterials into our day to day life, the potential for exposure is increasing daily. Whether or not nanomaterials exhibit deleterious effects to human life and the ecosystems is not well understood. As such, an evaluation of interaction of nanomaterials with biological systems is highly warranted. Of the various types of nanomaterials available, the toxicity evaluation of the engineered (manufactured) nanoparticles is perhaps the most important as the industrial production of manufactured nanomaterials is progressing rapidly. Recent studies reporting the toxicity of engineered

nanomaterials have led to concerns by scientific and regulatory agencies about the toxicity of engineered nanomaterials. The Organization for Economic Cooperation and Development Working Party on Manufactured Nanomaterials (OECD MPMN) has identified fourteen manufactured nanomaterials for evaluation. Materials identified include fullerenes, carbon nanotubes, metal oxides, nanoclays and CeO_2 nanoparticles [6]. At present, data regarding the potential toxicity of CeO_2 nanoparticles are limited.

Cerium is a rare earth metal and is the most reactive lanthanide metal. Cerium can exist in Ce^{3+} and Ce^{4+} states with Ce^{4+} being the most stable form. Nanoparticles made from cerium oxide (CeO_2) have been widely used in fuel cells, solar cells, for polishing of materials, in UV blockers and in the automobile industries as well for catalysts [7]. Cerium exhibits a fluorite like chemical structure that enables it to donate or receive the oxygen atoms depending on the partial pressure of oxygen in the surrounding environment [8]. This property of redox cycling makes cerium an efficient agent for reduction and oxidation reactions. At the nanoscale, CeO_2 nanoparticles have increased surface area, expansion of lattice [8], and a higher melting point when compared to their bulk counterparts. It is thought that these properties allow CeO_2 nanoparticles to exhibit anti-oxidant activity [9]. Recent studies have shown that CeO_2 nanoparticles can be used to scavenge reactive oxygen species (ROS) and this activity can protect against cardiomyopathy [10], oxidative neuronal toxicity [11], and radiation-induced tissue damage [12]. It has been proposed that CeO_2 nanoparticles may mimic the action of the superoxide dismutase (SOD) and catalase enzymes where they function to scavenge reactive oxygen species that are generated in the cell [13]. Whether CeO_2 nanoparticles exhibit toxic effects to cellular function is not well understood.

The most common route of exposure to CeO_2 nanoparticles is likely to be through inhalation or ingestion. The inhalation route is the most worrisome route of the exposure as the absorption of CeO_2 nanoparticles through ingestion is typically minimal [7]. Although there are limited studies on the toxicity of CeO_2 nanoparticles, most of these studies are centered on the toxicological evaluation on lung cells and lung tissues.

Studies on microorganisms such as *E. coli* have shown that CeO_2 nanoparticles (7nm) can induce cell death and the oxidative stress might be the possible mechanism of toxicity[14]. *In vitro* studies using human bronchoalveolar carcinoma cell line (BEAS-2B) and lung epithelial cell lines (A549) demonstrated that exposure to CeO_2 nanoparticles (20 nm) is associated with reduced cell viability and increased oxidative stress[15]. Conversely, CeO_2 nanoparticles were not shown to be toxic to T98G (glioblastoma cell line) and H9C2 (cardiomyoblast) cell lines [16] . *In vivo* studies on male Sprague- Dawley rats showed that exposure to CeO_2 nanoparticles (20nm) can cause lung damage and fibrosis [17]. These changes in the lung structure were associated with increased infiltration of inflammatory cells and increased accumulation of nanoparticles in the alveolar spaces. This work also demonstrated that CeO_2 nanoparticles can cause lung damage by increasing oxidative stress causing apoptosis of the lung macrophages. Nonetheless, it is not yet mechanistically clear how exposure to CeO_2 nanoparticles may induce oxidative stress in the intact animal.

Some studies have proposed that CeO_2 nanoparticles can catalyze Fenton-like reactions that result in the production of reactive radicals [9]. Other *in vitro* studies have suggested that exposure to CeO_2 nanoparticles can diminish the amounts of glutathione and α-tocopherol [16] while other work has demonstrated that CeO_2 nanoparticles can generate ROS in cells[18].

Recent *in vitro* studies have suggested that the oxidative stress induced by CeO_2 nanoparticles is mediated through the p38-Nrf-2 signaling pathway [19]. Whether similar cell signaling events occur *in vivo* subsequent to CeO_2 nanoparticle exposure has, to our knowledge, not been investigated.

It is thought that inhaled nanoparticles can translocate to various other organs in the body including the liver, kidney, spleen, brain and heart through the systemic circulation[20]. Once reaching the cells, other work has demonstrated that nanomaterials can enter the nucleus, mitochondria, lipid vesicles and cell membranes and induce toxic effects [21-23]. One of the most studied pathways of the nanoparticle mediated toxicity is oxidative stress and apoptosis. Nanoparticles have been shown to induce oxidative stress by the production of ROS or by decreasing the antioxidant levels in the cell [24]. The oxidative stress is mediated through various stress responsive cell signaling events such as activation of the mitogen activated protein kinase (MAPK) signaling or through the activation of inflammatory mediators [24]. Depending on the magnitude of oxidative stress increase, either apoptosis or necrosis of the cell can result.

CeO_2 nanoparticles have shown to translocate to various other organs in the body through the systemic circulation [25]. Nonetheless, it is not clear if they induce any toxic effects on the liver. Studies on various other metal nanoparticles such as iron oxide, silver, copper and gold nanoparticles have shown that they can induce liver toxicity after intratracheal instillation [26-28]. As the liver is the major metabolizing organ of the body and a primary source of xenobiotic elimination, an examination of the toxicological effects of the CeO_2 nanoparticles on the liver is warranted. Herein, we propose to evaluate the role of MAPK signaling and caspases

4

in the oxidative stress and apoptosis induced by CeO_2 nanoparticles in lungs as well as we evaluate if CeO_2 nanoparticles exhibit toxic effects on the liver following intratracheal instillation.

Objectives and Specific Aims

Our long-term goal is to evaluate whether CeO_2 nanoparticles are toxic to the lungs and the liver. Based on previous studies from the literature using other nanoparticles [2, 17, 24], we hypothesize that:

i. CeO_2 nanoparticle accumulation in the lungs will be associated with oxidative stress. The oxidative stress induced by CeO_2 nanoparticles will activate stress responsive MAPK protein signaling and inflammatory protein signaling. Finally, CeO_2 nanoparticle- induced increases in oxidative stress and inflammation in the lungs will be associated with increases in apoptosis.

ii. Inhaled CeO_2 nanoparticles will translocate to liver.

iii. CeO_2 nanoparticle toxicity in the liver will be mediated through oxidative stress and apoptosis and will increase with the duration of the exposure to CeO_2 nanoparticles.

Specific Aims

i. **Specific Aim I**: To investigate the role of MAPK signaling and inflammatory protein signaling in the oxidative stress and apoptosis induced by CeO_2 nanoparticles in the lungs (Figure 1.1).

ii. **Specific Aim II**: To investigate if intratracheal instillation of CeO_2 nanoparticles is associated with the deposition of ceria in the liver, kidney, spleen and heart of rats.

iii. **Specific Aim III**: To investigate if the intratracheal instillation of CeO_2 nanoparticles is associated with increased hepatic oxidative stress and apoptosis (Figure 1.2)

Layouts for the toxicological evaluation studies (Figures 1.1 and 1.2)

Figure 1-1: Layout of study design for Specific Aim 1
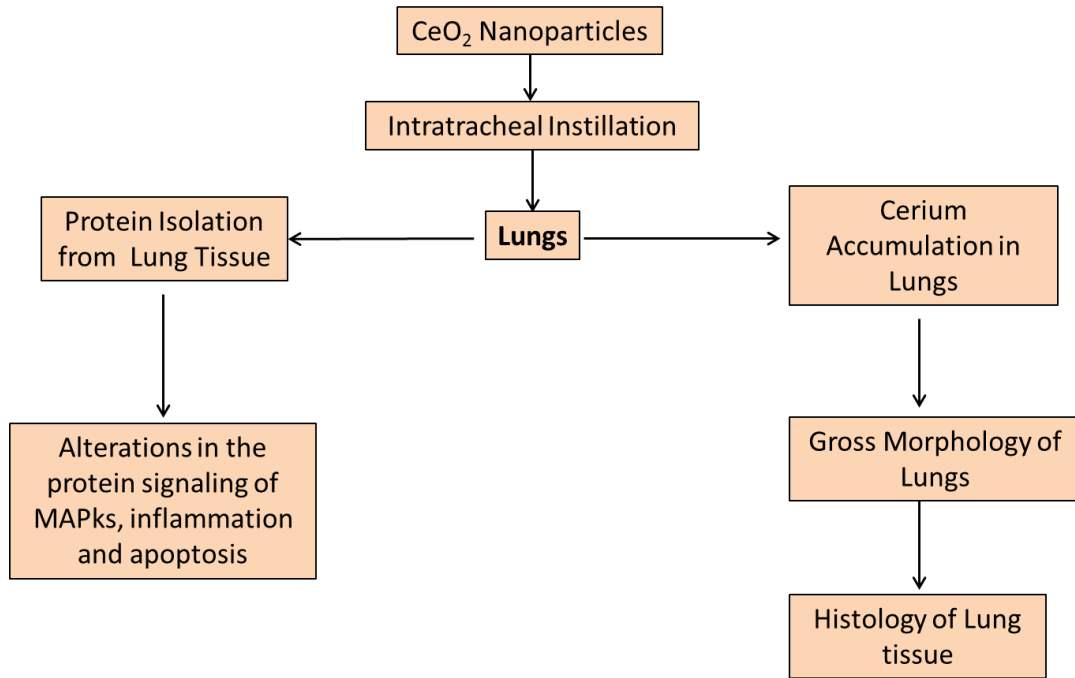
Figure 1-2: Layout of study design for specific aims 2 and 3
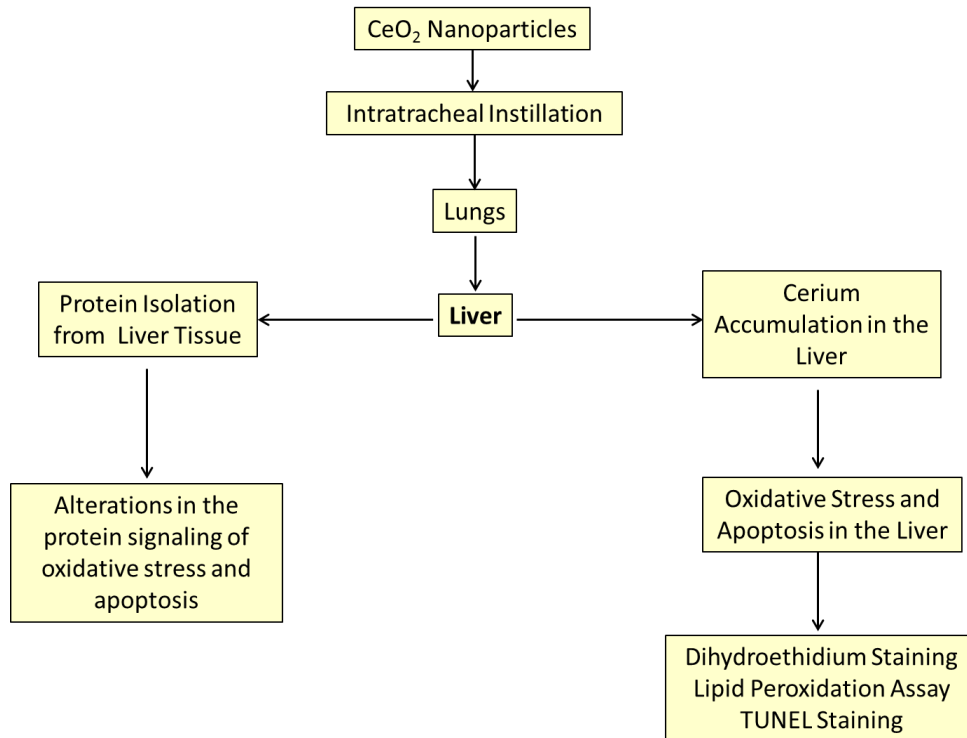
Chapter 2

2.1 Review of the literature

The following chapter presents a review of the literature concerning nanotechnology and the toxicity of CeO_2 nanoparticles. Specifically, we will address the current literature on nanotechnology, the unique properties and applications of the nanomaterials, the toxicity of the nanomaterials, factors responsible for the nanomaterial toxicity, routes of exposure to nanomaterials, cellular uptake and the effects of the nanomaterials on the cell, role of the oxidative stress and apoptosis in the toxicity induced by nanoparticles, the structure and unique properties of CeO_2 nanoparticles and the potential toxicity of CeO_2 nanoparticles.

2.2 Introduction to nanotechnology

The use of nanotechnology is rapidly increasing as industry strives to develop new products that are cheaper, better, and less harmful to the environment. It is estimated that investments in the nanotechnology industry grew from \$13 billion in 2004 to \$50 billion in 2006 and recent data has suggested that this growth will reach \$2.6 trillion dollars by 2014 [29, 30]. The National Science Foundation has proposed that the worldwide market for nanomaterials will reach \$1 trillion between 2010 and 2015 [30] with the pharmaceutical industry alone contributing approximately \$180 billion [31].

Nanotechnology can be defined as the design, synthesis, and application of materials and devices whose size and shape have been engineered at the nanoscale (1-100 nm). Materials that have structural components smaller than 100 nm in at least one dimension are

8

referred to as nanomaterials. Particles with at least one dimension smaller than 100 nm and potentially as small as atomic and molecular length scales (~0.2 nm) are termed nanoparticles [1, 2]. (Figure 2.1: How big are nanomaterials?). There are two types of nanoparticles (NPs): (1) naturally occurring NPs (e.g., produced naturally in volcanoes, forest fires or as combustion by-products) and (2) engineered nanoparticles (ENPs) which have been deliberately developed to exhibit some specific property or composition [e.g., carbon black, fumed silica, titanium dioxide (TiO_2), iron oxide (FeO_x), quantum dots (QDs), fullerenes, and carbon nanotubes (CNTs)][1, 2].

Figure 2-1: How big are nanomaterials?

Source: http://www.sustainpack.com/nanotechnology.html
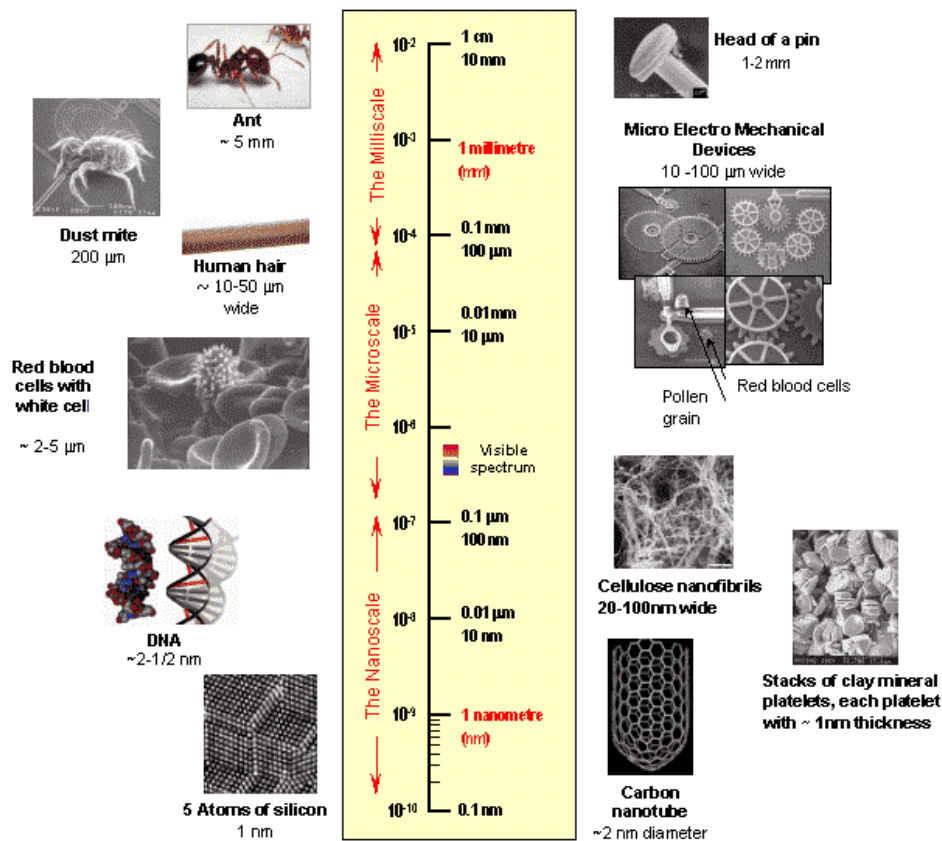
Recently the Organization for Economic Co-operation and Development (OECD) has formed a committee called the Working Party on Manufactured Nanomaterials (WPMN) to evaluate more than hundred different types of ENPs available as of today. Work from this effort has identified fourteen different ENPs for further evaluation due to their widespread use or unusual chemical or physical properties [32, 33] (Table 1).

Table 1: Engineered nanoparticles chosen by the WPMN for evaluation

- Fullerenes (C60)

- Single-walled carbon nanotubes (SWCNTs)

- Multi-walled carbon nanotubes (MWCNTs)

- Silver nanoparticles

- Iron nanoparticles

- Carbon black

- Titanium dioxide

- Aluminium oxide

- Cerium oxide

- Zinc oxide

- Silicon dioxide

- Polystyrene Dendrimers

- Nano clays

2.3 Unique properties and applications of nanomaterials

Nanomaterials exhibit unique chemical and physical properties due to their small size and increased surface area to volume ratio which allow them to behave differently from their bulk counterparts [1, 34]. These unique properties can give rise to increased chemical reactivity as well as different optical, electrical and magnetic properties [35]. For example, in its bulk form gold is yellow in color; however, gold nanoparticles can be different combinations of red, blue or green depending on their size [36, 37] (Figure 2.2).

Figure 2-2: Effect of size on the optical properties of gold
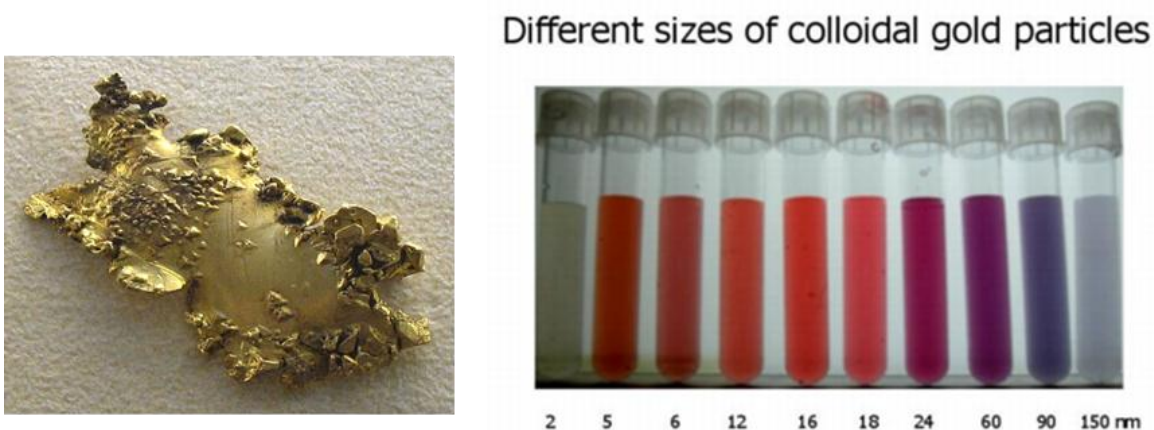
Source: http://www.ansci.wisc.edu/facstaff/Faculty/pages/albrecht/albrecht_web/Programs/microscopy/colloid.html

It is estimated that more than 800 products containing some form of nanomaterials are being manufactured by 322 companies the world over [38]. Industries utilizing nanomaterials include electronics manufacturers (chips, screens), energy (production, catalysis, and storage), materials (lubricants, abrasives, paints, tires and sportswear), consumer products (clothes, goggles, skin lotions and sun screens), automotive, soil/water remediation (pollution absorption, water filtering, and disinfection), pesticides, chemicals and the pharmaceutical

sector [1, 2, 30, 39, 40]. Other work is centered on utilizing nanomaterials in food products (additives, packaging), medical imaging and as drug delivery systems [41-44]. This development, in turn, has led to increasing concerns over the potential ramification of nanomaterial exposure to humans and the environment.

2.4 Toxicity of nanomaterials

It is thought that the ENPs pose the greatest threat to man and the environment given their widespread use and growing importance. Even with the proper precautions it is possible for exposure to occur during each phase of the material lifecycle (production, utilization, disposal, and recycling) [45]. Potential routes of exposure include inhalation, ingestion, absorption through the skin and via the food chain through contamination of food and water (Figure 2.3) [7, 46-48].

Exposure to nanomaterials is a growing concern. A recent clinical report [49], which was the first of its kind, examined seven Chinese women who worked in the paint industry and detailed how industrial exposure led to severe respiratory stress and shortness of breath. Pathological examination of the worker's lungs found nonspecific pulmonary inflammation, pulmonary fibrosis and foreign-body granulomas of the pleura. Additional transmission electron microscopy (TEM) studies confirmed the presence of round polyacrylate nanoparticles ~30 nm in diameter in the cytoplasm, karyoplasm of pulmonary epithelium, mesothelial cells, and in chest fluid. Based on these observations, the authors concluded that the long-term exposure to polyacrylate nanoparticles could result in serious damage to human lungs.

2.5 Factors responsible for the nanomaterial toxicity

Nanomaterials display different chemical and electronic properties/reactivity than their bulk counterparts [2, 50]. In addition, because of their small size, nanomaterials can easily penetrate into subcellular components of the cells where they can cause toxicological effects [2, 51, 52]. The shape of the nanomaterials may also play a role in governing potential toxicity [53]. In general, nanomaterials with a rod or needle shape are more toxic than the ones with round shape. Indeed, recent data has suggested that single walled carbon nanotubes (rods) are more toxic than fullerenes (cylindrical) of comparable size. Why shape may influence toxicity is not well understood; however, it is likely that shape may mediate, at least in part, particle absorption and deposition [54-56]. In addition to size and shape, other work has demonstrated that chemical composition along with other physicochemical properties (agglomeration state, crystal structure, chemical composition, surface area, and surface chemistry, surface charge, etc.) may also influence toxicity [35, 57]. Other studies have shown that the surface properties of nanoparticles can influence how they interact with proteins, leading to different types of corona and biological effects[58].

2.6 Respiratory Route of Exposure

Although nanoparticle exposure can occur via several different routes (respiratory, ingestion, dermal and drug delivery), it is thought that the uptake of nanoparticles into the body is most likely to occur via the respiratory system [1, 2]. If inhaled, nanomaterials can become phagocytized by alveolar macrophages or lodged in the lungs after diffusion through

the epithelial cell layer [2]. Upon becoming lodged in the lungs, it is possible for nanomaterials to pass across the epithelia of the respiratory track by transcytosis into the interstitium where they can enter into the blood either directly or via the lymphatic system [1, 2]. Once within the blood, the nanomaterials can then travel to the liver, kidney, spleen heart, brain and bone marrow (Figure 2.3) [2, 20, 59, 60]. Research using copper, nickel, gold and manganese oxide nanoparticles has shown that nanoparticles can enter into the nervous system through the sensory nerve fibers endings that are embedded in the airway epithelia [61-65]. If small enough, ENPs can also cross the blood brain barrier [63]. Clearance of the nanoparticles from the respiratory system can occur by either physical or chemical processes [1, 2, 66]. The physical process of elimination involves mucociliary movement, phagocytosis by macrophages, endocytosis into epithelial cells, interstitial translocation and eventual clearance into the blood and lymphatic circulation [66]. The chemical process of elimination can occur by protein binding or leaching or through the dissolution of the particles or components of the particles that are either lipid soluble or soluble in intracellular and extracellular fluids [2]. It is thought that the chemical process of elimination appears to be largely dependent upon local extracellular and intracellular conditions [67, 68]

Evaluation of the toxicity of nanomaterials through the respiratory route of exposure in animals involves either inhalation of the materials or intratracheal instillation into the lungs. Although, the inhalation route provides natural route of entry of the material into the lungs, it has several limitations. For example, the inhalation route of exposure needs special facilities, while it is also difficult to know with certainty how much of the inhaled material that enters the

lungs. As such, it is thought that the intratracheal instillation route is the most preferable method to study inhalation toxicity [69].

Figure 2-3: Potential routes of nanomaterial exposure
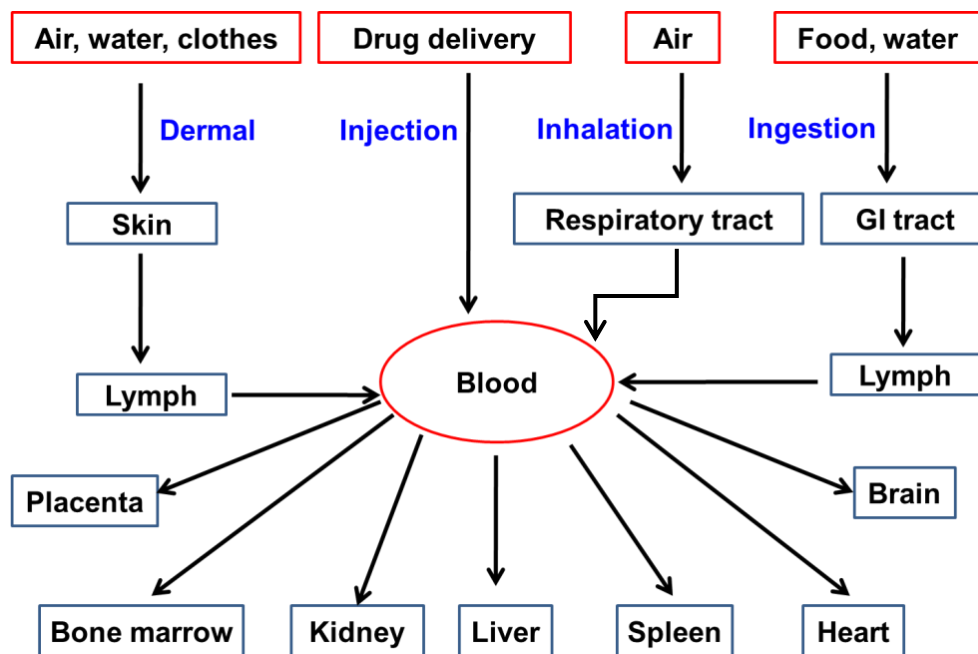
Modified from "Nanotoxicology: An Emerging Discipline Evolving from Studies of Ultrafine Particles G. Oberdörster *et al.*, Environmental Health Perspectives Volume 113, Number 7, 2005"

2.7 Cellular effects of engineered nanoparticles

2.7.1 Cellular uptake of engineered nanoparticles

Once in the circulation, nanomaterials are taken up into cells by endocytosis (phagocytosis or pinocytosis), membrane penetration or passive diffusion through

transmembrane channels [2]. The transmembrane passage of nanomaterials is dependent, on many factors including the physicochemical properties of the particles (chemical composition, size, shape and agglomeration status), cell type (professional phagocytes such as macrophages vs. non-professional phagocytes), serum components, and surfactant [1]. After internalization, nanomaterials can travel to several different locations within the cell including the outer-cell membrane [70], cytoplasm [70], mitochondria [21], lipid vesicles [22], nuclear membrane [71], or become lodged within the nucleus itself [23, 72]. If the concentration is high enough, nanomaterials can damage cellular organelles and DNA which can result in cell death and, at times, disease development (Figure 2.4).

2.8 Mechanisms of nanoparticle toxicity

Mechanisms of nanoparticle toxicity include oxidative stress, inflammation, genetic damage, the inhibition of cell division and cell death [3, 24, 73, 74]. Most work to date has suggested that oxidative stress and consequent generation of ROS is a common mechanism of nanomaterial toxicity [24, 75]. *In vitro* studies have shown that TiO_2[76] and carbon nanotubes [77] all cause toxicity by the generation of ROS. Other work has shown that some nanomaterials (e.g. ZnO, SiO_2, fullerenes) can generate excited electrons when exposed to light which, in the presence of oxygen, can form superoxide radicals by direct electron transfer [78].

Figure 2-4: Various effects of the nanomaterials after cellular internalization[1].

NANOPARTICLES INTERNALIZED IN CELLS

Mithocondrion
Nucleus
Cytoplasm
Membrane
Lipid vesicle

Nanoparticles ingestion

Gastro-intestinal system
(Crohn's disease, colon cancer)

Orthopedic implant wear debris
(Auto-immune diseases, dermatitis, urticaria, vasculitis)

Nanoparticle inhalation

Brain *(neurological diseases: Parkinson's, Alzheimer's disease)*

Lungs *(Asthma, bronchitis, emphysema, cancer)*

Circulatory system *(Artheriosclerosis, vasoconstriction, thrombus, high blood pressure)*

Heart *(arrythmia, heart disease, death)*

Other organs *(disease of unknown etiology in kidneys, liver)*

Lymphatic system *(Podoconiosis, Kaposi's sarcoma)*

Skin *(Auto-immune diseases, dermatitis)*

Source: Buzea, Pacheco, and Robbie: Nanomaterials and nanoparticles: Sources and toxicity

Biointerphases, Vol. 2, No. 4, December 2007

Oxidative stress can be caused either by the depletion of antioxidants or increased production of ROS or reactive nitrogen species (RNS). Potential ROS include superoxide anion ($O^{2-.}$), peroxide ($O_2^{-2.}$), hydroxyl radical (·OH), and singlet oxygen ($^1O_2$), an excited form of oxygen. Oxygen-derived radicals are generated constantly as part of normal aerobic life. A prominent feature of ROS is that they have extremely high chemical reactivity which may help

to explain their damaging effects on cells. When produced in excess, ROS can damage proteins, lipids and DNA. If the damage is excessive cell death can be induced.

2.8.2 Role of MAP kinases in the nanoparticle induced oxidative stress

Oxidative stress has been shown to activate stress responsive mitogen-activated protein kinases (MAPKs), which are thought to regulate, at least in part, the fate of the cell to go through proliferation, differentiation, or cell death [79, 80]. Different studies have shown that the suppression of extracellular signal-regulated kinase (ERK1/2-MAPK) and activation of c-Jun N-terminal kinase (JNK) and p38 MAPKs play a role in apoptosis in different cell lines [80, 81]. It has been revealed that ERK1/2-MAPKs are activated in response to growth factor stimulation where they play a very important role in the processes of cellular proliferation and differentiation [82, 83]. Conversely, the JNK and p38 MAPKs have been shown to be activated in response to cellular stresses such as UV light, osmotic stress, DNA damaging agents and proinflammatory cytokines [84, 85] (Figure 2.5). An increased expression of JNK and p38-MAPKs has been proposed to cause apoptosis in various cell lines [86]. It has been observed that silver nanoparticles can activate JNK protein signaling and apoptosis in a variety of cells [87]. Similarly, *in vitro* studies with CeO_2 nanoparticles have shown that they can activate p38 MAPK signaling in bronchoalveolar cells [16]. However, the role of MAPKs signaling in nanoparticles induced oxidative stress remains largely unknown.

Figure 2-5: Modulation of various MAP kinases by stresses to induce varied cellular effects

Stimulus	Growth Factors	Inflammatory cytokines, ROS and cellular stresses	
MAPKKK	Raf	TPL2 MEKK	MLK/DLK TAK ASK
MAPKK	MEK1/2	MKK4/7	MKK3/6
MAPK	ERK1/2	JNK/SAPK	P38 MAPK
Response	Proliferation, Differentiation and Development	Inflammation and Apoptosis	
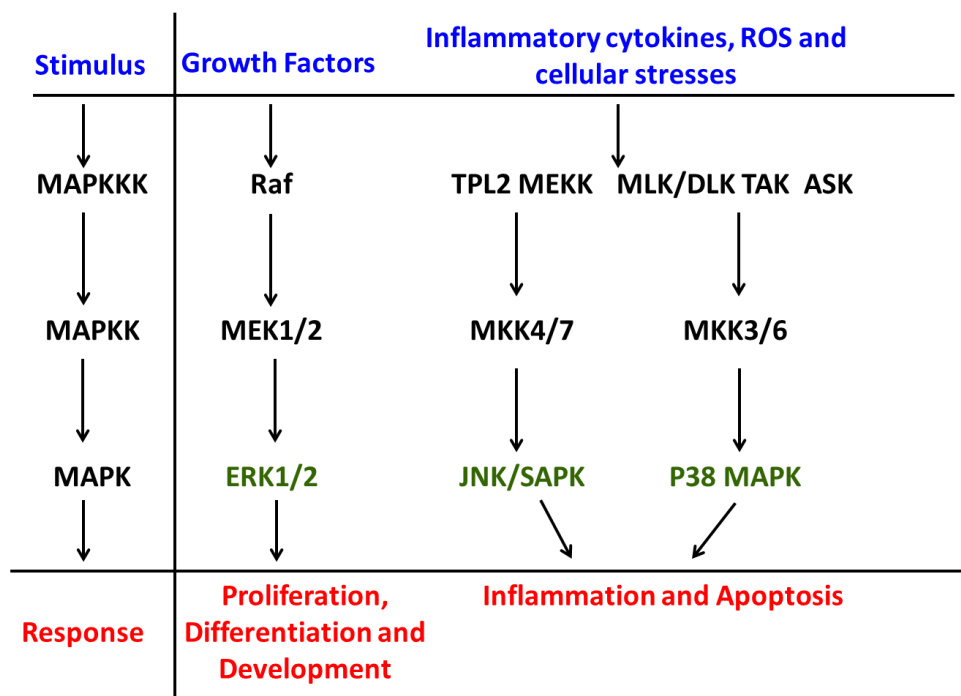
2.8.3 Mechanisms of ROS production and apoptosis

ROS can be generated directly when both oxidants and free radicals are present on the surface of the particles [88-90]. Some nanoparticles have been shown to activate inflammatory cells such as the alveolar macrophages and neutrophils which can result in the increased production of ROS [90-92]. Other nanomaterials such as TiO_2, ZnO, CeO_2 and silver nanoparticles have been shown to deposit on the cellular surface or inside the subcellular organelles and induce oxidative stress signaling cascades that eventually results in the oxidative stress to the cell [1]. It appears that the mitochondria are one of the major target organelles for nanoparticle-induced oxidative stress [21]. Upon entry into the mitochondria, nanomaterials appear to be capable of inducing structural damage which can lead to the impairment of

mitochondrial function [93]. It is well known that high levels of ROS in the mitochondria can result in damage to membrane phospholipids which can lead to mitochondrial membrane depolarization. In addition, the deposition of nanomaterials in mitochondria can alter normal functioning of mitochondria by disrupting the electron transport chain, ultimately resulting in the production of ROS. During oxidative phosphorylation, electrons occasionally escape from the electron transport chain where they can be accepted by molecular oxygen to form the extremely reactive superoxide anion radical ($O^{2-\bullet}$) which can get further converted to hydrogen peroxide (H_2O_2) or partially reduced to hydroxyl radical ($OH^\bullet$), one of the strongest oxidants in nature [93]. Nanomaterials can increase the rate of superoxide anion production, either by blocking the electron transport or by accepting an electron from a respiratory carrier and transferring it to molecular oxygen [88, 94]. Mitochondrial damage, if extensive, can trigger activation of caspases and cellular apoptosis.

2.8.4 Mitochondrial pathway of apoptosis

Apart from affecting the cellular proteins, lipids and DNA, ROS have a very crucial role in inducing apoptosis in the mitochondria. Conditions of excessive oxidative stress can result in the cellular apoptosis or necrosis. Apoptosis has been implicated as a major mechanism of cellular death due to nanomaterial-induced toxicity [57, 87, 95, 96]. Among the different apoptotic pathways, the mitochondrial pathway seems to play a predominant role. In this process, the generation of excessive ROS leads to changes in mitochondrial membrane

potential, an increase in cytochrome C release from the damaged mitochondria and the activation of caspase-3.

The decision to proceed to apoptosis is regulated by the Bcl-2 family of proteins. Bcl-2 family members can interact with each other or exert function independently and are comprised of several different members including those that inhibit (Bcl-2, Bcl-xL, etc.,) or favor (Bax, Bak, Bad, etc) apoptosis. Bcl-2 is an anti-apoptotic protein which is predominately present in mitochondria. The Bcl-2 protein prevents apoptosis by suppressing oxyradical mediated membrane damage and stabilizing mitochondria membrane potential. Conversely, the proapoptotic protein Bax can trigger the release of cytochrome C into the cytosol. Once released, cytochrome C interacts with APAF-1 and procaspse-9 which results in the formation of the apoptosome. The apoptosome then cleaves procaspase-9 into its active form which causes the cleavage and activation of the effector caspase, procaspase-3. Once active, caspase-3 then initiates cleavage of nuclear and cytosolic proteins resulting in the apoptotic death of the cell [94, 97-99].

2.8.5 Engineered nanoparticles induced inflammation

Inflammation is the protective mechanism of the organism against adverse reactions induced by foreign chemicals or organisms. If limited, inflammation is often times protective in nature, but if excessive, inflammation can cause cellular dysfunction. Fullerenes, carbon nanotubes, silver nanoparticles and TiO_2 nanoparticles have been shown to increase the level of inflammatory mediators or cytokines in the circulation which can result in the generation of

ROS, hypersensitive reactions, allergic response or granulomas in the target organs [52, 73, 100, 101]. Nanomaterials have also been shown to activate the nuclear factor kappa B (NF-Kβ) transcription factor, which when active, translocates to the nucleus. Once in the nucleus, NF-Kβ can induce transcription of the several pro-inflammatory mediators including TNF-alpha, IL-8, IL-2 and IL-6 which can lead to increased inflammation and oxidative stress [102, 103].

Increased production of cytokines can transduce various cell signaling mechanisms. The Janus kinase/ signal transducers and activators of transcription (Jak/STAT) pathway is one important signaling mechanism that can be transduced by various cytokines [104]. After binding of cytokines, the activation of the receptor-associated tyrosine kinases Jak1 and Tyk2 induces tyrosine phosphorylation of the receptor subunits and several STAT proteins, which form homodimers and/or heterodimers that translocate to the nucleus and regulate the transcription of specific target genes that are involved in inflammation [105]. It has been shown that STAT proteins can activate p38 MAPK which may play an important role in inflammation and apoptosis of the cells [106].

2.9 Literature review on cerium oxide nanoparticles

2.9.1 Cerium oxide nanoparticles structure and applications

Cerium is a lanthanide metal that is also the most reactive rare earth metal. Cerium exists in either the Ce^{4+} or Ce^{3+} state with the Ce^{4+} state being the most stable structure. Cerium oxide (CeO_2) is one of the most stable forms of cerium. There are several synonyms for CeO_2 including cerium oxide, cerium dioxide, ceric oxide and ceria. The fluorite structure, with its

large crystal lattice energy, provides an exceptionally strong stabilizing influence on the CeO_2 [8] (Figure 2.5: Lattice structure of CeO_2).

Figure 2-6: The cubic structure of the cerium dioxide[8]
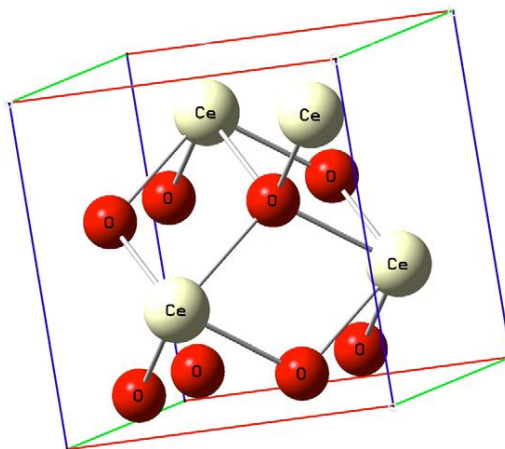
CeO_2 is used in a number of different materials and industrial applications including petroleum refineries, solid cell fuel cells, and as polishing materials [7]. CeO_2 nanoparticles are somewhat unique in that they have the ability to undergo reversible oxygenation / deoxygenation cycles based on the partial pressure of the oxygen in the surrounding environment [107]. At the nanoscale, CeO_2 particles exhibit increased electrical conductivity and increased catalytic properties [8].

CeO_2 is widely used as a catalyst and has been incorporated into automobile mufflers to reduce toxic engine emissions [108]. CeO_2 nanoparticles have been used as an additive to diesel fuel since 1999 where they function to reduce particulate emissions as well as to increase fuel efficiency [7]. Commercially available cerium based fuel additives include Envirox™ [109], Platinum Plus produced by Clean Diesel Technologies Inc. and Eoly DPX-9 (Rhodia) [7]. CeO_2 nanoparticles have also been used in sunscreens as they can absorb UV radiation [110].

23

In addition to their use in industry, CeO_2 nanoparticles may also have biomedical applications. CeO_2 nanoparticles have been shown to be able to scavenge ROS generated in the cell and have demonstrated potential application for the treatment of cardiovascular disease, neuronal injury and radiation-induced tissue damage in animals [10-12]. How CeO_2 nanoparticles may function to scavenge ROS is not fully understood. Recent work has proposed that scavenging of ROS by CeO_2 nanoparticles may be due to the ability of CeO_2 to cycle back and forth between its Ce^{3+} and Ce^{4+} states [9, 111].

$$Ce^{4+} + e^- \longleftrightarrow Ce^{3+}$$

$$Ce^{3+} + OH^{\cdot -} \longleftrightarrow Ce^{4+} + OH^-$$

$$Ce^{4+} + O^{2\cdot -} \longleftrightarrow Ce^{3+} + O_2$$
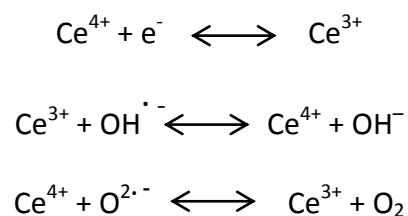
Other work has suggested that CeO_2 nanoparticles can mimic superoxide dismutase (SOD) and catalase [111]. It has also been demonstrated that there is a positive correlation between the trivalent oxidation state of CeO_2 nanoparticles and superoxide dismutase mimetic activity. Additional studies have proposed that surface oxygen vacancies in the CeO_2 nanoparticle may play an indirect role in the radical scavenging properties [112].

2.9.2 Sources of exposure and bio distribution of cerium oxide nanoparticles

Potential sources of CeO_2 nanoparticles include particles generated by the manufacturing industries and diesel exhaust. Recent studies have found that the use of ceria as

a diesel fuel additive can result in exhaust emissions containing CeO_2 nanoparticles [109]. Routes of CeO_2 nanoparticle exposure include inhalation and ingestion [113].

Recent work using radiolabeled CeO_2 nanoparticles has shown that nearly 80% of the inhaled nanoparticles are still present in the lungs at 24 hours [113]. Previous studies with other nanomaterials have shown that nanoparticles can be internalized into epithelial cells or penetrate into the interstitial space where they can then be taken up into the circulation [2]. Studies with CeO_2 nanoparticles have shown that the concentration of the cerium in the blood is elevated after inhalation and that cerium can accumulate in the liver, kidney, spleen and bone [113]. The half-life of cerium elimination has been shown to be 103 days. Approximately 90% of ingested CeO_2 nanoparticles are eliminated through the feces [113]. Thus far, little is known about the systemic toxicological effects of CeO_2 nanoparticles.

2.9.3 Cerium oxide nanoparticle toxicity

Recent data suggest that CeO_2 nanoparticles are toxic to microorganisms. Thill and coworkers demonstrated that large amounts of CeO_2 nanoparticles can be adsorbed onto the surface of E. coli and that this adsorption can reduce bacterial viability through the generation of ROS [14].

Studies conducted using murine macrophage cells have suggested that the major mechanism of CeO_2 nanoparticle uptake into the cell is through phagocytosis and diffusion through the cell membrane. CeO_2 nanoparticles have been shown to localize in cytosol and lysosomes [114]. Lin and colleagues studied the toxic effects of 20 nm CeO_2 nanoparticles on

25

the lung cancer cell line A549. They demonstrated that exposure to CeO_2 nanoparticles is associated with reduced cell viability, increased oxidative stress, reduced glutathione, increased lipid peroxidation and increased membrane damage [18]. Work by Park and coworkers using the human bronchial epithelial cell (BEAS-2B) line showed that exposure to 30 nm CeO_2 nanoparticles is characterized by nanoparticle internalization, increased oxidative stress and diminished cell viability in a concentration and time dependent fashion [16]. Additional data from their study also demonstrated that CeO_2 nanoparticles can induce chromatin condensation and cellular apoptosis via the activation of caspase 3.

Eom and coworkers studied the possible molecular events associated with the CeO_2 nanoparticle-induced oxidative stress in BEAS-2B cells [19]. This work examined the effect of CeO_2 nanoparticle exposure on mitogen activated protein kinases (MAPK) signaling and the regulation of redox sensitive transcription factors. They demonstrated that exposure to CeO_2 nanoparticles was associated with the activation of caspase 3 and p38 MAPK but not ERK1/2-MAPK or JNK MAPK signaling. In addition, they also found that the CeO_2 nanoparticles can induce the translocation of the redox sensitive transcription factor, Nrf-2 into the nucleus and the activation of heme oxygenase-1 but not superoxide dismutase or NF-KB. They proposed that the activation of HO-1 may be mediated through p38 MAPK signaling.

2.9.4 *In vivo* toxicity of Cerium Oxide nanoparticles

Work by Hirst and colleagues showed that the intravenous administration of CeO_2 nanoparticles is associated with increased kidney and liver weights that are dose and time

dependent [25]. These researchers also demonstrated the accumulation of cerium in various organs. Cerium concentrations were highest in spleen and elevated in the liver and brain. In the liver, they noted cerium oxide agglomerates in Kupffer cells and in the hepatocytes [6].

In vivo studies conducted by Ma and coworkers using rats showed that the inhalation of CeO_2 nanoparticles causes lung inflammation and alveolar macrophage apoptosis via increased oxidative stress [17]. These scientists also found that the CeO_2 nanoparticles are taken up by alveolar macrophages and that exposure to CeO_2 nanoparticles is associated with lung fibrosis. He and colleagues studied whether inhaled CeO_2 nanoparticles can translocate to other organs in the body using rats as a model system [113]. They observed that cerium can undergo extra pulmonary translocation where it can accumulate in the liver, spleen, bone, kidney and blood. Whether the accumulation of CeO_2 nanoparticles was associated with organ dysfunction was not addressed.

2.9.5 Possible mechanisms of ROS production by cerium oxide nanoparticles

CeO_2 nanoparticles have been shown to gain entry into the cell through diffusion and phagocytosis. Asati and colleagues showed that CeO_2 nanoparticles can become localized to the lysosome where they can induce cellular toxicity via the up regulation of oxidative stress signaling [115]. How CeO_2 nanoparticles might cause elevations in oxidative stress is not very well understood. Lin and coworkers have proposed that the Ce^{3+} state produced by the reduction of Ce^{4+} can interact with oxygen molecules to generate superoxide anions [18]. The two superoxide anions formed can then interact with each other to form hydrogen peroxide,

which then can be converted to hydroxyl radicals (reactions 1-4 below). It is also possible to produce alkoxyl radicals from lipid peroxide (LOOH) (reaction 5). In addition, they also proposed that physiologically relevant reductants such as ascorbate and thiol could interact with the CeO_2 nanoparticles and undergo oxidation to produce free radicals and reactive species.

$$Ce^{4+} + A^-_{red} \longrightarrow Ce^{3+} + A_{ox} \qquad (1)$$

$$Ce^{3+} + O_2 \longrightarrow Ce^{4+} + O_2^- \qquad (2)$$

$$O_2^- + O_2^- + 2H^+ \longrightarrow O_2 + H_2O_2 \qquad (3)$$

$$H_2O_2 + Ce^{3+} \longrightarrow Ce^{4+} + OH^- + OH^{\cdot} \qquad (4)$$

$$LOOH + Ce^{3+} \longrightarrow Ce^{4+} + LO^{\cdot} + OH^- \qquad (5)$$
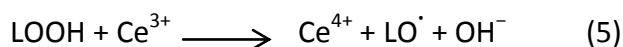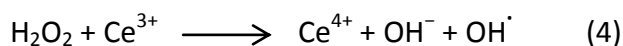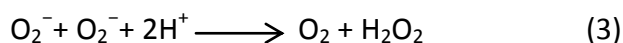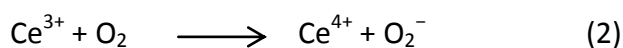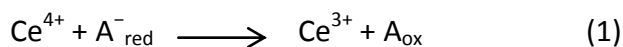
In reaction 1, A^-_{red} refer to physiologically relevant reductants, such as ascorbate and thiol compounds, whereas A_{ox} are their oxidized states.

3.0 Summary of the review of the literature

The field of nanotechnology is growing tremendously with applications in various industrial sectors including electronics, energy, consumer products, automotive and pharmaceutical industries [1, 2, 39]. With the increased application of nanomaterials, there is an increased risk of exposure to humans and the ecosystem. The evaluation of nanomaterial toxicity is of growing importance. Due to their widespread industrial use, CeO_2 nanoparticles have been chose by regulatory agencies for toxicology evaluation [7]. Studies conducted with

other metallic nanoparticles such as gold, silver, titanium and zinc have shown that the toxicity of nanoparticles is characterized by increased oxidative stress and cellular apoptosis [28, 116, 117]. Whether exposure to CeO_2 nanoparticles is associated with similar changes in the lung and liver is currently not clear.

Chapter 3

The following chapter includes three different research papers describing in detail the research experiments conducted to test our hypotheses set forth for the specific aims I, II and III of this dissertation project

PAPER I

Specific Aim 1: To investigate the role of stress responsive MAPKs and inflammatory protein signaling in the oxidative stress and apoptosis induced by CeO$_2$ nanoparticles in the lungs

Exposure to cerium oxide nanoparticles is associated with activation of MAPK signaling and apoptosis in the rat lung

Abstract

Whether exposure to cerium oxide (CeO_2) nanoparticles is associated with increased oxidative stress and apoptosis in rat lung has not been investigated. Specific pathogen free male Sprague-Dawley rats were instilled with either vehicle (saline) or CeO_2 nanoparticles at 7.0 mg/kg and euthanized 1, 3, 14, 28, 56 or 90 days post exposure. Lung tissues were collected and evaluated for evidence of oxidative stress and cellular apoptosis. Compared to age-matched control animals, exposure to CeO_2 nanoparticles increased lung weight to body weight ratio by ~8%, 34%, 15%, 36%, 80% and 69% at 1, 3, 14, 28, 56 and 90 days post exposure, respectively ($P<0.05$). Changes in lung weight were associated with the cerium accumulation in the lungs, elevations in serum inflammatory markers, an increased Bax to Bcl-2 ratio, elevated caspase-3 protein levels, increased phosphorylation of p38-MAPK and diminished phosphorylation of ERK1/2-MAPK ($P<0.05$). Taken together, these data suggest that exposure to CeO_2 nanoparticles is associated with lung remodeling, oxidative stress and cellular apoptosis.

Introduction

Cerium is a lanthanide metal that can undergo redox cycling depending on the partial pressure of oxygen in the surrounding environment [9]. The industrial production and utilization of cerium oxide (CeO_2) nanoparticles is increasing rapidly in the polishing, energy, electronic, automobile and biomedical industries [8]. Recently, CeO_2 nanoparticles have been used as catalysts in combustion engines to reduce particulate emissions and increase fuel efficiency [118]. Other work has demonstrated that CeO_2 nanoparticles may exhibit antioxidant activity [111] which has led to the suggestion that these particles may be useful for the treatment of cardiovascular disease [10], neuronal injury [11] and for the prevention of radiation-induced damage [12].

In addition to investigating the beneficial applications of CeO_2 nanoparticles, other research has begun to examine whether these materials may also be toxic. *In vitro* studies using A549 lung cancer cells [18] and bronchial alveolar epithelial cells (BEAS2B) [19] has suggested that cellular exposure to CeO_2 nanoparticles may be associated with increased production of reactive oxygen species (ROS) and the induction of cellular apoptosis. Other work using the intact rat has demonstrated that CeO_2 nanoparticles exposure can cause lung inflammation and fibrosis [17]. How exposure to CeO_2 nanoparticles may induce lung inflammation and remodeling has not been fully elucidated.

The mitogen activated protein kinases (MAPKs) including the extracellular signal-regulated kinase (ERK1/2-MAPK), p38-MAPK and c-Jun amino terminal kinase (JNK) are a family of serine / threonine specific kinases that transduce extracellular stimuli and are involved in the regulation of cell proliferation, gene expression and apoptosis [79, 80]. Previous work has

suggested that several metals, including arsenic, zinc and chromium can induce the phosphorylation of MAPK proteins [119]. Whether exposure to CeO_2 nanoparticles can elicit similar activity in the intact lung, has to our knowledge, not been examined.

The primary goal of this study was to determine if exposure to CeO_2 nanoparticles is associated with the activation of MAPK signaling and cellular apoptosis in the rat lung. Our data suggest that exposure to CeO_2 nanoparticles is associated with an increased lung weight to body weight ratio, the accumulation of cerium in the lungs, elevations in serum inflammatory markers, an increased Bax to Bcl-2 ratio, elevated caspase-3 protein levels, increased phosphorylation of p38-MAPK and diminished phosphorylation of ERK1/2-MAPK ($P<0.05$). Taken together, these data suggest that exposure to CeO_2 nanoparticles is associated with activation increased pulmonary ROS and cellular apoptosis.

Materials and Methods

Particle characterization

CeO_2 nanoparticles, average diameter at ~20 nm, were obtained from Sigma-Aldrich (St Louis, MO, USA) as previously outlined [17]. Normal saline was used to suspend the nanoparticles prior to instillation. Diluted particle suspensions were filtered, sputter coated, and examined with a Hitachi Model S-4800 Field Emission scanning electron microscope (Schaumburg, IL, USA) at 5 and 20 kV or placed on a formvar-coated copper grid to dry and imaged with a JEOL 1220 transmission electron microscope (Tokyo, Japan).

Animal handling and instillation of CeO₂ nanoparticles

All procedures were performed in accordance with the Marshall University Animal Care and Use Committee guidelines, using the criteria outlined by the Assessment and Accreditation of Laboratory Animal Care (AAALAC). Five week old (150-174 g) specific pathogen-free male Sprague-Dawley (Hla: SD-CVF) rats were purchased from Hilltop Lab Animals, Inc. (Scottdale, PA, USA). Rats were housed two per cage in an AAALAC approved vivarium with a 12-h light–dark cycle and maintained at 22 ± 2° C. Animals were allowed access to food and water *ad libitum*. All animals were allowed to acclimatize for two weeks before initiation of the study. All animals were examined for precipitous weight loss, failure to thrive or unexpected gait. Periodic weight measurements were taken throughout the duration of the study. After acclimatization, animals were randomly divided into 12 groups (n=6 per group). Animals underwent instillation with 0.3 ml of saline suspension or CeO₂ nanoparticles at a dosage of 7.0 mg/kg as described elsewhere[17].

Tissue collection

Rats were anesthetized at 1, 3, 14, 28, 56 or 90 days post exposure with ketamine (40 mg/kg) – xylazine (10 mg/kg) cocktail and supplemented as necessary for loss of reflexive response. After midline laparotomy, the lungs were removed and washed with oxygenated Krebs–Ringer bicarbonate buffer to remove any blood. After washing, lungs were trimmed of connective tissue, weighed and immediately snap frozen in liquid nitrogen.

Determination of cerium content in the lung

Cerium content in the lung was estimated by induction coupled plasma-mass spectrometry (ICP-MS) at Elemental Analysis Inc. (Lexington, KY, USA) according to standard protocols. Cerium concentration was estimated for 1, 3, 14, 28 and 90 day post exposure groups. Briefly, lung samples (n=4 for each group) were prepared using EPA Method 3050B for the analysis of total cerium by ICP-MS. A 1.0 g sample was weighed to the nearest 0.0001 g and digested with concentrated nitric acid, 30% hydrogen peroxide, and concentrated hydrochloric acid. A method blank, laboratory control sample, a laboratory duplicate, and a pre-digestion matrix spike were prepared for each sample. After digestion, the extracts and the quality control samples were diluted to a final volume of 50 mL before analysis using an Agilent 7500cx ICP-MS. The instrument was calibrated for Ce-140 with 0, 0.1, 1.0, 10.0, and 100 µg/L standards prepared from a certified reference standard traceable to NIST reference materials. A second source calibration verification standard traceable to NIST reference materials was analyzed to verify the calibration standards. A continuing calibration verification standard and a continuing calibration blank were analyzed at the beginning of the run, after every ten samples, and at the conclusion of the run.

Histopathological examination

Tissues from lungs were embedded in paraffin wax, sectioned at 5-µm, mounted on glass slides and stained with hematoxylin-eosin using standard histopathological techniques. Sections were examined by light microscopy in a blinded fashion by a board certified pathologist.

Immunoblotting analysis

Portions of individual lung tissues (100 - 150mg) were homogenized in buffer (T-PER, 8 mL/g tissue; Pierce, Rockford, IL, USA) containing protease (P8340, Sigma-Aldrich, Inc., St. Louis, MO, USA) and phosphatase inhibitors (P5726, Sigma-Aldrich, Inc., St. Louis, MO, USA). Tissue homogenates were sonicated for three cycles for 30 sec at 150W. The supernatant protein was collected by centrifuging the tissue homogenate at 12,000 x g for 5 min at 4 °C. Protein concentration of homogenates was determined via the 660 nm assay method (Fisher Scientific, Rockford, IL, USA). Equal concentrations of the protein samples were prepared from individual animals by adding the equal quantities of Laemmli 2X sample buffer (Sigma- Aldrich, Inc., St. Louis, MO, USA) and adjusting the protein concentration with the T-PER lysis buffer. Samples were boiled in a Laemmli 2X sample buffer for 5 min. Thirty two µg of total protein for each sample was separated on a 10% PAGEr Gold Precast gel (Lonza, Rockland, ME, USA) and then transferred to nitrocellulose membranes. Gels were stained with a RAPID Stain protein stain reagent (G-Biosciences, St. Louis, MO, USA) to verify transfer efficiency to membrane. Membranes were stained with Ponceau S and the amount of protein quantified by densitometric analysis to confirm successful transfer of proteins and equal loading of lanes as detailed somewhere else[120]. Membranes were blocked with 5% milk in Tris Buffered Saline (TBS) containing 0.05% Tween-20 (TBST) for 1 h and then incubated with primary antibody overnight at 4°C. After washing with TBST, the membranes were incubated with the corresponding secondary antibodies conjugating with horseradish peroxidase (HRP) (anti-rabbit (#7074) or anti-mouse (#7076), Cell Signaling Technology, Danvers, MA, USA) for 1 h at room temperature. Protein bands were visualized following reaction with ECL reagent (Amersham

ECL Western Blotting reagent RPN 2106, GE Healthcare Bio-Sciences Corp., Piscataway, NJ, USA). Target protein levels were quantified by AlphaView image analysis software (Alpha Innotech, San Leandro, CA, USA). Primary antibodies against caspase-3 (#9662), cleaved caspase-3 (#9661S), Bax (#2772), Bcl2 (#2870S), caspase-9 (#9506), ERK1/2-MAPK Thr 202/Tyr204 (#9106S), Phospho ERK1/2-MAPK Thr 202/Tyr204 (#4377S), JNK (#9252), Phospho JNK Thr 183/Tyr185 (#9251S), p38 MAPK (#9212), Phospho p38 MAPK Thr 180/ Tyr 182 (#9216L), JAK2 (#3229), Phospho JAK2 Tyr1007/100 (#3776), STAT3 (#9132) and Phospho STAT3 Tyr 705 (#9131S) were purchased from Cell Signaling Technology (Beverly, MA, USA).

Multiplexed serum protein immunoassays

Pooled serum samples from six animals in 1, 3, 28 and 90 day exposure groups were shipped on dry ice to Rules Based Medicine (Austin, Texas) for Rodent MAP® version 2.0 Antigen analysis using a Luminex 100 instrument as detailed elsewhere [121]. The antigen panel consisted of fifty-nine proteins, which included proteins involved in inflammation, cytokines, growth factors and tissue factors. Each analyte was quantified using 4 and 5 parameter, weighted and non-weighted curve fitting algorithms using proprietary data analysis software developed at Rules-Based Medicine.

Data Analysis

Results are presented as mean ± SEM. Data were analyzed using the Sigma Plot 11.0 statistical program. One-way analysis of variance and two-way analysis of variance were

performed for overall comparisons, while the Student–Newman–Keuls *post hoc* test used to determine differences between groups. Values of $P < 0.05$ were considered to be statistically significant.

Results

Nanoparticle characterization

Similar to previous work[17], using the same batch of CeO_2 nanoparticles, analysis of nanoparticle size by TEM and scanning electron microscopy (SEM) confirmed the presence of single and agglomerated CeO_2 nanoparticles in the suspension as shown in early studies[17, 121]. Field emission scanning electron microscopy showed that the CeO_2 nanoparticles were generally dispersed into submicron groups with an average size of 9.26 ± 0.58 nm. The diameter of the primary CeO_2 particles was determined to be 10.14 ± 0.76 nm by TEM (Figure 3.1).

Exposure to CeO_2 nanoparticles increases lung weight to body weight ratio

Cerium oxide nanoparticles exposure had no effect on feed intake or body weight gain (data not shown). Compared to age-matched control animals, the lung weight to body weight ratio was higher for the CeO_2 nanoparticles exposure group at each time point of exposure (Day 1 control: 5.42 ± 0.66 vs. Day 1 CeO_2 nanoparticles exposure: 5.84 ± 0.24 ($P < 0.05$), Day 3 control: 4.97 ± 0.68 vs. Day 3 CeO_2: 6.64 ± 0.66 ($P < 0.05$), Day 14 control: 5.55 ± 0.66 vs. Day 14 CeO_2 exposure: 6.40 ± 0.89 ($P < 0.05$), Day 28 control: 4.44 ± 0.38 vs. Day 28 CeO_2 exposure: 6.03 ± 0.69

(P<0.05), Day 56 control: 3.50± 0.57 vs. Day 56 CeO$_2$ exposure: 6.30±1.19 (P<0.05), and Day 90 control: 3.11± 0.27 vs. Day 90 CeO$_2$ exposure: 5.27±0.64 (P<0.05) (Table 2).

Accumulation of cerium in the lung with the days of post exposure

The concentration of cerium in the lung was estimated with the elemental analysis technique ICP-MS (Elemental Analysis, Inc., Lexington, KY, USA). The concentration of cerium in the lung was decreased with increasing at 1- day post exposure (Post exposure Day 1: 250 ± 33 ppm vs. Day 3: 223 ± 41 ppm vs. Day 14: 143 ± 12 ppm vs. Day28: 177 ± 38 ppm, and Day 90 132 ± 31 ppm (P<0.05) (Figure 3.2). However, total cerium content in the lung tissue appears to increase post day 1 exposure that stays unaltered with the progression in the days of exposure (Data not shown).

Exposure to CeO$_2$ nanoparticles alters the gross histological appearance of the lung

Alterations in appearance of the lungs following exposure to CeO$_2$ nanoparticles included increased lung weight, the presence of black spots and white pustular nodules on the surface of the lungs that appeared to increase over time (Figure 3.3). Histological alterations included an increased number of alveolar macrophages, increased number of polymorphonuclear cells and the apparent accumulation of particulate material in the alveolar spaces (Figure 3.4).

CeO$_2$ nanoparticles increase apoptotic protein signaling in the lung

Compared to day 1 control animals, the Bax to Bcl-2 protein ratio in exposed animals was 16% higher at day 1 and 99% higher at day 3 post exposure (P<0.05) before declining thereafter (Figure 3.5). Similarly, the Bax to Bcl-2 ratio was 37%, 23%, and 14% lower at days 14, 28 and 56, respectively in CeO$_2$ nanoparticles exposed animals. Conversely, the Bax to Bcl-2 ratio was 22% higher for day 90 exposure animals compared to that observed in the day 1 control animals.

In an effort to extend these findings, we next examined the regulation of the initiator (caspase-9) and the executor caspases (caspase-3) [98]. Compared to day 1 control animals, total caspase-9 protein levels were reduced by 28%, 6%, 23%, 5%, 21%, and 32% (P<0.05) in the day 1, 3, 14, 28, 56, and 90 exposure groups, respectively (P<0.05). Compared to saline day 1 controls, the expression of the 38kDa and 40 kDa cleaved fragments of caspase-9 was increased 20%, 20%, and 20% for day3, day 14 and day 28 post exposure groups, respectively (P<0.05; Figure 3.6).

Caspase-3 protein expression levels were increased by 56% (P<0.05) and 20% (P<0.05) for the day 3 and 14 exposure groups when compared to day 1 controls. Compared to saline day 1 control animals, the amount of cleaved caspase-3 (17kDa and 19 kDa) was increased by 10%, 88%, 66%, 119%, 77%, and 39% higher for the day 1, 3, 14, 28, 56 and 90 exposure groups (P<0.05; Figure 3.7).

CeO$_2$ nanoparticle exposure is associated with activation of MAPK signaling

Compared to day 1 controls, the ratio of phosphorylated p38 MAPK (Thr180/Tyr182) to total p38 MAPK was 22% and 14% lower for day1 and day3 post exposure groups (P<0.05). Conversely, this ratio was elevated by 52%, 15%, and 10% for day 14, 28 and 56 exposure groups, before declining by 19% in the 90 day animals (P<0.05; Figure 3.8).

The ratio of phosphorylated ERK1/2-MAPK (Thr202/Tyr204) to total ERK1/2-MAPK was reduced by 43%, 57%, 56%, 62%, 53% and 41% at day 1, 3, 14, 28, 56 and 90 post exposure groups when compared to day 1 saline controls (P<0.05; Figure 3.9). There were no significant differences in the expression of phosphorylated (Thr183/Tyr185) JNK to total JNK ratio with the nanoparticle exposure (Figure 3.10).

CeO$_2$ nanoparticles increase inflammatory protein signaling

It is known that JAK2 and STAT3 play crucial roles in the inflammation[104]. When compared to saline control day1, phosphorylated (Tyr705) to total STAT3 protein levels were 111%, 193%, 106%, 15% and 20% higher for day 3, 14, 28, 56 and 90 exposure groups (P<0.05; Figure 3.11). Phosphorylated (Tyr1007/1008) JAK2 to total JAK2 ratio was 25%, 23%, and 103% (P<0.05) higher for the day 1, 56, and 90 animals when compared to saline control animals (Figure 3.12).

In order to determine the role of inflammatory mediators that are released into the circulation, we determined the expression of serum biomarkers that include inflammatory cytokines, interleukins, chemokines, tissue factors and growth factors. Among the 55 parameters, we have included 12 parameters that are thought to play an important role in the

inflammation. Data are presented as percentage change in the expression when compared with the saline control day 1. Compared to saline control day 1, CeO$_2$ nanoparticle exposure at day 1 has increased the expression of all the parameters that are under the study (Figure 3.13 a). Compared to saline control day 1, post exposure day 3 group showed elevation of expression for 3 parameters, lowered expression for 8 parameters and no changes in the expression of 1 parameter (Figure 3.13 b). Compared to saline control day1, day28 post exposure group showed an elevation of 4 parameters, a lowered expression for 7 parameters and no change in the expression of 2 parameters (Figure 3.13 c). Compared to saline control day 1, day 90 post exposure group showed lowered expression for 10 parameters and no change in the expression for 2 parameters (Figure 3.13 d).

Discussion

Previous *in vitro* and *in vivo* studies have suggested that exposure to CeO$_2$ nanoparticles can elicit toxic effects; however the underlying mechanism(s) is not well understood [16-18, 118]. The primary findings of the current work are that pulmonary exposure to CeO$_2$ nanoparticles is associated with increases in the lung to body weight ratio, histological evidence of lung inflammation, the activation of MAPK signaling, the phosphorylation of STAT-3, increases in caspase-3 cleavage, and inflammation.

Our data demonstrated that exposure to CeO$_2$ nanoparticles results in increased lung weight to body weight ratio (Table 2). To determine the potential mechanism of increased lung weight we next examined the lungs for the presence of CeO$_2$ nanoparticles. As indicated by our ICP-MS data, the instillation of CeO$_2$ nanoparticles leads to the deposition of cerium in the lungs

43

(Figure 3.2). Whether this cerium deposition is responsible for the increased lung to body weight ratio is currently unclear. With increased lung to body weight ratio we also observed that exposure to CeO_2 nanoparticles was associated with the development of white nodular structures on the lung surface (Table 2, Figures 3.3 and 3.4). Recent work has shown that nanoparticles such as carbon nanotubes, TiO_2 nanoparticles, and polyacrylate nanoparticles can induce granulomas on the lung surface [49, 122, 123]. It is possible that the white nodules we observed in the present study may be the byproduct of an ongoing inflammatory reaction, which could result in either the clearance of the nanoparticles or advance further to form granulomas on the surface of lungs [123, 124]. The aforementioned possibility is consistent with our histopathological analysis where we observed an increase in the number of alveolar macrophages and polymorph nuclear white blood cells in the lungs of animals that had been exposed to the CeO_2 nanoparticles. It is thought that the toxic effects of most nanoparticles (silver, silica, titanium dioxide, zinc oxide and carbonaceous nanoparticles) are characterized by increased oxidative stress [24, 73, 125-127]. Whether these increases in oxidative stress are due to increased ROS generation or decreased ROS scavenging is currently unclear, however, many metallic oxide nanoparticles have been shown to increase ROS production [1, 102].

Increase in the ROS may also induce apoptotic signaling. Here, we observed an increase in the proapoptotic Bax to Bcl-2 ratio after 3 days of the exposure before declining thereafter (Figure 3-5). Given that the Bax to Bcl-2 ratio is a primary determinant of whether a cell undergoes apoptosis or survival [97, 98] we next examined the possibility that CeO_2 nanoparticle exposure is associated with the activation of caspase-3. Consistent with the Bax/Bcl-2 data, we found that caspase-3 cleavage (activation) is elevated at days 3, 14, 28 and

56. Why caspase-3 cleavage may exist in the absence of elevation in the Bax/Bcl-2 ratio is currently unclear. Other signaling pathways (extrinsic or intrinsic pathway) that activate the apoptotic pathway may explain the possible activation of effector caspase 3 in the absence of elevated Bax/Bcl-2 ratio. It is thought that mild lung injury will result in repair of the damaged tissue whereas excessive apoptotic cell death may lead to the development of lung remodeling and fibrosis [128]. Bearing this in mind, the activation of caspase 3 we find in the current study may help to explain the findings of increased lung fibrosis following CeO_2 nanoparticle exposure shown in previous work [17].

The MAPKs are stress responsive proteins that can be activated by the growth factors, chemicals, ultraviolet radiation, heat, synthesis inhibitors, metals or foreign organisms [129]. The MAPKs pathway plays an important role in the nanoparticle and metal induced oxidative stress and inflammation [102, 119]. The primary members of the MAPKs signaling family include p38 MAPK, JNK-MAPK and ERK1/2-MAPK. MAPKs proteins are thought to phosphorylate (activate) transcription factors that are involved in regulating the cell survival or death. Here we observed that CeO_2 nanoparticle exposure is associated with increased p38 MAPK phosphorylation at days 14, 28 and 56 of exposure. Conversely, we found that ERK1/2-MAPK activity appeared to be impaired by CeO_2 nanoparticles (Figures 3.8 and 3.9). Given that ERK1/2- MAPK is thought to play an important role in cell survival and that p38 MAPK may play an important role in apoptosis [129], these differences in MAPK signaling may help to explain the discrepancies that we observed in the proapoptotic Bax to Bcl-2 ratio.

It is well known that nanoparticle exposure is often associated with increased levels of inflammatory mediators such as cytokines, interleukins and other mediators of inflammation [1,

73, 102]. The Janus kinase / signal transducers and activators of transcription (JAK/STAT) pathway is a particularly important pathway in mediating inflammation [104]. Interestingly, JAK2 did not appear to have an important role in the toxicological response, as its phosphorylation (Tyr1007/1008) was elevated only at day 1 and day 90 of exposure (Figure 3.12). Conversely the phosphorylation of STAT-3 (Tyr705) seemed to parallel p38 MAPK activation (Figure 3.11). Previous work has demonstrated that p38 MAPK can act as an upstream activator of STAT-3, which when activated, can induce apoptosis [106]. These data, considered together with our findings of an increased Bax/Bcl-2 ratio, are consistent with the possibility that CeO_2 nanoparticles induced apoptosis is mediated through the activation of the p38 MAPK and STAT-3 signaling pathways.

In addition to evidence for increased inflammatory signaling, we also noted increased levels of several inflammatory cytokines and chemokines (Figures 3.13a, b, c and d). Of particular note was the finding that CD40 Ligand (CD40L) was elevated at day1 and 3 post exposure. Previous studies using ultrafine particles present in the air pollutants and diesel exhausts showed activation of CD40L which can strongly activate CD40 bearing cells such as white blood cells, endothelial cells and platelets and thereby can cause increased coagulation and inflammation [130]. It is also thought that CD40L plays an important role in activating macrophages where it causes macrophages to increase their phagocytic activity. Other work has shown that CD40L can induce the production of IL-4 by T-cells [130] (Figure-13a). Whether this activity is the cause of the increased levels of IL-4 seen in the current study, is currently unclear. Other studies have shown that CD40L can induce endothelial cells to produce ROS, chemokines and cytokines that can damage the cell [131]. In addition to CD40L, we also noted

the increased expression of several other serum chemokines and cytokines including IL-7, IL-1 alpha, monocyte chemo attractant proteins (MCP) and Eotaxin; all of which are thought to play an important role in inflammation [73, 132, 133]. How these factors may work together to cause the inflammatory response we observe in the present study is unfortunately, beyond the scope of the current study and will require additional experimentation.

In summary, our data suggest that exposure to CeO_2 nanoparticles can increase lung to body weight ratio and the increased lung weights are associated with increased accumulation of cerium in the lungs. Our studies demonstrated that exposure to CeO_2 nanoparticles can cause gross and histological alterations to lungs. CeO_2 nanoparticles appear to activate oxidative stress, inflammation and apoptotic protein signaling in the lungs. Data from our studies demonstrate that the apoptosis induced by CeO_2 nanoparticles appears to be mediated through activation of caspase protein signaling. Given these findings, additional research to evaluate the role of subcellular organelles in inducing the apoptosis is likely warranted.

Table 2: CeO$_2$ nanoparticle exposure increases the lung weight to body weight ratio

Days of exposure	Body weight (g)		Lung weight (g)		Coefficient of lung weight to bodyweight	
	Saline Control	CeO2-7.0mg/kg	Saline Control	CeO2-7.0mg/kg	Saline Control	CeO2-7.0mg/kg
1	319.67±15.92	319.67±15.20	1.74±0.0.28	1.88±0.08	5.42±0.66	5.84 ±0.24
3	310.33±28.10	331.67±24	1.54±0.27	2.19±0.15	4.97± 0.68	6.64± 0.66†
14	345.67±27.11	332.33±21.07	1.90±0.31	2.12±0.23	5.55±0.66	6.40± 0.89†
28	411.33±29.2^{*μ}	403.67±28.94^{*μ}	1.82±0.09	2.43±0.30	4.44 ±0.38	6.03 ±0.69†
56	451.67±26.21^{*αμ}	451.33±34.6^{*αμ¶}	1.56±0.24	2.84±0.58	3.50± 0.57^{*αμ}	6.30±1.19†
90	523.33±60.87$^{*αμ¶\#}$	519.33±44.84$^{*αμ¶\#}$	1.62±0.11	2.75±0.51	3.11±0.27^{*αμ¶}	5.27±0.64^{†α}

† Significantly different from the control in each day of exposure
*Significantly different from the 1 Day exposure group in each condition
^{α} Significantly different from the 3 Day exposure group in each condition
μ Significantly different from the 14 Day exposure group in each condition
¶ Significantly different from the 28days exposure group
\# Significantly different from the 56days exposure group

Figure 3-1: Characterization of the cerium oxide nanoparticles by (a) TEM micrograph (scale bar = 200 nm) and (b) Field emission SEM of a dilute cerium oxide suspension.

a
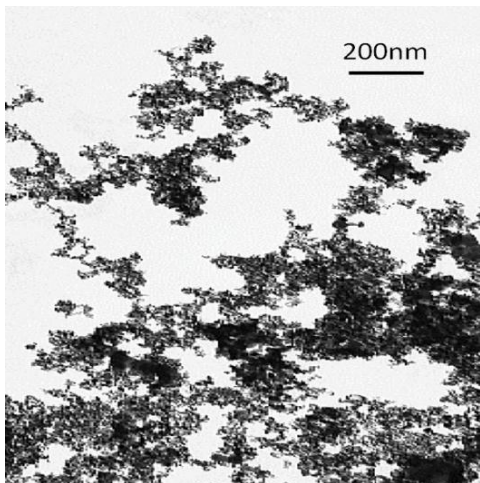
b
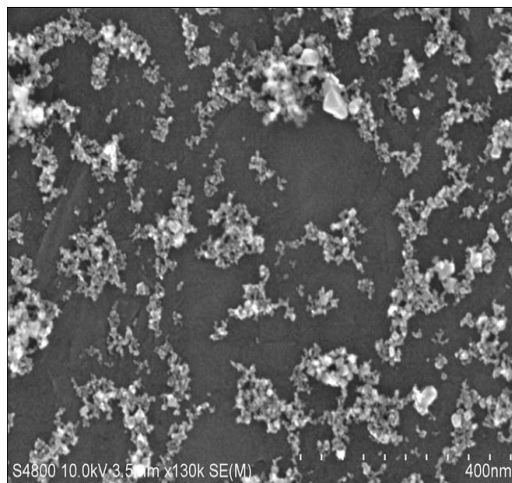
Figure 3-2: Cerium deposition in the lung appears to diminish over time.

Con-1 represents saline control day1, CeO$_2$-1, 3, 14, 28 and 90 represents animal groups post

exposed to CeO$_2$ nanoparticles at 1, 3, 14, 28 and 90 days respectively.
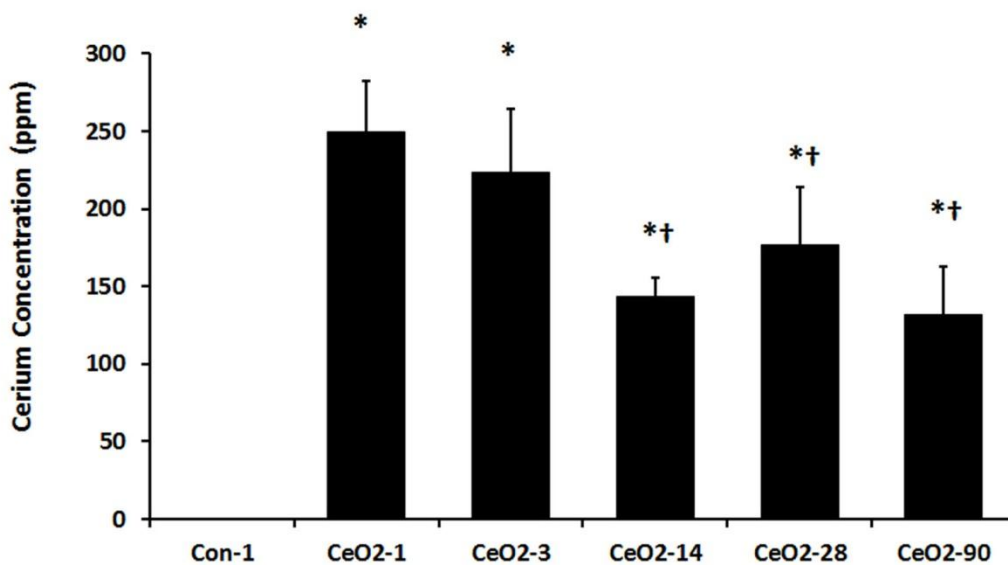
∗ Significantly different from the saline control day-1

† Significantly different from the CeO$_2$-day-1

Figure 3-3: Gross alterations in the lungs with CeO$_2$ nanoparticles instillation include increases in the lung weight, appearance of white nodules on the surface (Arrow) and appearance of black spots on lung surface

Saline-control-Day1-lungs

CeO$_2$ 7.0 mg/kg-lungs-28days

CeO$_2$ 7.0 mg/kg-lungs-56days

CeO$_2$ 7.0 mg/kg-lungs-90days

Enlarged image

CeO$_2$-7.0mg/kg- Lungs-56 days
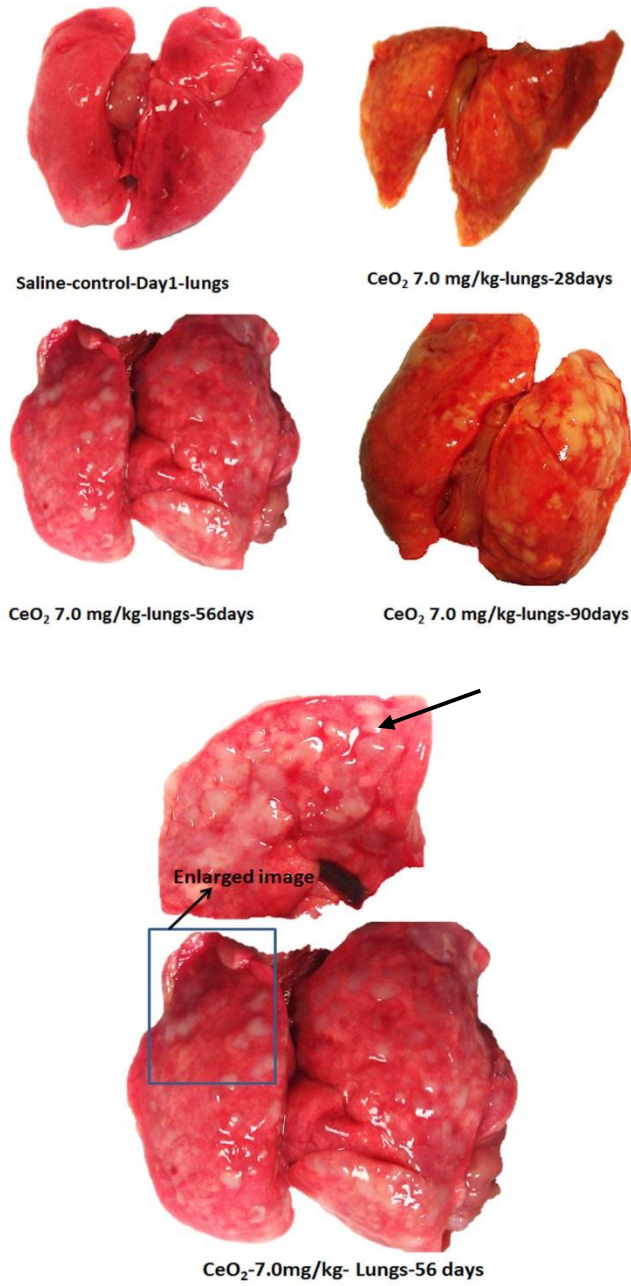
Figure 3-4: Alterations in histological appearance of lungs with CeO$_2$ nanoparticle instillation include increases in the number of alveolar macrophages, increases in the polymorphonuclear white blood cells (Arrow head) and increased accumulation of particulate matter (Arrow) in the air spaces (400X)
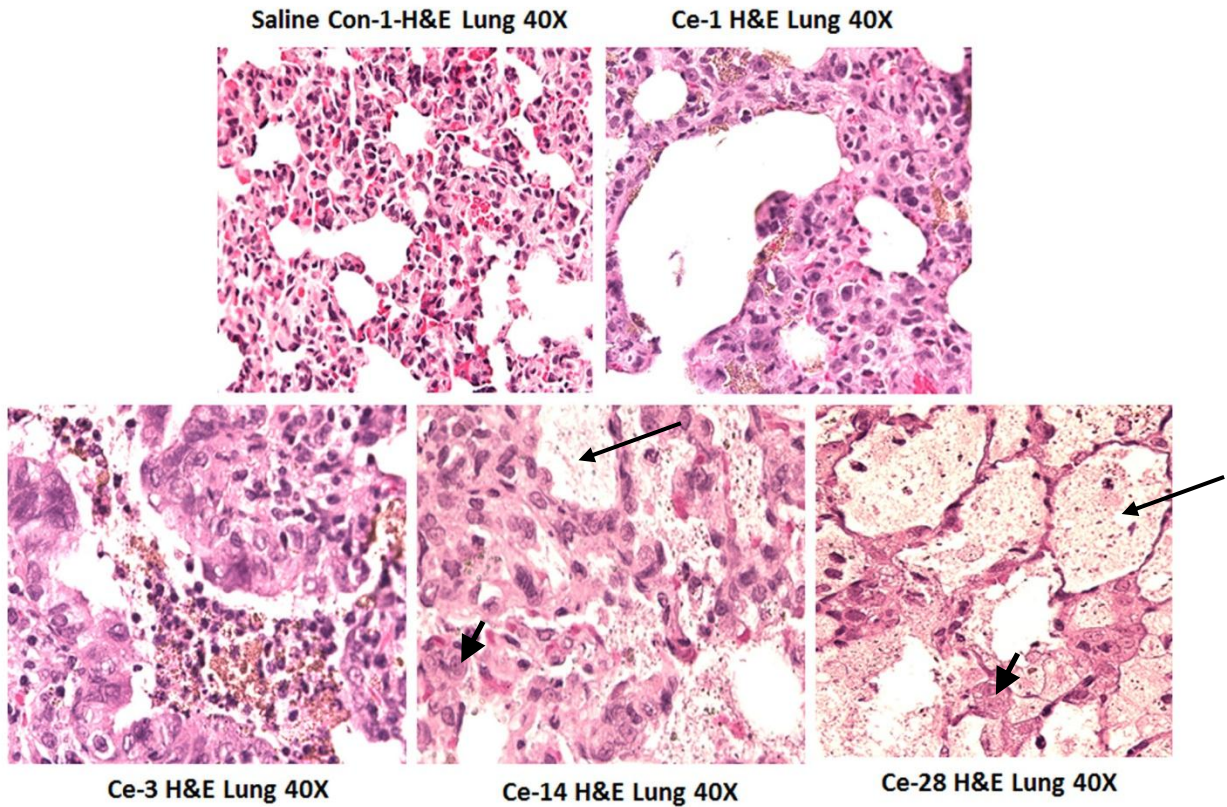
Figure 3-5: CeO$_2$ nanoparticles can increase the proapoptotic protein signaling in the lungs. Protein bands of the Bax and Bcl-2 proteins and corresponding GAPDH are represented in the figure. Bands corresponding to the X-axis labels are shown in the immunoblotting images. Protein levels were adjusted by GAPDH levels and compared with the control day-1.
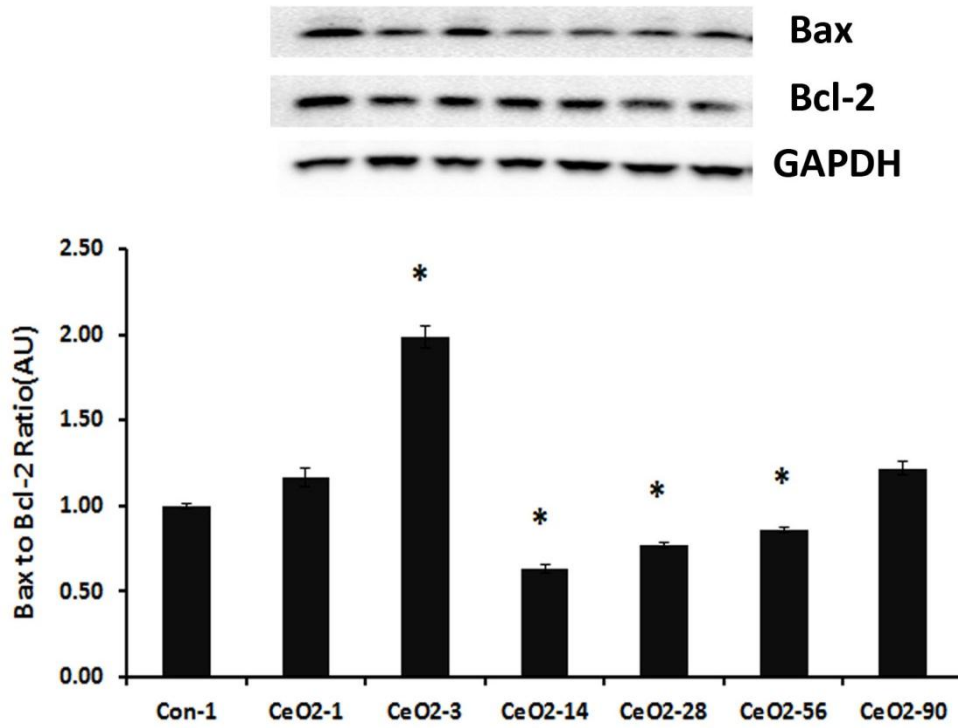
＊Significantly different from the saline control day-1

Figure 3-6: Increased expression of initiator caspase-9 with CeO$_2$ nanoparticles instillation.

Protein bands of the caspase-9 and cleaved caspase-9 proteins and corresponding GAPDH are represented in the figure. Bands corresponding to the X-axis labels are shown in the immunoblotting images. Protein levels were adjusted by GAPDH levels and compared with the control day-1.
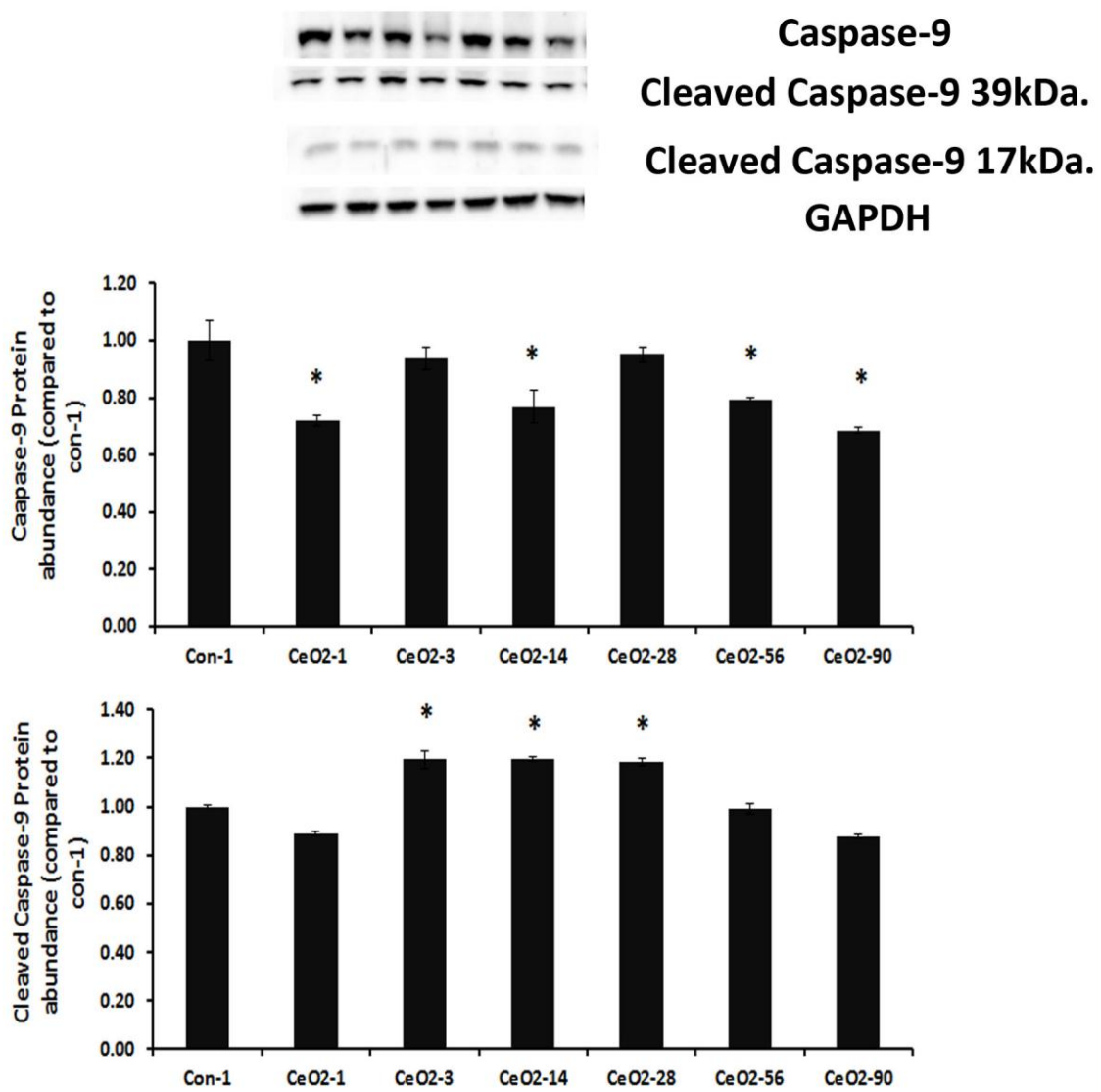
* Significantly different from the saline control day-1

Figure 3-7: Increased expression of executor caspase-3 with CeO$_2$ nanoparticles exposure.

Protein bands of the caspase-3 and cleaved caspase-3 proteins and corresponding GAPDH are represented in the figure. Bands corresponding to the X-axis labels are shown in the immunoblotting images. Protein levels were adjusted by GAPDH levels and compared with the control day-1.

∗ Significantly different from the saline control day-1
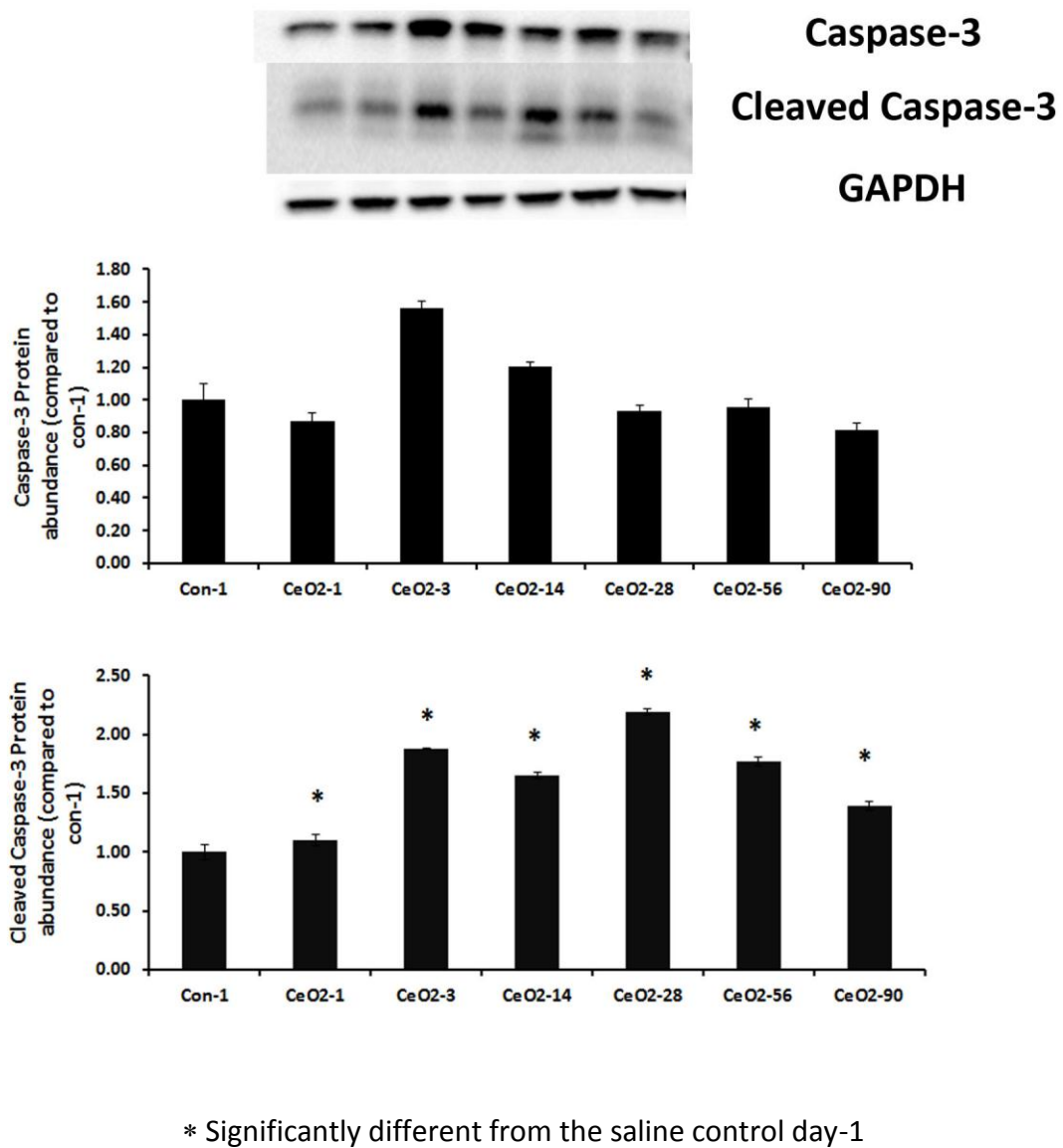
Figure 3-8: Activation of p38 MAPK activity with the CeO_2 nanoparticles instillation.

Protein bands of the p38MAPk and Phospho p38 MAPK proteins and corresponding GAPDH are represented in the figure Bands corresponding to the X-axis labels are shown in the immunoblotting images. Protein levels were adjusted by GAPDH levels and compared with the control day-1.
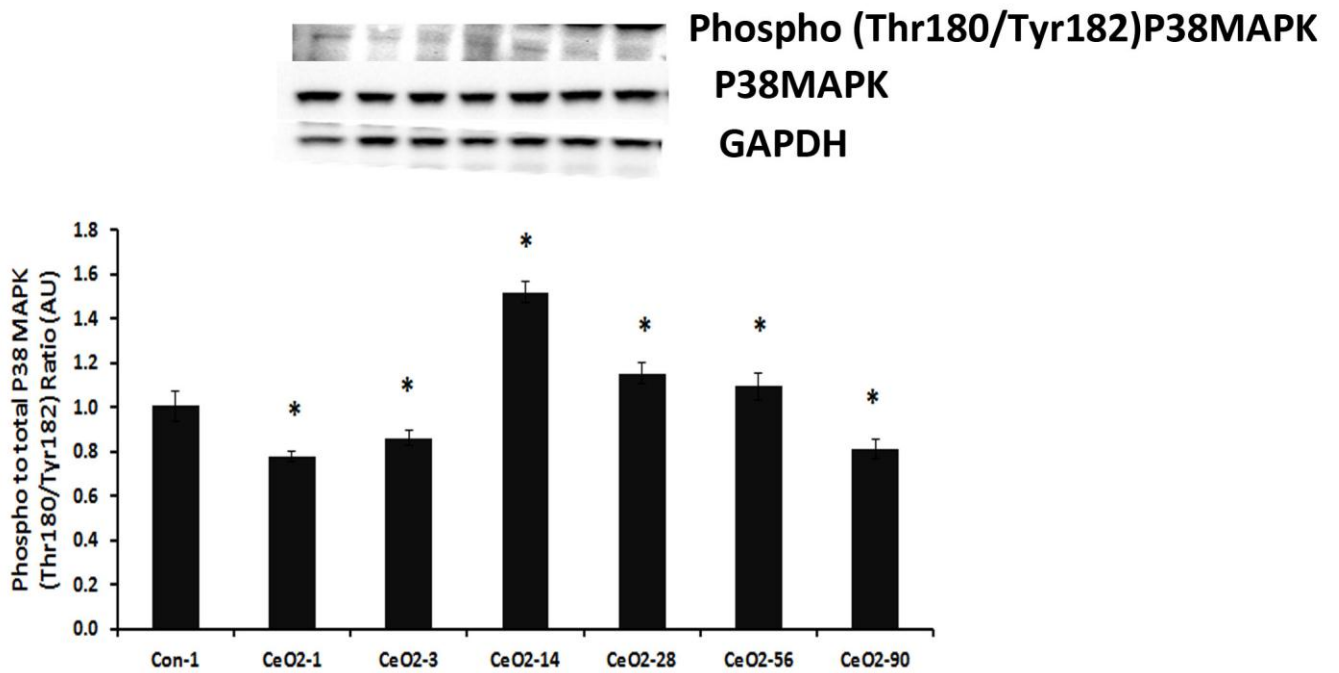
∗ Significantly different from the saline control day-1

Figure 3-9: Inhibition of ERK1/2-MAPK activity with the CeO₂ nanoparticles instillation.

Protein bands of the ERK1/2-MAPK and Phospho ERK1/2-MAPK proteins and corresponding GAPDH are represented in the figure. Bands corresponding to the X-axis labels are shown in the immunoblotting images. Protein levels were adjusted by GAPDH levels and compared with the control day-1.
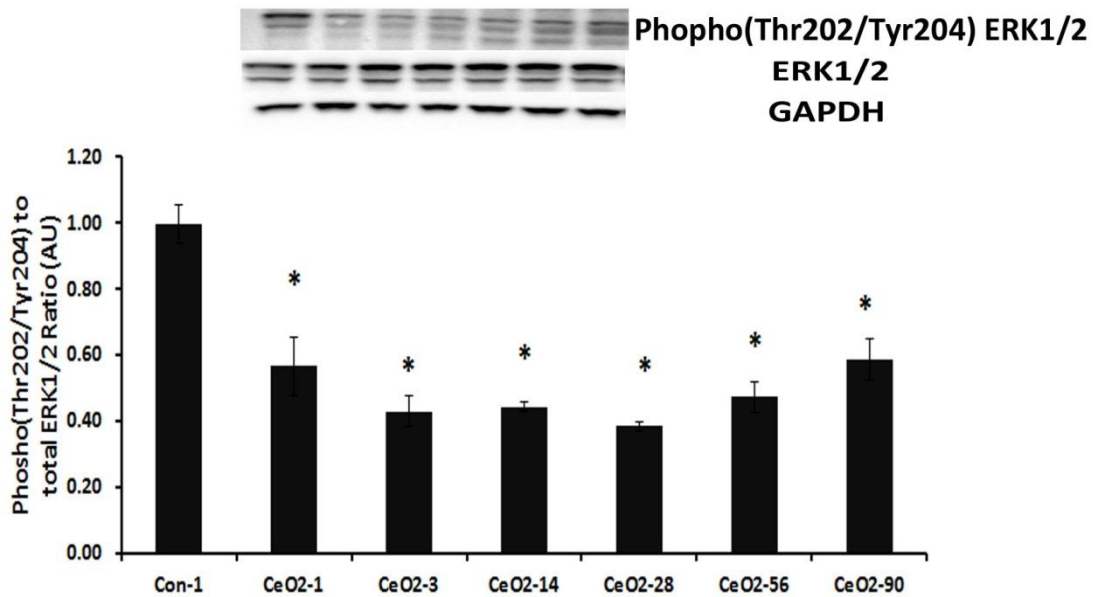
∗ Significantly different from the saline control day-1

Figure 3-10: CeO$_2$ nanoparticles do not appear to modulate the JNK activity.

Protein bands of the JNK and Phospho JNK proteins and corresponding GAPDH are represented in the figure. Bands corresponding to the X-axis labels are shown in the immunoblotting images. Protein levels were adjusted by GAPDH levels and compared with the control day-1.
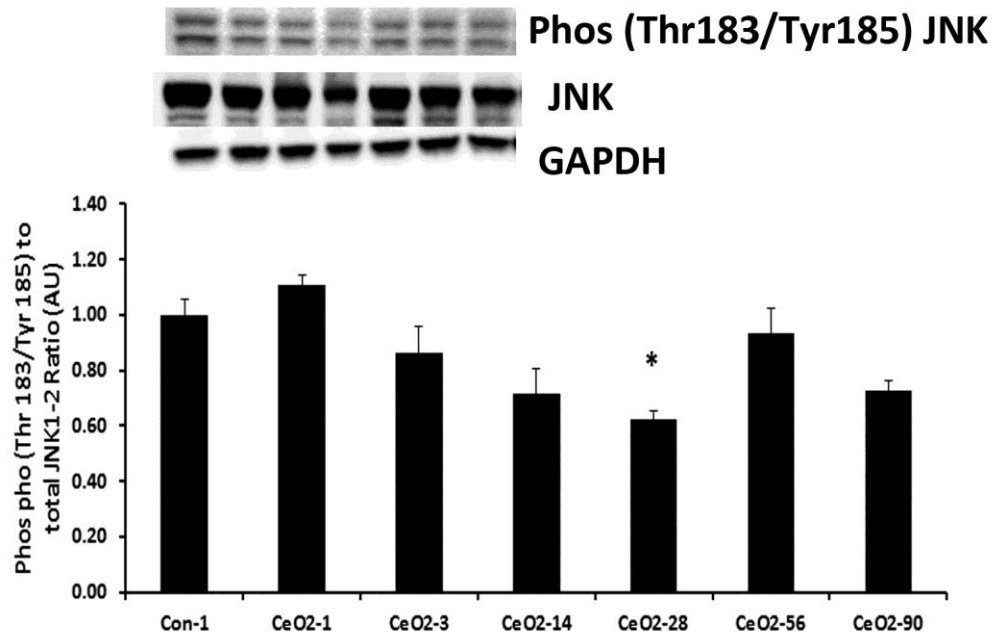
＊Significantly different from the saline control day-1

Figure 3-11: Activation of STAT-3 with CeO$_2$ nanoparticles exposure follows the activation of p38 MAPK.

Protein bands of the STAT-3 and Phospho STAT-3 proteins and corresponding GAPDH are represented in the figure. Bands corresponding to the X-axis labels are shown in the immunoblotting images. Protein levels were adjusted by GAPDH levels and compared with the control day-1.
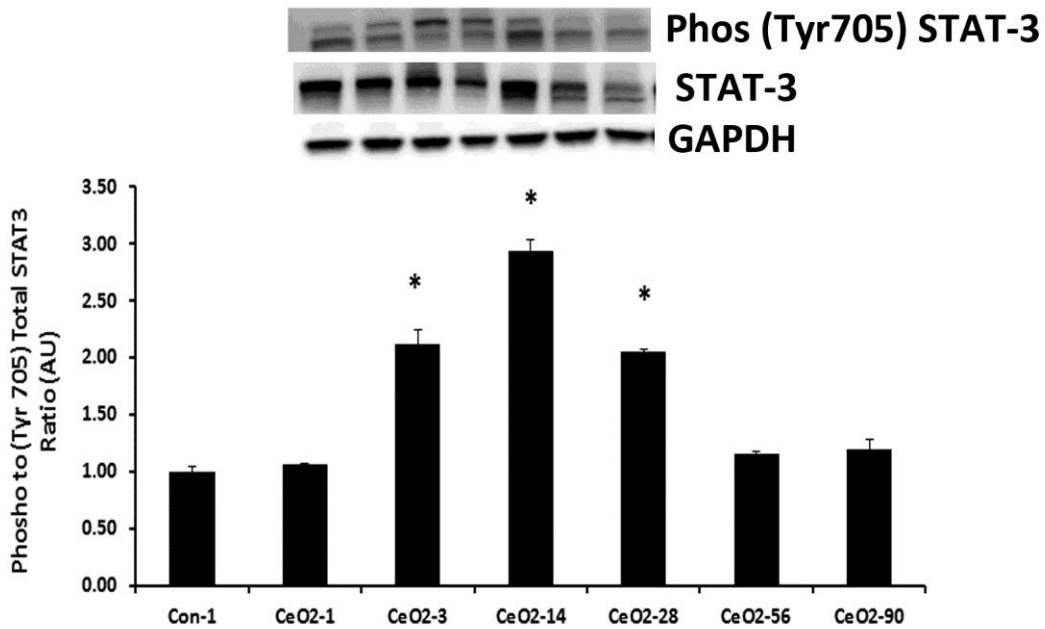
* Significantly different from the saline control day-1

Figure 3-12: Alteration in the expression of JAK2 protein expression with CeO_2 nanoparticles instillation.

Protein bands of the JAK2 and Phospho JAK2 proteins and corresponding GAPDH are represented in the figure. Bands corresponding to the X-axis labels are shown in the immunoblotting images. Protein levels were adjusted by GAPDH levels and compared with the control day-1.
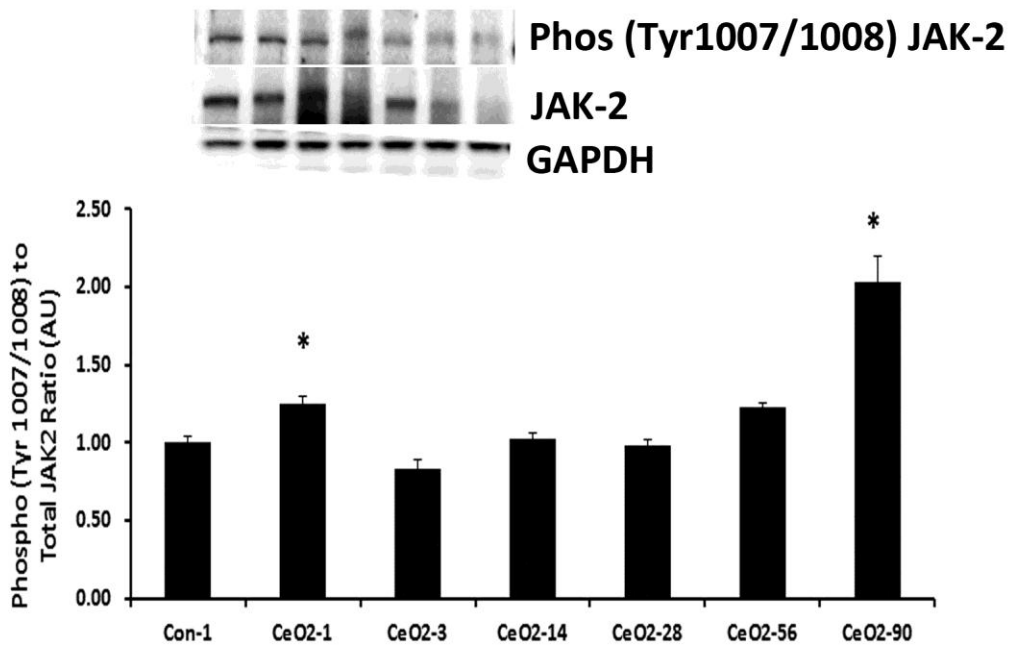
∗ Significantly different from the saline control day-1

Figure 3-13: Activation of pro-inflammatory cytokines and chemokines in the serum with CeO$_2$

nanoparticles exposure
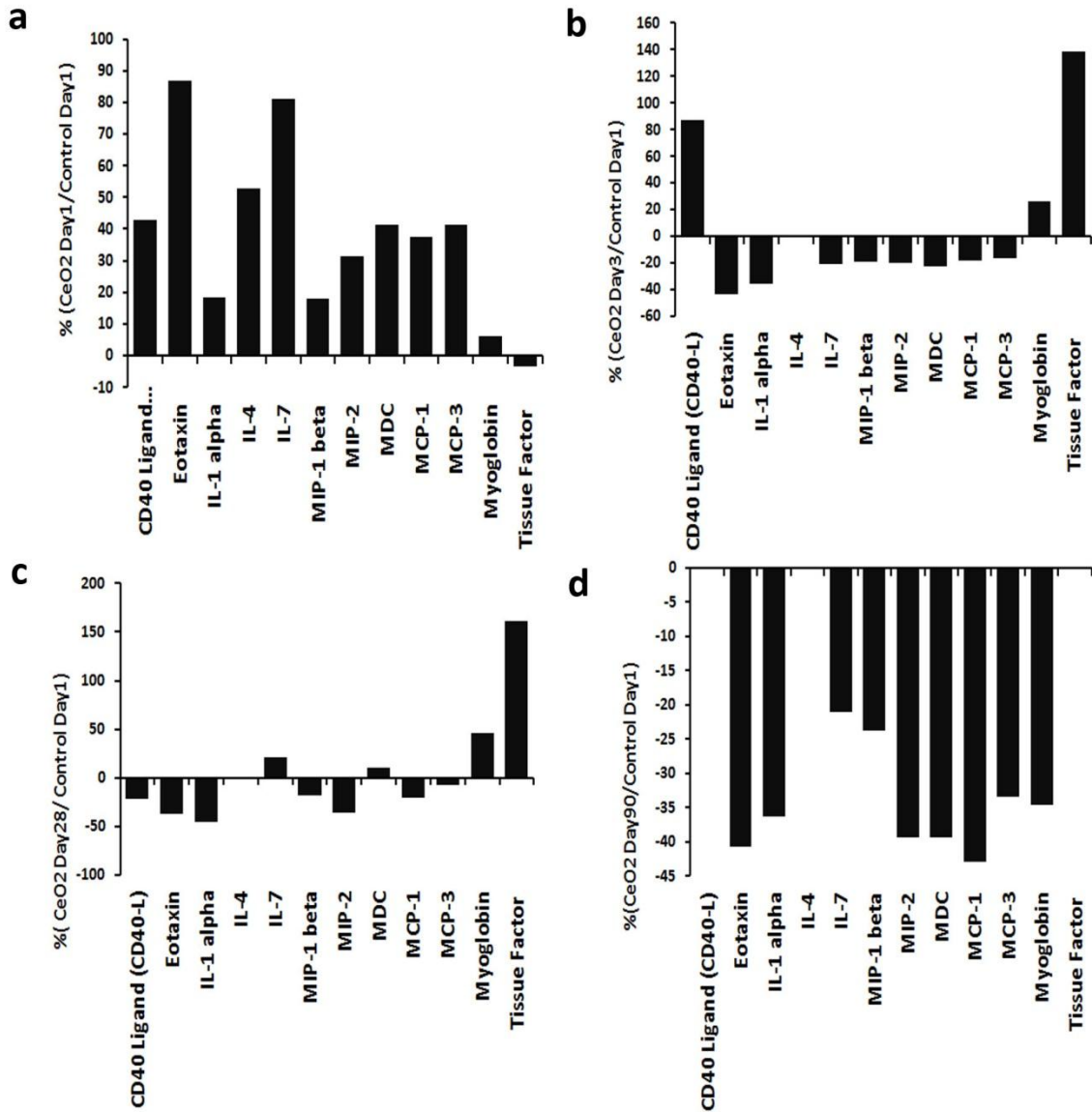
Paper-II

Specific Aim-2: To investigate if intratracheal instillation of CeO_2 nanoparticles has any toxic effects on the liver, kidney, spleen and heart of rats

Note: Animal studies and procedures such as exposure to CeO_2 nanoparticles and scarifying of the animals mentioned in this part were conducted at NIOSH, where we collected the vital organs such as liver, kidney, spleen and heart and used to perform the experiments explained in this part.

Note: This paper has been previously published:

Intratracheal instillation of cerium oxide nanoparticles induces hepatic toxicity in male Sprague Dawley rats

Abstract

Cerium oxide (CeO_2) nanoparticles have been posited to have both beneficial and toxic effects on biological systems. Herein, we examine if a single intratracheal instillation of CeO_2 nanoparticles (1.0 mg/kg, 3.5 mg/kg or 7.0 mg/kg) after 28 days is associated with systemic toxicity in male Sprague-Dawley rats. Compared to control animals, CeO_2 nanoparticle exposure was associated with increased liver ceria levels, elevations in serum alanine transaminase levels, reduced albumin levels, diminished sodium-potassium ratio and decreased serum triglyceride levels ($P<0.05$). Consistent with these data, rats exposed to CeO_2 nanoparticles also exhibited reductions in liver weight ($P<0.05$) and dose dependent hydropic degeneration, hepatocyte enlargement, sinusoidal dilatation and the accumulation of granular material. No histopathological alterations were observed in the kidney, spleen and heart. Analysis of the serum biomarkers suggested that there was an elevation of acute phase reactants and markers of hepatocytes injury in the CeO_2 nanoparticles exposed rats. Taken together, these data suggest that intratracheal instillation of CeO_2 nanoparticles can result in liver damage.

Introduction

Cerium is a rare earth lanthanide metal that is a strong oxidizing agent. Cerium exists both in the trivalent (Ce^{3+}, cerous) and in a very stable tetravalent state (Ce^{4+}, ceric) as cerium oxide (CeO_2) [8]. CeO_2 is widely used as a polishing agent for glass mirrors, television tubes and ophthalmic lenses [7]. In addition, CeO_2 can also act as a catalyst as it can both accept and give up oxygen [134]. This latter property has led to the widespread use of CeO_2 in the automobile industry where it has been used to increase fuel efficiency and reduce particulate emissions [108, 109, 118]. It appears that CeO_2 nanoparticles may also be capable of acting as antioxidants which has led some to postulate that these particles may be useful for the treatment of cardiovascular disease [10], neurodegenerative disease [11] and radiation-induced tissue damage [12, 135]. Nonetheless, other *in vitro* work has shown that CeO_2 nanoparticles can also cause oxidative stress [19].

The Organization for Economic Co-operation and Development (OECD) Working Party on Manufactured Nanomaterials (WPMN) has demarcated CeO_2 nanoparticles along with fourteen other nanoparticles as a high-priority for evaluation [136]. Given current industrial applications, it is thought that the most common route of CeO_2 exposure is likely to be through inhalation and/or ingestion. Although previous studies have shown that intratracheal instillation of CeO_2 nanoparticles can cause a toxicological response in the lung, whether these particles also exhibit systemic toxicity is currently unclear [7, 17]. The purpose, therefore, of the current study was to determine if the intratracheal instillation of CeO_2 nanoparticles is associated with indices of systemic toxicity and pathological change. On the basis of previous work examining the translocation of carbon nanotubes from the lung [137], we hypothesized

that intratracheal instillation of CeO_2 nanoparticles may be associated with nanoparticle deposition in other organs through the circulation. Consistent with this hypothesis, our data suggest that the intratracheal instillation of CeO_2 nanoparticles is associated with increased liver ceria levels, reductions in liver weight and evidence of liver damage.

Materials and Methods

Particle characterization

CeO$_2$ nanoparticles, 10 wt % in water (average diameter at ~20 nm), were obtained from Sigma-Aldrich (St Louis, MO, USA) as previously outlined [13]. Normal saline was used as vehicle to suspend the nanoparticles prior to instillation. Diluted particle suspensions were also filtered, sputter coated, and examined with a Hitachi Model S-4800 Field Emission scanning electron microscope (Schaumburg, IL, USA) at 5 and 20 kV or placed on a formvar-coated copper grid to dry and imaged with a JEOL 1220 transmission electron microscope (Tokyo, Japan).

Animal handling and instillation of CeO_2 nanoparticles

Specific pathogen-free male Sprague-Dawley (Hla: SD-CVF) rats (6 weeks old) were purchased from Hilltop Laboratories (Scottdale, PA, USA). Rats were kept in cages individually and ventilated with HEPA filtered air in an animal facility accredited by the Association for Assessment and Accreditation of Laboratory Animal Care International. After acclimatization for 1 week, rats were randomly divided into four groups (n=7 per group): vehicle control (saline,

0.9% NaCl), or instillation with 1.0, 3.5, or 7.0 mg/kg CeO_2 nanoparticles. Rats were anesthetized and placed on an inclined restraint board before instillation with 0.3 ml of saline suspension or CeO_2 nanoparticles. Animals were euthanized 28 days post-exposure by drug overdose using the combination of xylazine and ketamine according to the Guide for the Care and Use of Laboratory Animals and as approved by the National Institute for Occupational Safety and Health Animal Care and Use Committee. All animals were humanely treated and were monitored for any potential suffering.

Determination of cerium content in the liver

Liver cerium content was estimated by Induction Coupled Plasma-Mass Spectrometry (ICP-MS) at Elemental Analysis Inc. (Lexington, KY, USA) according to standard protocol [137]. Briefly, liver samples (n=4 for each group) were prepared using EPA Method 3050B for the analysis of total Cerium by ICP-MS. A 2.5 g sample was weighed to the nearest 0.0001g and digested with concentrated nitric acid, 30% hydrogen peroxide, and concentrated hydrochloric acid. A method blank, laboratory control sample, a laboratory duplicate, and a pre-digestion matrix spike were prepared for each sample. After digestion, the extracts and the quality control samples were diluted to a final volume of 50 mL before analysis using an Agilent 7500cx ICP-MS. The instrument was calibrated for Ce-140 with 0, 0.1, 1.0, 10.0, and 100 µg/L standards prepared from a certified reference standard traceable to NIST reference materials. A second source calibration verification standard traceable to NIST reference materials was analyzed to verify the calibration standards. A continuing calibration verification standard and a continuing

calibration blank were analyzed at the beginning of the run, after every ten samples, and at the conclusion of the run.

Serum biochemical and lipid profile analysis

Blood was collected from the euthanized animals by cardiac puncture into a serum collection tube (BD Vacutainer® SST™ Tubes; #367986) before centrifugation at 800 x g for 15 minutes. Serum was collected and used for biochemical assays using Abaxis VetScan® analyzer (Abaxis, Union City, CA, USA). Serum biochemical parameters: alanine aminotransferase (ALT), alkaline phosphatase (ALP), bilirubin, blood urea nitrogen (BUN), albumin (ALB), calcium (Ca^{+2}), creatinine (CRE), amylase (AMY), globulin (GLOB), potassium (K^+), sodium (Na^+), phosphorous (PHOS), total bilirubin (TBIL) and total protein were evaluated with a Comprehensive Diagnostic Profile Disk. The lipid profile: total cholesterol, triglycerides and HDL were measured using lipid profile-Glu cassettes (Cholestech LDX) and a Cholestech LDX® analyzer. The remaining serum was stored at -80 °C.

Multiplexed serum protein immunoassays

Pooled serum samples from all 7 animals in each experimental group were shipped on dry ice to Rules Based Medicine (Austin, Texas) for RodentMAP® version 2.0 Antigen analysis using a Luminex 100 instrument as detailed elsewhere [137]. The antigen panel consisted of fifty-nine proteins, which included proteins involved in inflammation, cytokines, growth factors and tissue factors. Each analyte was quantified using 4 and 5 parameter, weighted and non-

weighted curve fitting algorithms using proprietary data analysis software developed at Rules-Based Medicine.

Tissue collection

Liver, kidney, spleen and heart were collected at the time of death. Each tissue was weighed and then fixed in FineFIX™ (Milestone Medicals, Shelton, Connecticut) preservative for later histopathological examination.

Histopathological examination

Tissues from liver, spleen, kidney and heart were embedded in paraffin wax, sectioned at 5-µm, mounted on glass slide and stained with hematoxylin-eosin using standard histopathological techniques. Sections were examined by light microscopy in a blinded fashion by a board certified pathologist.

Data Analysis

Results are presented as mean ± SEM. Data were analyzed using the SigmaPlot 11.0 statistical program. One-way analysis of variance was performed for overall comparisons, while the Student–Newman–Keuls post hoc test used to determine differences between groups [17]. Values of $P<0.05$ were considered to be statistically significant.

Results

Nanoparticle characterization

Similar to previous work using the same batch of CeO_2 nanoparticles [13], analysis of nanoparticle size by TEM and SEM confirmed the presence of single and agglomerated CeO_2 nanoparticles in the suspensions.

CeO_2 instillation decreases liver wet weight

CeO_2 instillation had no significant effect on rat body, heart, kidney, or spleen weight. Compared to control animals, CeO_2 instillation decreased liver weight (Saline control 14.55 ± 0.27 vs. CeO_2 7.0 mg/kg 12.50 ± 0.54; *P< 0.05*, Table 3).

CeO_2 instillation increases liver ceria content

The ceria content of animals instilled with 7.0 mg/kg CeO_2 nanoparticles was higher than that observed in the other groups (Saline control: non-detectable vs. 1.0 mg/kg CeO_2 0.05 ± 0.01 ppm vs. 3.5 mg/kg CeO_2 0.11 ± 0.02 ppm vs. CeO_2 7.0 mg/kg: 0.50 ± 0.18 ppm; *P< 0.05;* Figure 3.14).

Effect of CeO_2 instillation on serum biochemical profile

Table 4 shows the alterations of the serum biochemical parameters following CeO_2 nanoparticle exposure. Compared to control animals, CeO_2 instillation increased serum ALT levels, reduced albumin levels and diminished the sodium-potassium ratio. The serum lipid

profile analysis (Table 4b) indicated a reduction in the triglyceride levels with CeO_2 nanoparticle exposure.

CeO_2 nanoparticle exposure is associated with evidence of liver pathology

The primary alterations considered for liver tissue damage were hydropic degeneration of the hepatocytes, dilation of the sinusoids, portal inflammation and fibrosis of the liver. Alterations considered for the kidney pathologies were necrosis of the proximal tubular epithelium, tubular accommodation of proteinaceous material, and inflammatory reaction in the interstitial areas of the cortex and medulla. For the spleen and heart tissues were examined for any histological alterations in structure along with the infiltration of inflammatory cells.

CeO_2 nanoparticle exposure showed wide spread hydropic degeneration of the hepatocytes around the central vein region with sparing of the immediate peri-portal region when compared with the controls (Figure 3.15). These changes were pan-lobular in nature. Along with hydropic degeneration, we also observed enlargement of the hepatocytes, enlargement of the nucleus in the hepatocyte, binucleation of some hepatocytes, dilatation of the sinusoids, and occasional focal necrosis areas in few of the exposed animals. As the dose of the nanoparticles was increased, the number of hepatocytes that show hydropic degeneration was also elevated suggesting that changes in hepatocyte structure were dose dependent. There was no evidence of granuloma, portal inflammation, fibrosis, or bile duct abnormalities except for the presence of some local inflammation of the lobules in some animals. We did not observe any alterations in the histological appearance or the infiltration of inflammatory cells in the heart, kidney and spleen with CeO_2 nanoparticle exposure.

Effect of CeO$_2$ instillation on serum protein expression

A panel of 59 protein biomarkers comprising cytokines, inflammatory markers, growth factors, and tissue factors were quantified in the serum samples collected in this study using the RBM RodentMAP$^®$ V2.0 multiplex immune assay service. Only the biomarkers which showed alterations in the serum protein biomarkers with the different experimental doses are depicted in Figure 3.16; Panels a, b, c). Among the 59 analytes, 20 analytes showed consistent changes across all the experimental groups. Among these 20 analytes, 8 analytes were up-regulated for CeO$_2$ 1.0 mg/kg dose group, 9 analytes were down regulated and 3 analytes did not change. For the 3.5 mg/kg CeO$_2$ dose group, 12 analytes were up regulated, 7 were down regulated and 1 did not change. Similarly, for the 7.0 mg/ kg CeO$_2$ exposure, 17 analytes were up regulated, while 3 analytes were down regulated. Analytes that were elevated in all the experimental groups include: C-reactive protein, eotaxin, fibroblast growth factor-basic, haptoglobin, immunoglobulin-A, matrix metalloproteinase-9, serum amyloid-protein, serum glutamic oxaloacetic transaminase (SGOT) and thrombopoietin (TPO), vascular endothelial growth factor-A (VEGF-A) and von Willebrands's factor (vWF).

Discussion

Investigation of the effects that nanomaterials may have on cellular function is essential for ensuring that the utilization of these materials in industrial or medical applications is safe. Although CeO_2 nanoparticles have demonstrated excellent potential for biomedical use [10], [11],[12] limited knowledge exists concerning potential systemic toxicity. The primary finding of this investigation was that the intratracheal instillation of CeO_2 nanoparticles results in increased liver ceria levels (Figure 3.14) and that these changes in liver ceria are associated with evidence of liver pathology (Figure 3.15), decreases in liver weight (Table 3) and alterations in blood chemistry (Table 4). Consistent with other reports examining CeO_2 [113], titanium dioxide [138], silica [139] and copper [140] nanoparticles, our data suggest that it is possible that CeO_2 nanoparticles are capable of translocating from the lung to the liver via the circulation.

The histopathological appearance of the liver following CeO_2 nanoparticle instillation is consistent with the possibility that ceria can induce several different pathological alterations including hydropic degeneration of the hepatocytes, enlargement of the hepatocytes, dilatation of the sinusoids and nuclear enlargement (Figure 3.15). As liver is the major organ for biotransformation of the toxins, it may be the first organ to be exposed to nanoparticles that are able to enter into the circulation. It is thought that hydropic degeneration can be caused by hypoxia [141], ischemia [142] or the treatment of hepatocytes with endotoxins [143] or chemicals [144]. Consistent with our findings, this response has also been observed following exposure to other toxic materials including copper nanoparticles [145] and carbon tetrachloride [146] or following the inhalation of anesthetics such as sevofulrane and desflurane [147]. How exposure to CeO_2 nanoparticles may induce hydropic degeneration or if these changes are

reversible is currently unclear. Sinusoidal dilatation is the increased gap between the hepatic cords in the hepatic lobule. Sinusoidal dilatation is a pathological change that has also been observed in aluminum-induced hepatic toxicity [148], carbon tetrachloride-induced hepatic toxicity [149], ischemia [150], as well as with the organophosphate insecticide mathidathion [151]. In addition, we also noted the accumulation of granular material inside the hepatocytes which appeared to be dose-dependent and perhaps related to the reduction of liver weight (Table 3). The molecular mechanism(s) responsible for this accumulation are unknown and will require further investigation.

To complement our study of liver histopathology we also investigated the effects that ceria might have on blood chemistry. Our data suggest that CeO_2 nanoparticle instillation in the rat is associated with an elevation of ALT and reductions in albumin (Table 4). It is well established that hepatocyte damage is associated with the release of liver enzymes into the circulation and reduced albumin levels [148]. In addition to changes in the level of circulating liver enzymes, CeO_2 nanoparticle instillation also appears to decrease the sodium-potassium ratio and the amount of triglycerides (Table 4). Whether alterations in the sodium-potassium ratio or triglyceride levels can be directly attributed solely to changes in liver, kidney or adrenal function or some combination thereof is currently unclear however it is interesting to note that these changes appear to occur coincident with decreases in liver weight.

To identify potential serum biomarkers following CeO_2 nanoparticle exposure, we examined 59 different analytes. Of the analytes studied, 20 biomarkers showed changes across all the groups. This may indicate that inhaled exposure to CeO_2 nanoparticles may trigger the concurrent activation of several biochemical pathways. Similar to other work examining other

types of nanoparticles [152, 153], we observed elevations in the amount of C-reactive protein (10%), haptoglobin (16%), serum amyloid-p protein (24%) and von Willebrand's factor (33%) following exposure to the CeO_2 nanoparticles. Consistent with our histopathological findings, and the possibility of hepatic injury, we also found evidence that CeO_2 nanoparticle instillation was associated with increases in the amount of serum thrombopoietin, fibroblast growth factor, SGOT and TPO (Figure 3.16). Elevation in these serum biomarkers is thought to be highly correlated with acute hepatic damage [144],[154]. Taken together, these data suggest that ceria deposition may be associated with liver damage. Given our findings that CeO_2 nanoparticle instillation, at least at the levels used in the current study, does not induce appreciable damage to the heart, kidney or spleen, it is possible that the liver, by acting to clear CeO_2 nanoparticles from the circulation, is functioning to prevent additional secondary or tertiary toxicological pathophysiology.

Conclusion

In summary, our data suggest that intratracheal instillation of CeO_2 nanoparticles can induce hepatotoxicity resulting in the potential loss of hepatic mass and function. The toxicity induced by the CeO_2 nanoparticles appear to be dose-dependent and the rats exposed with the 7.0 mg/kg body weight of the CeO_2 nanoparticles showed maximal toxic response when compared with other dosage groups. The toxicological response appears to be limited to the liver and may occur through extra pulmonary translocation of the CeO_2 nanoparticles into the systemic circulation. Given these findings, additional research to evaluate the health effects of CeO_2 nanoparticles is likely warranted.

Acknowledgments

Disclaimer

The findings and conclusions in this report have not been formally disseminated by the NIOSH and should not be construed to represent any agency determination or policy.

Table 3: Alterations in the absolute organ wet weight 28 days after the intratracheal instillation of cerium oxide nanoparticles. * Indicates significantly different from the vehicle control (p <0.05)

Organ weight (g)	Saline Control (n=7)	CeO₂ 1.0 mg/kg (n=7)	CeO₂ 3.5 mg/kg (n=7)	CeO₂ 7.0 mg/kg (n=7)
Heart (g)	1.52±0.15	1.35±0.05	1.27±0.07	1.23±0.05
Liver (g)	14.55±0.27	14.30±1.04	14.78±0.57	12.50±0.54*
Kidney (g)	2.67±0.31	2.55±0.21	2.54±0.33	2.43±0.31
Spleen (g)	0.58±0.06	0.65±0.10	0.56±0.08	0.64±0.04

Table 4: Changes in the serum biochemical parameters (a) and lipid profile (b) 28 days after the intratracheal instillation of cerium oxide nanoparticles. * Indicates significantly different from the vehicle control (P<0.05).

a

Analyte	Saline Control (N=7)	CeO$_2$ 1.0mg/kg (N=7)	CeO$_2$ 3.5mg/kg (N=7)	CeO$_2$ 7.0mg/kg (N=7)
Glucose (mg/dL)	186.4±9.7	208±16.3	197.6±15.2	231±35.4
ALP (U/L)	276.1±20.3	263±21.0	242±13.3	222.23±31.0
ALT (U/L)	58.3±4.0	83.4±10.8	88.3±11.9	130.5±38.6*
Amylase (U/L)	974.7±37.0	1055.1±47.0	991.4±44.0	908.4±105.0
Total Protein (g/dL)	6.0±0.1	5.9±0.2	6.2±0.2	5.4±0.5
Albumin (g/dL)	4.2±0.06	4.1±0.2	4.2±0.2	3.5±0.43*
Globulin (g/dL)	1.8±0.1	1.8±0.1	2.0±0.1	1.8±0.1
ALB-GLOB Ratio	2.3±0.1	2.3±0.1	2.2±0.1	1.9±0.2
BUN (mg/dL)	15.4±0.4	15±1.2	15.7±0.7	14.4±1.6
Creatinine (mg/dL)	0.3±0.03	0.27±0.02	0.23±0.02	0.28±0.03
Ca^{2+} (mg/dL)	11.4±0.2	10.7±0.5	11.5±0.4	10.4±0.9
Phosphorus (mg/dL)	8.6±0.4	7.9±0.5	8.7±0.4	8.2±0.7
Na$^+$ (mmo/L)	142.3±0.4	138±4.0	138.1±4.0	132.1±6.1
K$^+$ (mmo/L)	5.5±0.2	6.0±0.2	6.5±0.2	5.8±0.4
Na$^+$ - K$^+$ Ratio	25.8±0.8	22.9±0.6*	21.2±0.6*	22.8±2.5*

b

Analyte	Saline Control (N=7)	CeO$_2$ 1.0mg/kg (N=7)	CeO$_2$ 3.5mg/kg (N=7)	CeO$_2$ 7.0mg/kg (N=7)
Total Cholesterol (mg/dL)	100.7±1.9	100±0	100±0	103.1±8.3
Triglycerides (mg/dL)	143±25.5	109.6±7.0	190.3±55.0	93.1±16.3*
HDL (mg/dL)	21±1.0	19.4±3.8	20±5.5	19±3.7

Figure 3-14: Concentration of cerium in the liver following intratracheal instillation of cerium oxide nanoparticles * Indicates significantly different from the vehicle control (P<0.05).
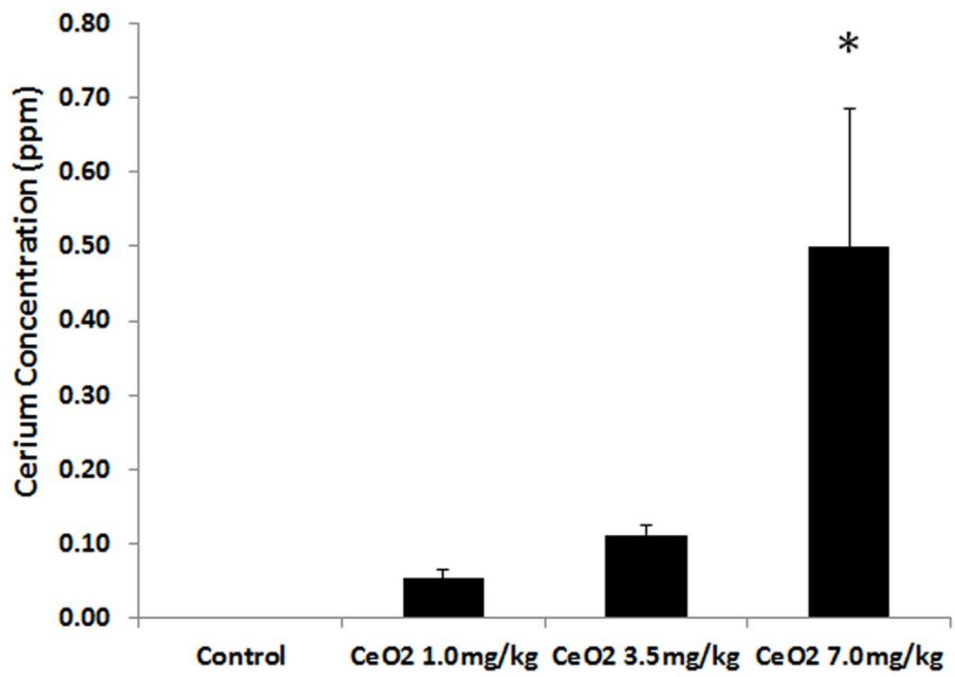
Figure 3-15: Cerium oxide nanoparticle exposure alters histopathological architecture of the liver. Panel a: saline control (400X), b: CeO$_2$ at 1.0 mg/kg (400X), c: CeO$_2$ 3.5 mg/kg (400X) and d: CeO$_2$ 7.0 mg/kg (400X). Note evidence of hydropic degeneration (arrow) with CeO$_2$ instillation.
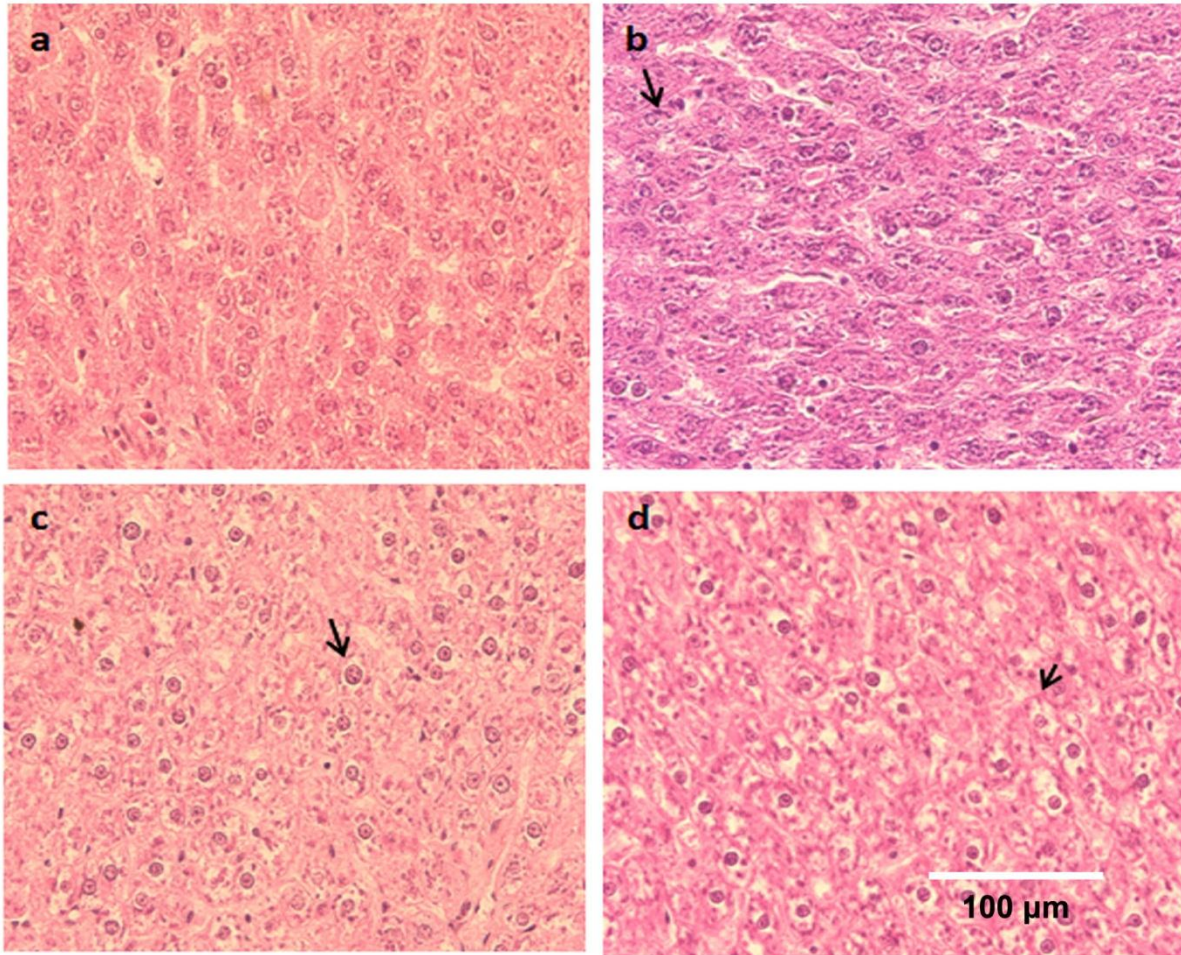
a. Saline Control
b. CeO$_2$ 1.0mg/kg

c. CeO$_2$ 3.5mg/kg
d. CeO$_2$ 7.0mg/kg

Arrow: Hydropic degeneration (400X)

Figure 3-16: Cerium oxide nanoparticles exposure results in alterations in the expression of serum protein biomarkers.
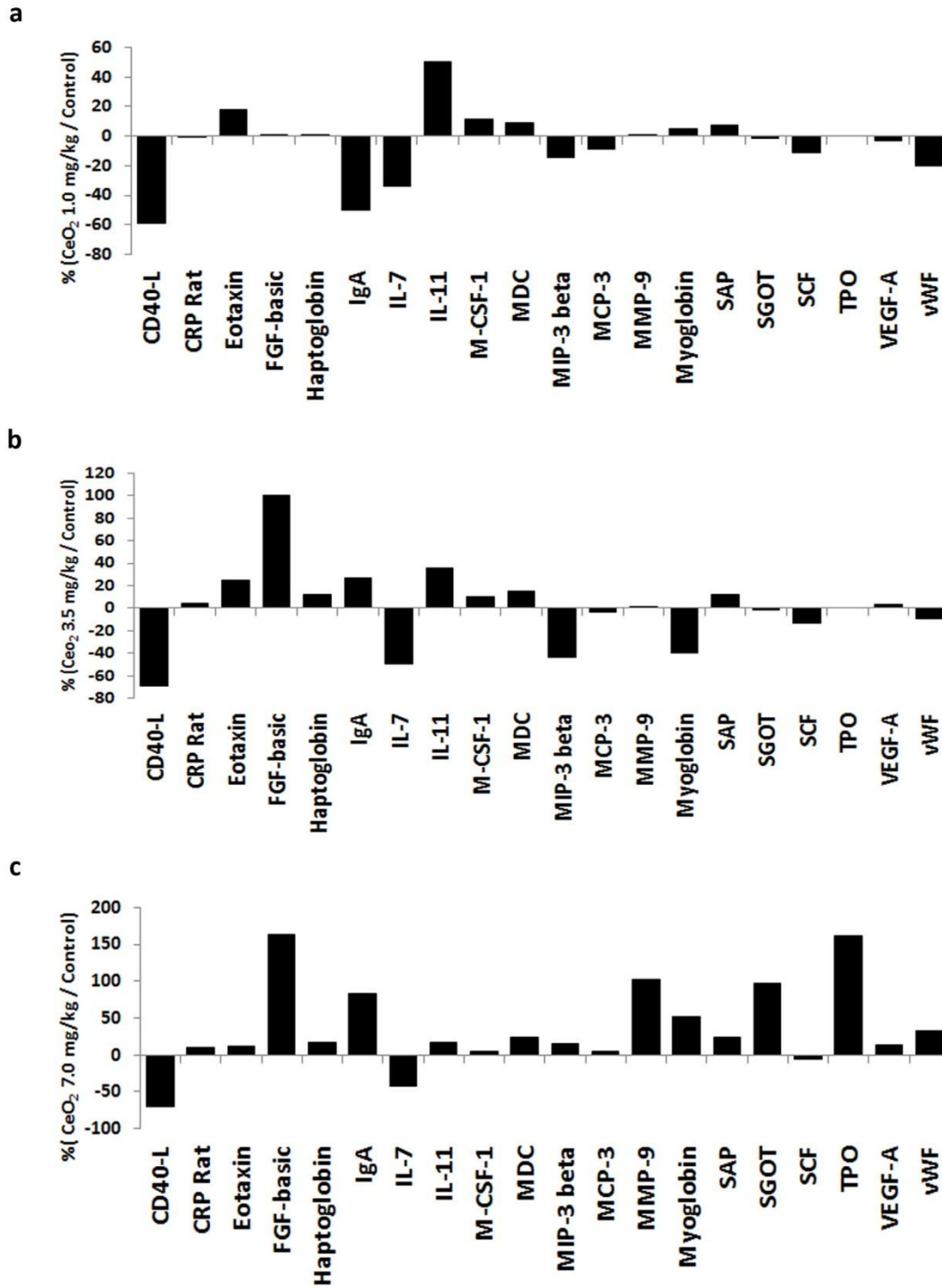
Paper-III

Specific Aim-3: To investigate the role of oxidative stress and apoptosis in the hepatic toxicity

induced by CeO2 nanoparticles following intratracheal instillation

Role of Oxidative Stress and Apoptosis in the Hepatic Toxicity induced by Cerium Oxide Nanoparticles Following Intratracheal Instillation in Male Sprague-Dawley Rats

Abstract

Inhaled cerium oxide (CeO_2) nanoparticles have been shown to be capable of translocation to the liver where they can cause dose dependent toxic effects [121]. Herein, we investigate if the deposition of ceria in the liver is associated with increased oxidative stress and cellular apoptosis. Specific pathogen free male Sprague-Dawley rats were instilled with either vehicle (saline) or CeO_2 nanoparticles (7.0 mg/kg) and euthanized 1, 3, 14, 28, 56, or 90 days post exposure. Liver samples were evaluated for evidence of ceria deposition, oxidative stress and apoptosis. Inductively coupled plasma mass spectroscopy demonstrated that ceria deposition increased over time. Analysis of lipid peroxidation, superoxide levels and number of TUNEL positive cells revealed evidence of increased oxidative stress and apoptosis at 1, 3, and 90 days post exposure. Immunoblotting showed that each of these time points was characterized by increases in the Bax/Bcl-2 ratio, elevations in caspase-9 protein levels and increased caspase-3 protein expression. Interestingly, we found no evidence of oxidative stress or apoptosis at day 14, 28, or 56 post-exposure. Taken together, these data demonstrate that the intratracheal instillation of CeO_2 nanoparticles is associated with increased liver ceria deposition and that this deposition causes a biphasic oxidative stress and apoptotic response.

Introduction

CeO$_2$ nanoparticles have been used as catalysts to increase fuel efficiency of automobile engines and to reduce particulate emissions from the incomplete combustion of fuels [25]. Recent data has also suggested that CeO$_2$ nanoparticles may also have biomedical use as potential scavengers of reactive oxygen species (ROS) to protect against cardiomyopathy [10], neuronal toxicity [11] and radiation damage [12]. Whether CeO$_2$ nanoparticles may exhibit toxic effects is not well understood. *In vitro* studies using the human bronchoalveolar carcinoma cell line (A549) and lung epithelial cell lines (BEAS2B) has demonstrated that CeO$_2$ nanoparticles (20nm) can reduce cell viability and induce oxidative stress [15]. *In vivo* studies using male Sprague-Dawley rats has shown that the intratracheal instillation of CeO$_2$ nanoparticles (20nm) can cause oxidative stress and apoptosis in pulmonary tissues [17]. Using this same model, Nalabotu and colleagues have shown that intratracheally instilled CeO$_2$ nanoparticles can travel from the lungs and cause liver toxicity in a dose-dependent fashion [121].

Similarly, other work has shown that inhaled nanoparticles such as silver, silica, copper, gold, TiO$_2$ and Zinc oxide nanoparticles can enter into the circulation and cause and apoptosis in the liver [116, 117, 155, 156]. It is thought that nanoparticle exposure is associated with increased production of ROS [53]. ROS generation is linked to membrane damage and cellular apoptosis and is also known to activate the mitogen activated protein kinase (MAPK) pathways which are important mediators of cell survival, differentiation and apoptosis [157]. Whether the intratracheal instillation of CeO$_2$ nanoparticles can cause increased oxidative stress and apoptosis in the liver is currently unclear.

The purpose of this investigation was to evaluate if the hepatic toxicity induced by CeO_2 nanoparticles is associated with activation of oxidative stress and apoptotic protein signaling in the liver. We hypothesized that bioaccumulation of cerium in the liver will be associated with generation of ROS that will cause damage to cells and that the oxidative stress induced by CeO_2 nanoparticles will activate apoptotic protein signaling in the liver. Taken together, our data suggest that intratracheal instillation of CeO_2 nanoparticles is associated with accumulation of cerium in the liver and the cerium can cause biphasic oxidative stress and apoptotic response in the liver.

Materials and Methods

Particle characterization

CeO_2 nanoparticles, 10 wt % in water (average diameter at ~20 nm), were obtained from Sigma-Aldrich (St Louis, MO, USA) as previously outlined [17]. Normal saline was used as vehicle to suspend the nanoparticles prior to instillation. Diluted particle suspensions were filtered, sputter coated, and examined with a Hitachi Model S-4800 Field Emission scanning electron microscope (Schaumburg, IL, USA) at 5 and 20 kV or placed on a formvar-coated copper grid to dry and imaged with a JEOL 1220 transmission electron microscope (Tokyo, Japan).

Animal handling, CeO_2 nanoparticles instillation and tissue collection

All procedures were performed in accordance with the Marshall University Animal Care and Use Committee guidelines, using the criteria outlined by the Assessment and Accreditation

of Laboratory Animal Care (AAALAC). Five week old (150-174 g) Specific pathogen-free male Sprague-Dawley (Hla: SD-CVF) rats were purchased from Hilltop Lab Animals, Inc. (Scottdale, PA, USA). Rats were housed two per cage in an AAALAC approved vivarium with a 12-h light–dark cycle. Housing temperature was maintained at 22 ± 2° C and the animals were given access to food and water *ad libitum*. All animals were allowed to acclimatize for 2 weeks before initiation of any treatment or procedures. All animals were examined for precipitous weight loss, failure to thrive or unexpected gait. Periodic weight measurements were taken throughout the duration of the study. After acclimatization, animals were divided randomly into 12 groups (n=6 per group). Animals underwent instillation with 0.3 ml of saline suspension or saline suspension containing CeO_2 nanoparticles as described previously [17]. Rats were euthanized with a combination of xylazine and ketamine and livers were collected at 1, 3, 14, 28, 56 or 90 days post exposure to either the CeO_2 nanoparticles or normal saline. After removal from the animals, livers were cleaned of blood and connective tissues, weighed, and immediately snap frozen in liquid nitrogen.

Determination of cerium content in the liver

Liver cerium content was estimated for the 1, 28, 56, and 90 day animals by induction coupled plasma-mass spectrometry (ICP-MS) at Elemental Analysis Inc. (Lexington, KY, USA) using EPA Method 3050B using methods identical to that detailed previously[158]. All Ce-140 calibration standards were prepared using a certified reference standard traceable to NIST reference materials. A continuing calibration verification standard and a continuing calibration

blank were analyzed at the beginning of the run, after every ten samples, and at the conclusion of the run.

Transmission electron microscopy (TEM)

Liver slices from 90 days control and 90 days post exposure are fixed in Karnovsky's fixative (2.5% glutaraldehyde, 3.5% paraformaldehyde in 0.1 M Sodium Cacodylate buffer), then embedded in 4% agarose and refixed for 2 h. The samples were post-fixed in 1% osmium tetroxide (120 min at 4°C), mordanted in 1% tannic acid (pH 7.0) and block stained in 0.5% uranyl acetate (both at room temperature for 60 minutes) all in a buffer of 8%sucrose and 0.9% sodium chloride. When the staining was complete, the solution was changed to 70% ethyl alcohol and then 90%, samples were then rinsed twice with 100% ethyl alcohol for 15 min each. Then placed into a solution of 1:1 100% ethyl alcohol to propylene oxide for 15 min, and finally into 100% propylene oxide changing the solution twice. The sample solution was replaced with a 1:1 of propylene oxide and LX112 embedding media, followed by a 3:1 solution for 30 min, and then finally into 100% solution of LX112 overnight on a rotating platform. This solution was changed again for an additional 4 h, then placed into embedding molds and placed into a 60°C oven for 48 h. Thick (0.5 μm) sections were cut and stained with a 1% toluidine blue (in 1% sodium borate) solution on a hot plate for 90 sec. Thin sections (70 nm) were placed on 200 mesh copper grids and stained with 4% aqueous uranyl acetate and Reynold's lead citrate for 15 and 20 min, respectively. Images were taken on a JEOL 1220 transmission electron microscope at 80 kV.

Lipid peroxidation assay

Lipid peroxidation assays were performed on liver tissues removed from the 1, 3, 14, 28, 56 and day 90 exposure animals and compared with the saline controls from each group. Briefly, individual liver pieces (200 mg) were homogenized in 1 ml phosphate buffered saline and the homogenizer probe then rinsed with an additional 1ml of PBS. Lipid peroxidation was measured as described previously [159]. The amount of malondialdehyde (MDA) was calculated based on a standard curve (range 1–40 nmol) using MDA (Aldrich, St. Louis, MO) and expressed as nmol MDA/g liver tissue.

Dihydroethidium staining

Liver tissues were serially sectioned (8 μm) using an IEC Microtome cryostat and the sections were collected on poly-lysine coated slides. The fluorescent superoxide indicator dihydroethidium (HE) was used to evaluate superoxide levels as detailed previously [98]. Upon oxidation, dihydroethidium intercalates with DNA exhibiting a bright fluorescent red. Briefly, frozen tissue sections were washed with phosphate-buffered saline (PBS) for 5 min and then incubated with 200 μl of 10 μM dihydroethidium (Molecular Probes, Eugene, OR, USA) for 1 h at room temperature. After washing with PBS (3 X 10 min), fluorescence was visualized under Texas red filter using an Olympus BX51 microscope (Olympus America, Melville, NY, USA) equipped with Olympus WH 209 wide field eyepieces and an Olympus UPlanF1 409/0.75 objective lens.

TUNEL staining

Liver tissues were serially sectioned (8 μm) using an IEC Microtome cryostat and the sections were collected on poly-lysine coated slides. DNA fragmentation was determined by TdT-mediated dUTP nick end labeling (TUNEL) according to the manufacturer's recommendations (In Situ Cell Death Detection Kit, Roche Diagnostics, Mannheim, Germany). TUNEL staining was performed on tissue sections obtained from saline controls and the day 1, 3, and 90 CeO_2 nanoparticle exposure groups (n=4/group) as described elsewhere [98]. Cross-sections from each tissue were treated with DNase-I to induce DNA fragmentation as a positive control. Liver sections were blocked with 3% BSA and incubated with anti-dystrophin antibody (NCL-DYS2, Novocastra Vector Laboratories, Burlingame, CA, USA) at a dilution of 1:200 to visualize the cell membrane. Nuclei were counter stained using DAPI (Vectashield HardSet Mounting Medium, Vector Laboratories, Burlingame, CA, USA). Liver cross sections were visualized by epifluorescence using an Olympus fluorescence microscope (Melville, NY, USA) fitted with 20X and 40X objectives and the images recorded digitally using a CCD camera (Olympus, Melville, NY, USA). The number of TUNEL positive nuclei was counted in three randomly selected regions in each slide. Four different animals were counted from each group.

Immunoblotting analysis

Portions of individual liver tissues (100-150mg) were homogenized in buffer (T-PER, 8 mL/g tissue; Pierce, Rockford, IL, USA) containing protease (P8340, Sigma-Aldrich, Inc., St. Louis, MO, USA) and phosphatase inhibitors (P5726, Sigma-Aldrich, Inc., St. Louis, MO, USA) and sonicated (3 x 30 sec at 150W). The supernatant protein was collected by centrifuging the

tissue homogenate at 12,000g for 5 minutes at 4°C. Protein concentration of homogenates was determined via the 660nm assay method (Fisher Scientific, Rockford, IL, USA). After boiling in Laemmli 2X sample buffer (Sigma-Aldrich, Inc., St. Louis, MO, USA) for 5 min, 32μg of total protein for each sample was separated on a 10% PAGEr Gold Precast gel (Lonza, Rockland, ME, USA) and then transferred to nitrocellulose membranes. Gels were stained with a RAPID Stain protein stain reagent (G-Biosciences, St. Louis, MO, USA) to verify transfer efficiency to membrane. Membranes were stained with Ponceau S and the amount of protein quantified by densitometric analysis to confirm successful transfer of proteins and equal loading of lanes as detailed somewhere else [120]. Membranes were blocked with 5% milk in Tris Buffered Saline (TBS) containing 0.05% Tween-20 (TBST) for 1 h and then incubated with primary antibody overnight at 4°C. After washing with TBST, the membranes were incubated with the corresponding secondary antibodies conjugated with horseradish peroxidase (HRP) (anti-rabbit (#7074) or anti-mouse (#7076), (Cell Signaling Technology, Danvers, MA, USA) for 1 h at room temperature. Protein bands were visualized following reaction with ECL reagent (Amersham ECL Western Blotting reagent RPN 2106, GE Healthcare Bio-Sciences Corp., Piscataway, NJ, USA). Target protein levels were quantified by AlphaView image analysis software (Alpha Innotech, San Leandro, CA, USA). Protein levels were normalized with the corresponding GAPDH protein level and expressed as increased expression when compared with the controls. Primary antibodies against caspase-3 (#9662), cleaved caspase-3 (#9661S), Bax (#2772), Bcl-2 (#2870S), caspase-9 (#9506), nuclear factor-kappa β p65 (#3034) , Phosho NF-kβ P65 (Ser536 # 3033), p38 MAPK (#9212), Phospho p38 MAPK (Thr180/Tyr182) (#9216L) were purchased from Cell Signaling Technology (Beverly, MA, USA).

Multiplexed serum protein immunoassays

Pooled serum samples from all six animals in the 1-, 3-, 28-, 56- and 90-day experimental groups were shipped on dry ice to Rules Based Medicine (Austin, Texas) for Rodent MAP® version 2.0 Antigen analysis using a Luminex 100 instrument as detailed elsewhere [121]. The antigen panel consisted of fifty-nine proteins, which included proteins involved in inflammation, cytokines, growth factors and tissue factors. Each analyte was quantified using 4 and 5 parameter, weighted and non-weighted curve fitting algorithms using proprietary data analysis software developed at Rules-Based Medicine.

Data Analysis

Results are presented as mean ± SEM. Data were analyzed using the Sigma Plot 11.0 statistical program. One-way analysis of variance and two-way analysis of variance were performed for overall comparisons, while the Student–Newman–Keuls *post hoc* test used to determine differences between groups. Values of *P<0.05* were considered to be statistically significant.

Results

Nanoparticle characterization

Similar to previous work [17, 121] which used the same batch of CeO_2 nanoparticles, TEM and scanning electron microscopy confirmed the presence of single and agglomerated CeO_2 nanoparticles in the suspensions. Field emission scanning electron microscopy showed that the CeO_2 nanoparticles were generally dispersed into submicron groups with an average size of 9.26 ± 0.58 nm. The diameter of the primary CeO_2 particles was determined to be 10.14 ± 0.76 nm by TEM.

Effect of CeO_2 nanoparticle exposure on feed intake, body weight gain and liver ceria levels

CeO_2 nanoparticle exposure had no effect on the average food intake or weight gain (Figure 3.17). Compared to saline control animals, CeO_2 nanoparticle exposure did not increase the liver weight to body weight ratio (Table 5). Compared to the day 1 exposure animals, the liver weight to body weight ratio was reduced in the day 3, 28, 56, and 90 day animals (Table 5). The concentration of cerium was undetectable in the saline control animals (Figure 3.18). The concentration of the cerium at day 1 post exposure was 0.03 ± 0.01 ppm and increased thereafter before peaking at 0.20 ± 0.04 ppm at day 90 (P<0.001). However, total cerium content in the liver also appears to increase with the progression of the days of exposure (Data not shown).

Alterations in the ultrastructure of hepatocytes

TEM image of the liver shows that the sub-μm sized nanoparticles are dispersed in the hepatocytes (Figure 3.19 a and b). Alterations observed in the ultrastructure of the liver with 90 days post CeO_2 nanoparticles exposure include reduced fat droplets when compared with the 90 days control animals, increased non-specific deposition of particulate material in the hepatocytes, altered mitochondrial structure and increased number of peroxisomes or lysosomes and splitting of endoplasmic reticulum.

CeO_2 nanoparticle exposure is associated with lipid peroxidation, elevations in hepatic superoxide levels and evidence of hepatic apoptosis.

Compared to age matched control animals, the concentration of MDA per gram of the liver tissue was elevated by 25%, 31%, and 20% at day 1, 3, and 90, respectively ($P < 0.05$) (Figure 3.20). Similarly, compared to control animals, dihydroethidium fluorescence intensity was increased by 122%, 145%, and 96% at days 1, 3, and 90, respectively ($P < 0.05$) (Figure 3.21). Compared to day 1 saline controls, CeO_2 nanoparticle exposure increased the number of TUNEL positive nuclei by 378%, 351% and 435% at days 1, 3 and day 90 post exposure (Figure 3.22).

Apoptosis induced by CeO_2 nanoparticles is associated with caspase cleavage

Compared to day 1 saline controls, the Bax to Bcl-2 protein ratio was 32% and 10% higher in the day 1 and 3 exposure groups ($P < 0.05$). After day 3, the Bax to Bcl-2 ratio began to

decline and was 55%, 62%, and 47% lower in the day 14, 28 and 56 exposure animals (P<0.05) (Figure 3.23).

Caspases are cysteine-dependent aspartate specific proteases that are activated during cell death. Compared to saline control day 1 animals, caspase-9 protein levels in CeO_2 nanoparticle exposed animals were 25%, 21% and 35% higher at days 1, 3, and 90 exposure, respectively (P<0.05). In a similar fashion, the amount of cleaved caspase-9 (activated) was 29%, 36% and 60% higher in the day 1, 3 and 90 animals, respectively (P<0.05) (Figure 3.24). Compared to saline control day 1, caspase 3 levels were 16% higher in day 1 exposure group (P<0.05). Compared to saline control day1, the amount of cleaved caspase-3 (activated) was 32%, 49% and 13% higher in the day 1, 3 and 90 exposure groups (P<0.05) (Figure 3.25).

CeO_2 nanoparticle exposure affects p38 MAPK and NF-Kβ phosphorylation in the liver

Compared to saline control day1, the ratio of phosphorylated p38 MAPK to total p38 MAPK ratio was reduced by 7%, 16%, and 50% in the day 1, 3, and 90 exposure animals (P<0.05). Conversely, the ratio of phosphorylated p38 MAPK (Thr180/Tyr 182) to total p38 MAPK ratio was elevated by 100%, 65%, and 91% in the day 14, 28 and 56 exposure groups (P<0.05) (Figure 3.26). Similar to p38 MAPK, it is thought that the NF-kβ p65 plays a protective role in the liver [160-162]. Compared to saline control day 1 animals, the ratio of phosphorylated NF-kβ p65 (Ser536) to total NF-kβ p65 protein was reduced by 14%, 5%, and 67% in the day 1, 3, and 90 exposure groups (P<0.05). Compared to saline control day 1

animals, phosphorylated NF-kβ p65 to total NF-kβ p65 protein levels were 26%, 34%, and 18% higher for day 14, 28 and 56 exposure groups (P<0.05) (Figure 3.27).

CeO$_2$ nanoparticle exposure alters serum inflammatory biomarkers

We monitored 55 serum biomarkers that include inflammatory cytokines, interleukins, chemokines, tissue factors and growth factors. Among the 55 parameters, 35 showed changes in the expression across all the groups. Compared to saline control day 1 animals, CeO$_2$ nanoparticle exposure increased the expression of 26 parameters, lowered expression of 8 parameters and failed to change the expression for one parameter (Figure 3.28 a). Compared to saline control day 1 animals, the 3 day exposure group showed an elevation of expression for 8 parameters, lowered expression for 22 parameters and no change in the expression of 5 parameters (Figure 3.28 b). Compared to saline control day 1 animals, animals in the day 28 exposure group showed an elevation of 10 parameters, lowered expression for 19 parameters and no change in the expression of 6 parameters (Figure 3.28 c). Compared to saline control day 1, the day 90 exposure group showed an elevation of 5 parameters, a lowered expression for 24 parameters and no change in the expression for 6 parameters (Figure 3.28 d).

Discussion

Previous investigations examining the toxicity of metallic nanoparticles have demonstrated that the exposure to silver, gold, silica, copper, zinc oxide and TiO$_2$ nanoparticles increases hepatic ROS and cell apoptosis [116, 117, 155, 156]. We found evidence of a similar phenomenon in the liver following the instillation of CeO$_2$ nanoparticles. Specifically, our

primary finding was that the deposition of ceria in the liver is associated with evidence of increased tissue ROS and cellular apoptosis.

One potential marker of increased oxidative stress is lipid peroxidation[163]. Lipid peroxidation is the end product of the oxidative degradation of lipids and can be assessed by the measurement of malondialdehyde (MDA) levels [163]. Here we observed that ceria deposition in the liver was associated with elevations in the amount of liver MDA at 1, 3 and 90 days after exposure (Figure 3.20). Interestingly, there was no evidence of elevated MDA levels at days 14, 28, or 56 of exposure. In addition to MDA levels, we also examined liver tissue sections for the presence of superoxide using dihydroethidium staining (Figure 3.21). Consistent with our MDA data, the HE staining procedure demonstrated that CeO_2 instillation at a dose of 7.0 mg/kg was associated with a robust increase in liver superoxide levels at day 1, 3 and 90 of exposure (Figure 3.22). Taken together, these data demonstrated that CeO_2 nanoparticles can induce the generation of ROS [164, 165] and in addition, that increases in hepatic ROS levels appear to be associated with increased hepatocyte lipid peroxidation. Why MDA and superoxide levels are increased at the early (days 1 and 3) and late (day 90) but not the middle time points is not clear. We suspect that the acute exposure to large dose of nanoparticles seen during the initial phase of the study is associated with the development of a systemic inflammatory response and increased oxidative stress which is then followed by a "remodeling phase". During this remodeling phase, ceria deposition continues in the liver which reaches a maximal level at day 90 (Figure 3.18) at which point the ceria levels may be high enough to initiate a second wave of inflammation and cell death. It is also observed that with the increased deposition of the CeO_2 nanoparticles in the hepatocytes as seen from the TEM

images of the liver, there are increased alterations in the structure of the organelles such as mitochondria and endoplasmic reticulum (Figure 3.19). More research, perhaps using additional time points longer than 90 days post exposure will be needed to mechanistically define the biphasic inflammatory response we observed in the liver.

To evaluate if the oxidative stress at days 1, 3 and 90 exposure groups was associated with the hepatocyte apoptosis, we next performed TUNEL staining to examine hepatocytes for the presence of double stranded DNA breaks. As predicted, our TUNEL analysis was consistent with the possibility of increased liver apoptosis at these time points (Figure 3.22). In an effort to better understand the potential mechanism(s) underlying these findings we next prepared protein isolates from the liver and used immunoblotting to examine the isolates for changes in apoptotic signaling. Immunoblotting was conducted on day 1 control isolates, and protein fractions from animals that had been exposed to the cerium oxide nanoparticles for 1, 3, 14, 28, 56, or 90 days. Our findings suggested that there was increased proapoptotic Bax/Bcl-2 protein signaling at day 1 and 3 post exposure that decreased thereafter. Proapoptotic protein signaling appeared to be diminished at day 14, 28, and 56 post exposure. Interestingly, and consistent with our oxidative stress data, we noted a robust increase in proapoptotic protein signaling in 90 day exposure group when compared to what was observed in the 56 day exposure animals (Figure 3.23).

Given that increases in the ratio of Bax/Bcl-2 can give rise to cellular apoptosis via the activation of intracellular caspases, we next examined our protein isolates for evidence of caspase cleavage. Our data suggested that there were increased levels of active caspase-9 (cleaved caspase-9) at day 1, 3, and day 90 post exposures (Figure 3.24). Conversely, the

expression of active caspase 9 appeared to be declined in the day 14, 28 and 56 exposure animals. Similar to our findings for Bax/Bcl-2 we also noted an increase in the amount of cleaved caspase-9 in the day 90 exposure group (Figure 3.24). To extend these findings, we repeated these experiments and examined if caspase-3 exhibited a similar trend. Like our data for caspase-9, caspase-3 cleavage also appeared to be increased at days 1, 3, and 90 (Figure 3.25). Taken together, these data, when considered in the context of our TUNEL findings, suggest that ceria deposition in the liver is associated with hepatic apoptosis and that these findings may be mediated by increased levels of oxidative stress. Why the apoptotic response appears to be biphasic in nature is not currently clear.

The p38 MAPK and NF-kβ-P65 are thought to play important roles in the protection of the liver from oxidative stress and apoptosis [160, 161, 166, 167]. When phosphorylated, p38 MAPK, and NF-kβ-P65 activate a number of different transcription factors which can then travel to the nucleus to induce changes in gene expression [161, 166]. Phosphorylated p38 MAPK has been shown to be involved in reducing the production of inflammatory factors [162, 168]. In the current study, we found that the ratio of phosphorylated to total p38 MAPK protein level was unaltered at days 1 and 3 post exposure while it was increased at days 14, 28, and 56 post exposure (Figure 3.26). Consistent with these findings, we also found that p38 MAPK activation (phosphorylation) appeared to be significantly reduced in the day 90 exposure group. Like p38 MAPK, the NF-kβ P65 is also thought to play a crucial role in hepatic cell survival and proliferation [160, 161]. Similar to our findings for p38 MAPK, we observed that the ratio of phosphorylated to total NF-kβ P65 protein levels appeared to be reduced in the day 1 and 3 exposure groups, elevated in the day 14, 28, and 56 before becoming significantly reduced in

the day 90 animals (Figure 3.27). Whether these decreases in p38 MAPK and NF-kβ activation can explain the increased susceptibility of the liver to exhibit increased oxidative stress and cellular apoptosis at day 90 post exposure is currently unclear and will require further investigation.

In addition to examining the effects of ceria deposition on the liver we also examined if exposure to CeO_2 nanoparticles elicited changes in proinflammatory cytokines. Our analysis of serum biomarkers suggested that CeO_2 nanoparticle exposure was associated with increased levels of cytokines, tissue factors and growth factors. In particular, our data suggested that ceria deposition in the liver was characterized by elevated acute phase reactant proteins such as fibrinogen, haptoglobin, serum amyloid P-component and Von Willebrand's factor at days 1, 3, 28, 56, and 90 [121, 152] (Figure 3.28). Our analysis of the serum also suggested that inhalation of CeO_2 nanoparticles was also associated with an allergic response. Eotaxin is a chemokine that attracts eosinophils to the site of injury to elicit an inflammatory response [169]. MCP-1, MCP-3, MIP-1 beta and MIP-2 are a group of chemokines that are induced by eotaxin, and have been shown to play a crucial role in the inflammation induced by eosinophils [170-172]. In addition, eotaxin also exhibits the ability to selectively prime eosinophils for chemotaxis, to direct their migration/chemotaxis, and to activate inflammatory activity in the cells attracted [171-173]. Two cell types that are candidates for mediating such an early or initial response are mast cells, a known source of IL-4 and TNF-alpha a finding which is consistent with our observation of increased IL-4 following CeO_2 nanoparticle exposure [171, 173].

Taken together, the data of the current study demonstrate that the exposure to CeO_2 nanoparticles is characterized by acute increases in hepatic oxidative stress, elevations in

hepatic apoptosis, and an eosinophil mediated inflammatory response that declines over time. Interestingly, at day 90 post exposure, oxidative stress and apoptosis once again increases. Although unable to demonstrate cause and effect, the increased oxidative stress and apoptosis at day 90 appears to be correlated with the increased bioaccumulation of cerium in the liver as well as diminished p38 MAPK and NF-kB activation. Further studies may be warranted to determine if exposure to CeO_2 nanoparticles is associated with any long term effects on hepatic structure and function.

Figure 3-17: Intratracheal instillation of CeO_2 nanoparticles does not alter feed intake and body

weight gain
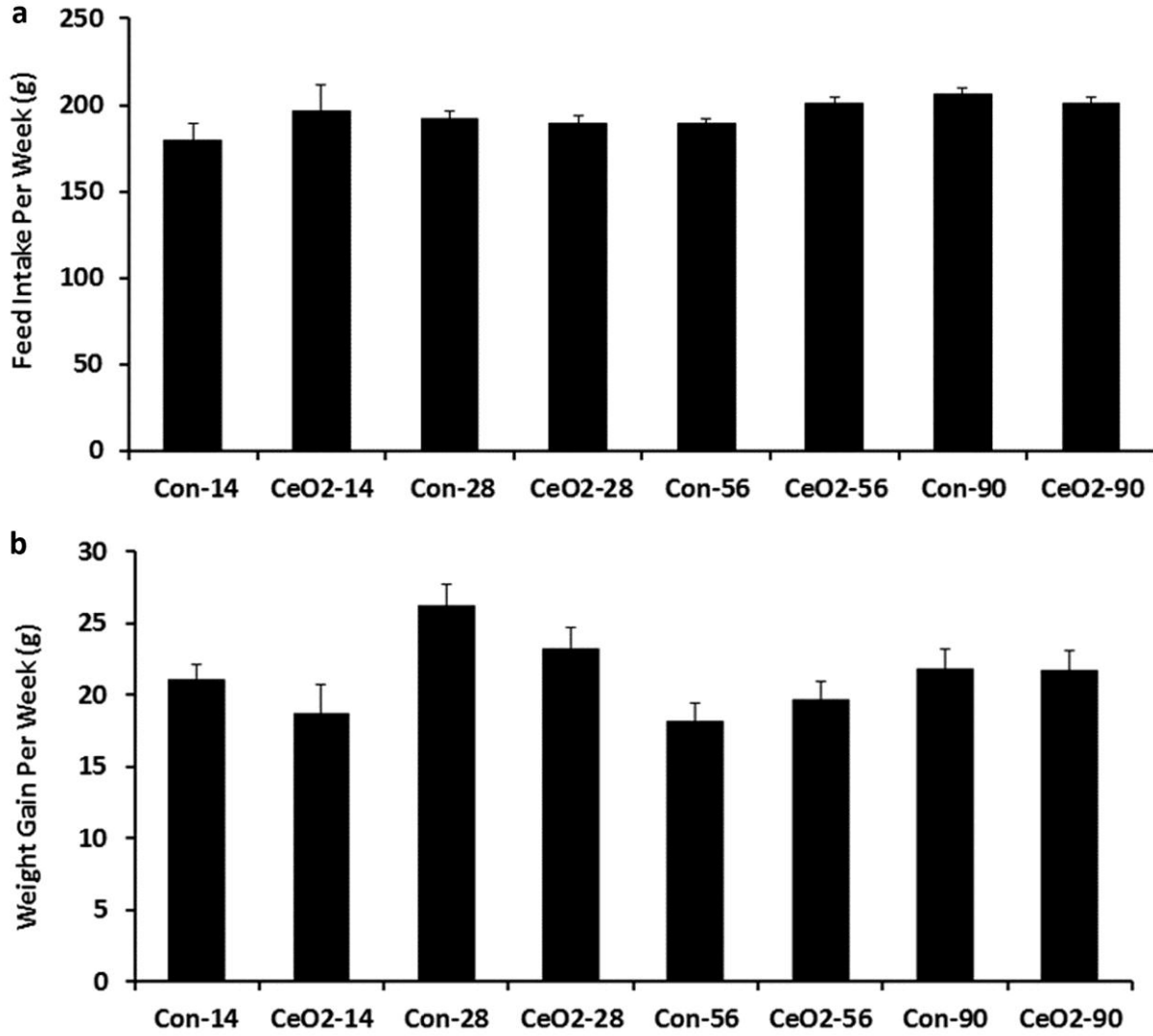
Table 5: Alterations in the liver weight, body weight and coefficient of liver weights with the ceO$_2$ nanoparticle exposure

Days of exposure	Body weight (g)		Liver weight (g)		Coefficient of liver weight to bodyweight	
	Saline Control	CeO2-7.0mg/kg	Saline Control	CeO2-7.0mg/kg	Saline Control	CeO2-7.0mg/kg
1	319.67±15.92	319.67±15.20	13.18±0.68	13.00±1.05	41.27±2.2	40.61 ±2.34
3	310.33±28.10	331.67±24	12.27±1.58	11.85±1.06	39.44± 1.86	35.85± 3.7*
14	345.67±27.11	332.33±21.07	13.31±2.00	13.31±2.00	38.40 ±3.80	38.04± 4.05
28	411.33±29.2$^{*\mu}$	403.67±28.94$^{*\mu}$	15.00±0.80$^{\alpha}$	14.70±1.55$^{\alpha}$	36.60 ±2.64*	36.30 ±1.88*
56	451.67±26.21$^{*\alpha\mu}$	451.33±34.6$^{*\alpha\mu\P}$	15.34±1.30$^{\alpha}$	15.34±1.30$^{\alpha}$	33.96± 2.02*	33.55± 2.69*¶
90	523.33±60.87$^{*\alpha\mu\P\#}$	519.33±44.84$^{*\alpha\mu\P\#}$	17.56±2.35$^{*\alpha\mu}$	17.06±1.80$^{*\alpha\mu}$	33.60 ±2.62*	32.82± 1.45*¶

*Significant difference from the 1 Day exposure group in each condition
$^{\alpha}$ Significant difference from the 3 Day exposure group in each condition
μ Significant difference from the 14 Day exposure group in each condition
$\P$ Significant difference from the 28days exposure group
Significant difference from the 56days exposure group

Figure 3-18: Accumulation of cerium in the liver with the days of the exposure to CeO$_2$

nanoparticles
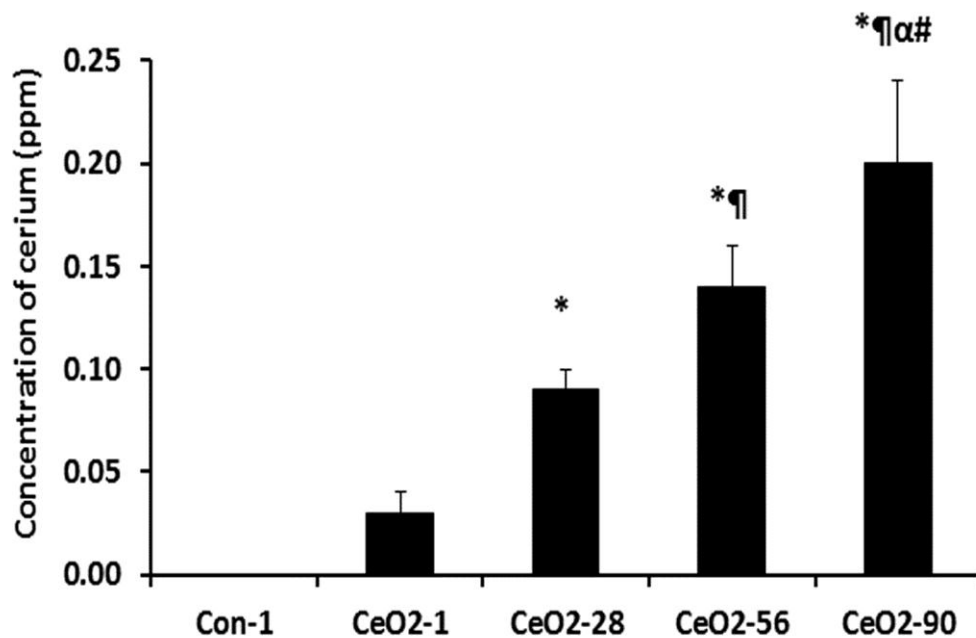
* Significant difference from control-1
¶ Significant difference from Day-1 exposure
α Significant difference from Day-28 exposure
Significant difference from Day-56 exposure

Figure 3-19: Alterations in the ultrastructure of the hepatocytes as observed with TEM a) 90

days control, b) 90 days CeO$_2$ nanoparticles exposed liver
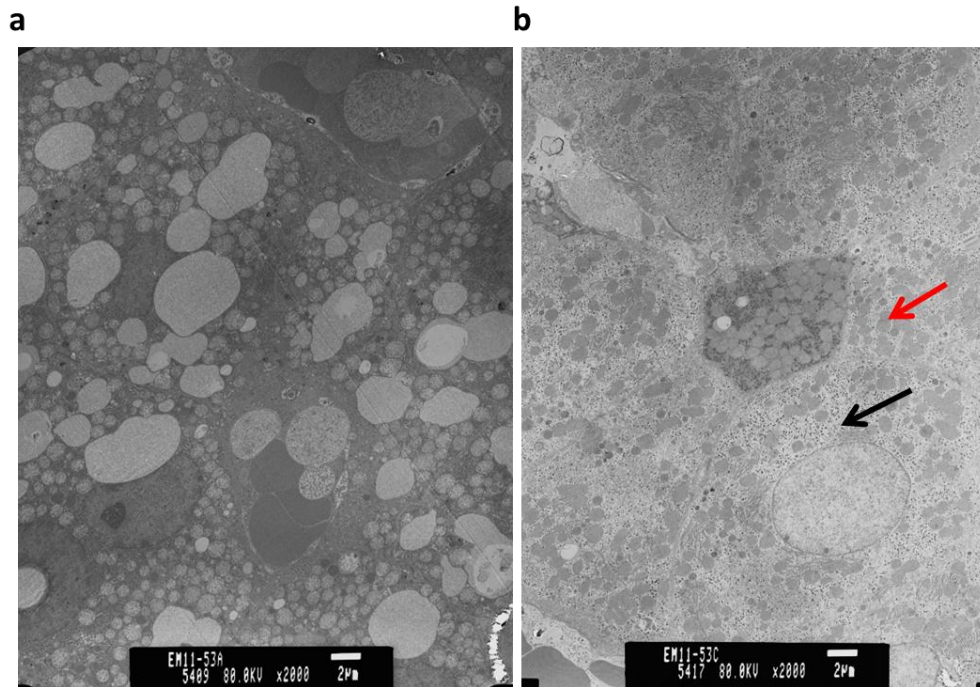
Black Arrow: Deposition of CeO$_2$ nanoparticles

Red Arrow: Altered mitochondrial structure with CeO$_2$ nanoparticle exposure

Figure 3-20: CeO$_2$ nanoparticles can cause lipid peroxidation of the hepatic cell membranes
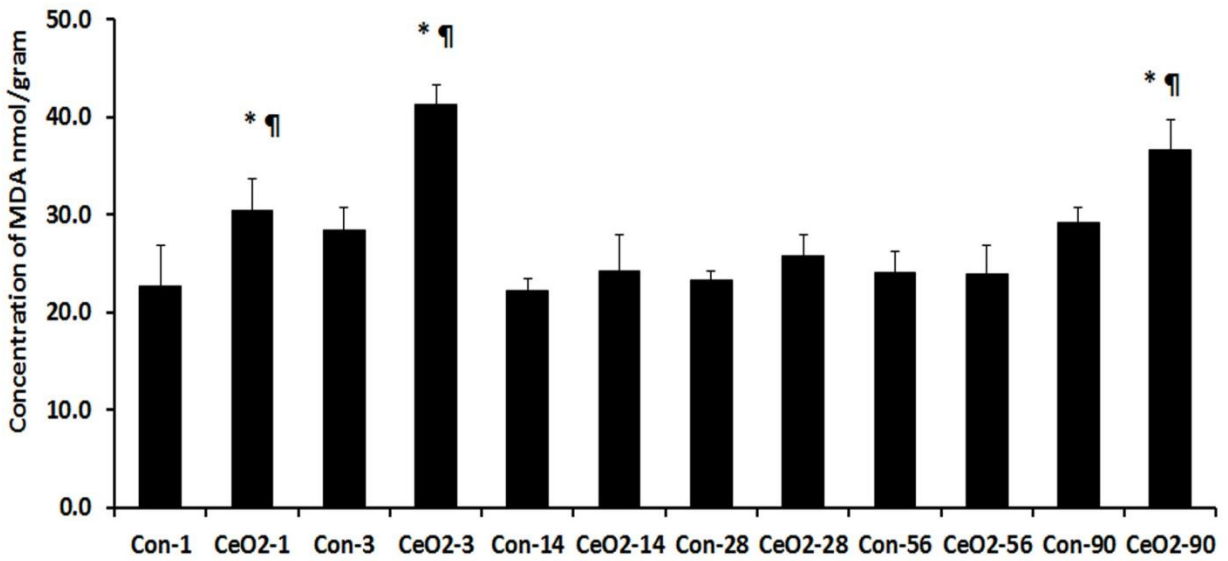
* Significant difference from the controls in each group
¶ Significant difference from the 14, 28 and 56 days CeO2 exposure group

Figure 3-21: Increased generation of superoxide radicals in the liver with the intratracheal instillation of CeO₂ nanoparticles
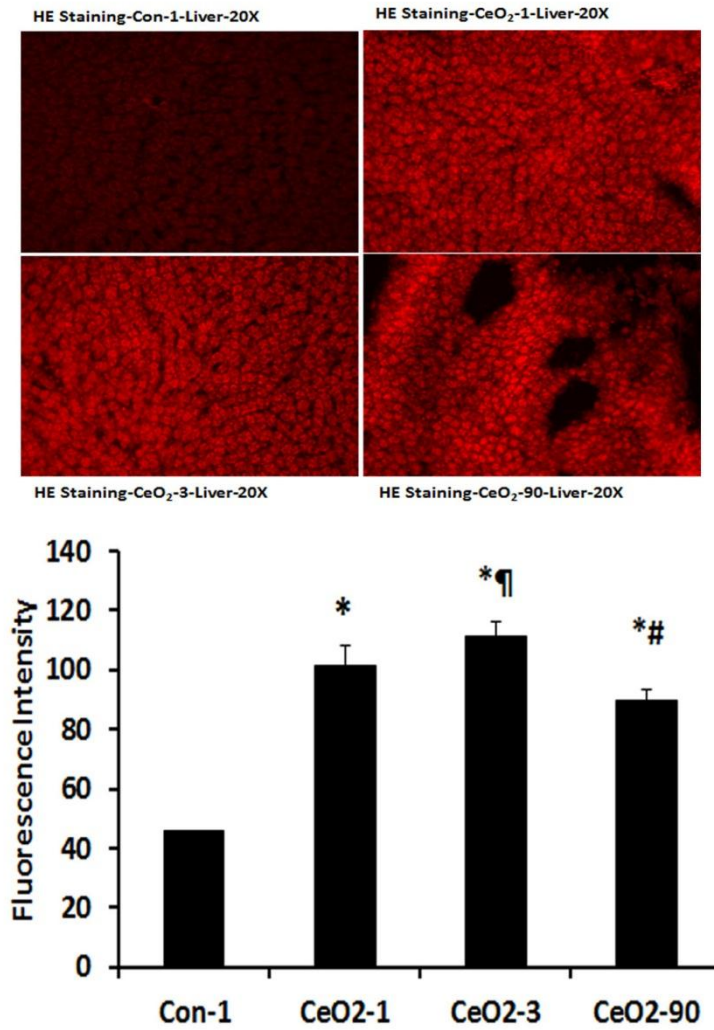
* Significant difference from control-1
¶ Significant difference from Day-1 exposure
# Significant difference from Day-3 exposure

Figure 3-22: CeO$_2$ nanoparticles exposure can increase TUNEL positive nuclei in the liver
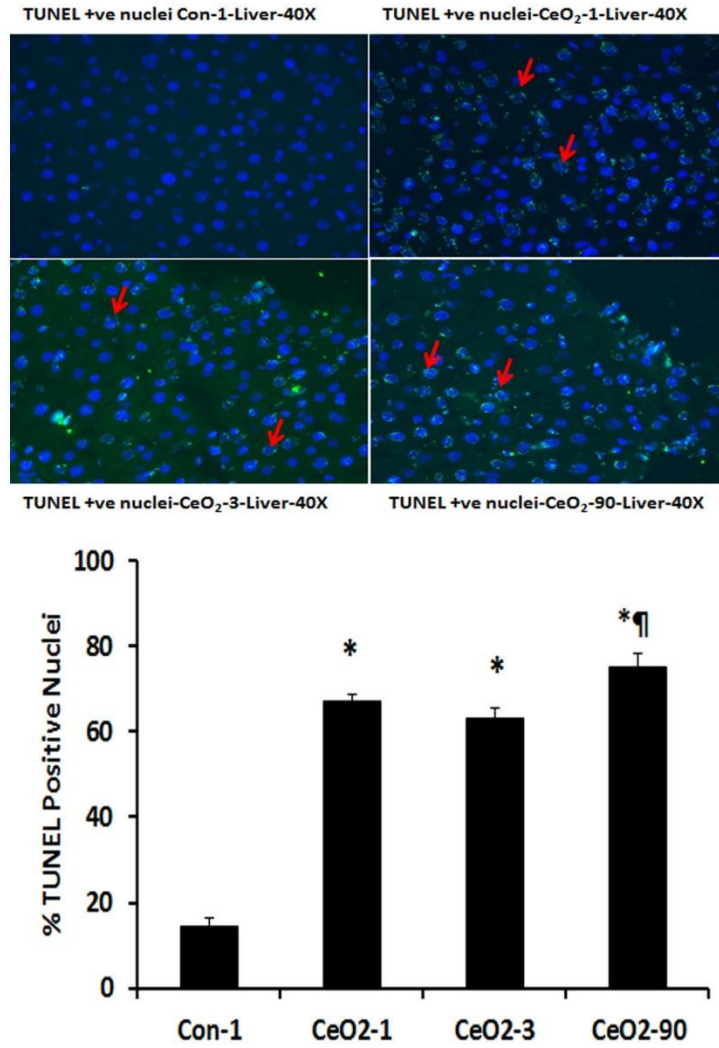
* Significant difference from control-1
¶ Significant difference from Day-3 exposure

Figure 3-23: Activation of proapoptotic protein signaling in the liver following intratracheal instillation of CeO$_2$ nanoparticles.

Protein bands of the Bax and Bcl-2 proteins and corresponding GAPDH are represented in the figure. Bands corresponding to the X-axis labels are shown in the immunoblotting images. Protein levels were adjusted by GAPDH levels and compared with the control day-1.

* Significant difference from control-1
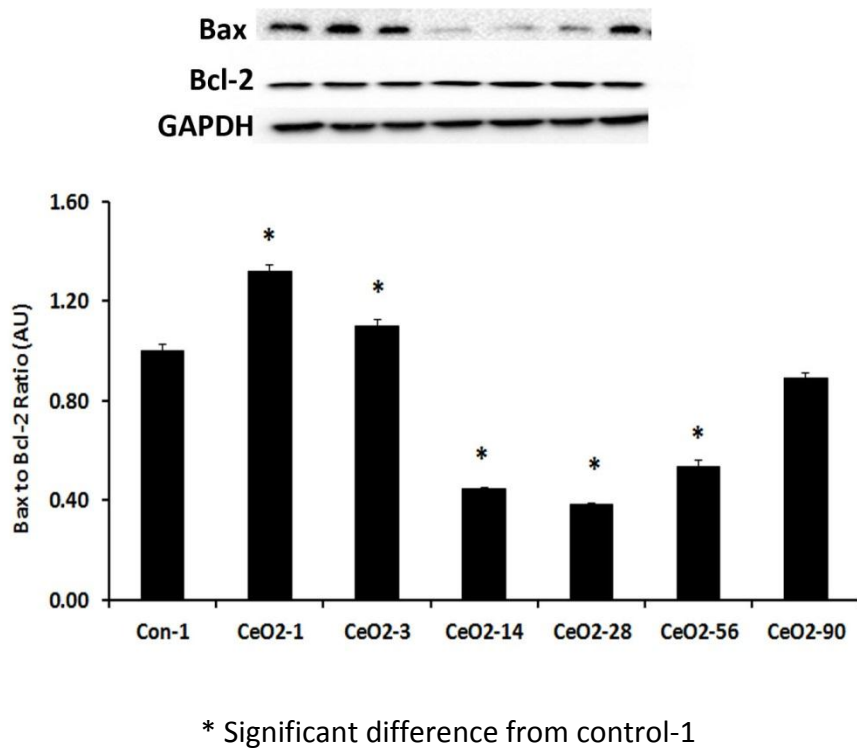
Figure 3-24: CeO₂ nanoparticle exposure can activate initiator caspase-9

Protein bands of the Caspase-9 and cleaved caspase-9 proteins and corresponding GAPDH are represented in the figure. Bands corresponding to the X-axis labels are shown in the immunoblotting images. Protein levels were adjusted by GAPDH levels and compared with the control day-1.
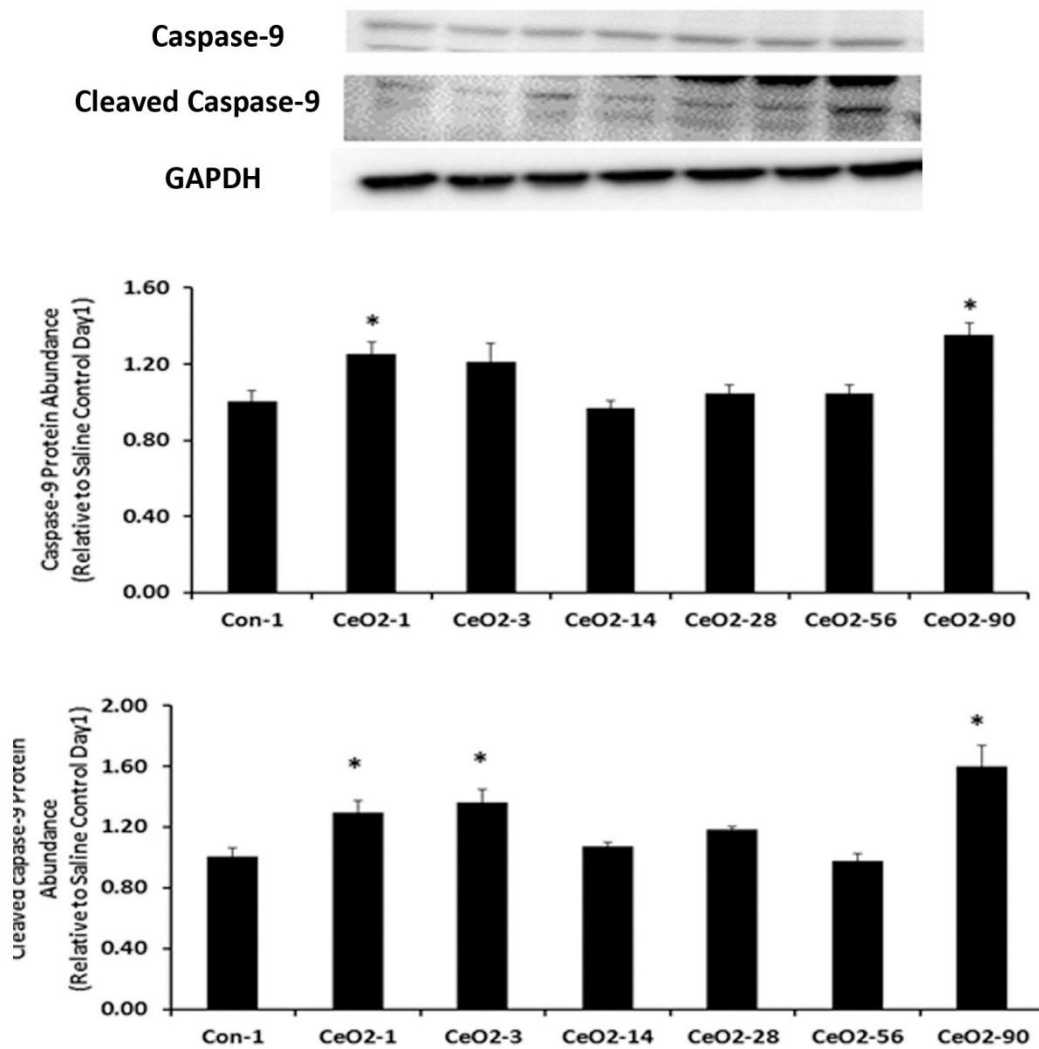
* Significant difference from control-1

Figure 3-25: CeO$_2$ nanoparticle exposure can activate executor caspase-3

Protein bands of the Caspase-3 and cleaved caspase-3 proteins and corresponding GAPDH are represented in the figure. Bands corresponding to the X-axis labels are shown in the immunoblotting images. Protein levels were adjusted by GAPDH levels and compared with the control day-1.
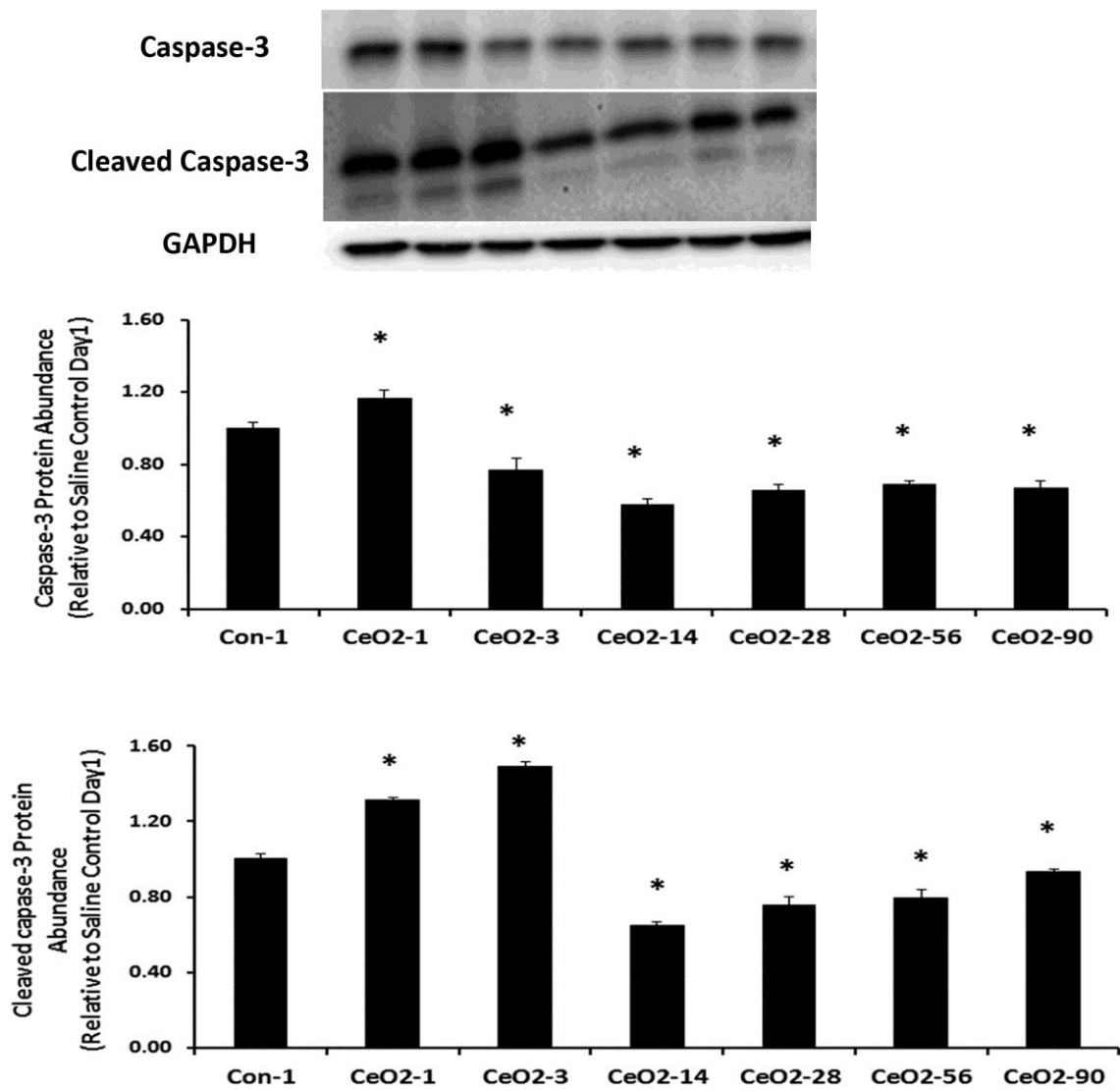
* Significant difference from day 1 control animals

Figure 3-26: CeO$_2$ nanoparticle exposure can alter the cell protective signaling in the liver by modulating the activity of p38 MAPK

Protein bands of the p38 MAPK and phospho p38 MAPK proteins and corresponding GAPDH are represented in the figure. Bands corresponding to the X-axis labels are shown in the immunoblotting images. Protein levels were adjusted by GAPDH levels and compared with the control day-1.
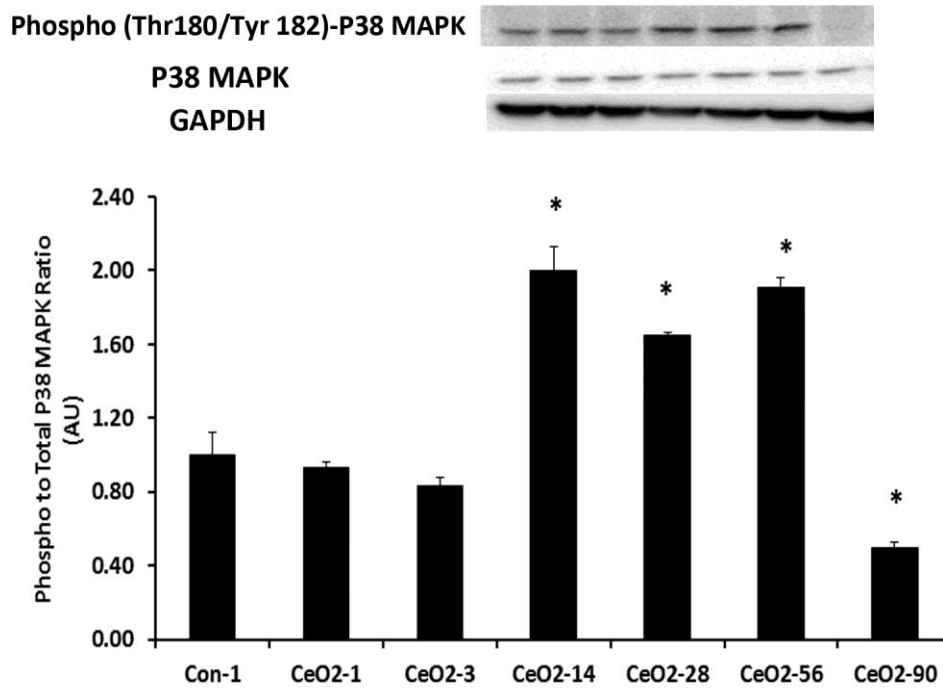
* Significant difference from day 1 control animals

Figure 3-27: CeO$_2$ nanoparticle exposure can alter the cell protective signaling in the liver by modulating the activity of NF-kβ activity

Protein bands of the NF-kβ and phospho NF-kβ p65 proteins and corresponding GAPDH are represented in the figure. Bands corresponding to the X-axis labels are shown in the immunoblotting images. Protein levels were adjusted by GAPDH levels and compared with the control day-1.
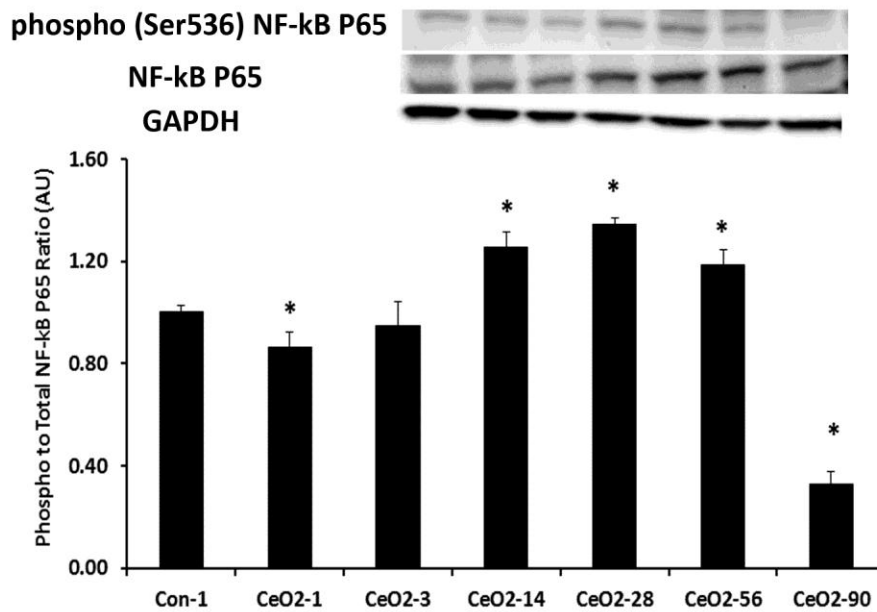
* Significant difference from day 1 control animals

Figure 3-28: Intratracheal instillation of CeO$_2$ nanoparticles can alter the expression of serum biomarkers that play an important role in the inflammation and/ or act as inflammatory cytokines and tissue factors
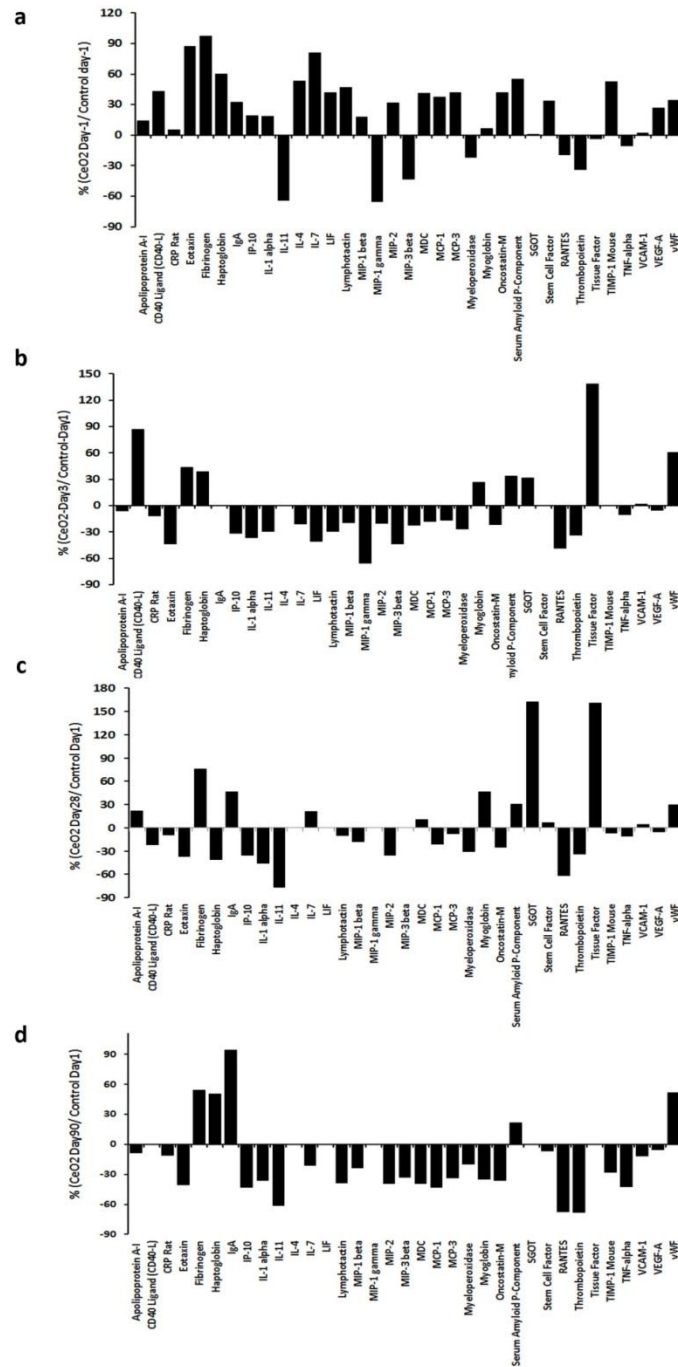
Chapter 4

General Discussion

The applications of nanotechnology are growing tremendously in several sectors including electronics (chips, screens), energy (production, catalysis, and storage), materials (lubricants, abrasives, paints, tires and sportswear), consumer products (clothes, goggles, skin lotions and sun screens), automotive, soil/water remediation (pollution absorption, water filtering, and disinfection), pesticides, chemicals and pharmaceutical industries [1, 2, 30, 39, 40]. It is estimated that there are almost 800 nanoproducts currently available [5]. With increased production and utilization of nanomaterials, there is increased chance of exposure to nanomaterials. The primary goal of this study was to investigate the potential toxic effects induced by CeO_2 nanoparticles following intratracheal instillation.

CeO_2 nanoparticles have application in fuel cells, solid cells, the polishing industries and biomedical fields [7]. Potential sources of CeO_2 nanoparticles exposure to the humans include environmental and industrial sources. While inhalation is the most common route of exposure, ingestion is also possible. But the inhalation route of exposure is the route of exposure of most concern as the absorption through oral route is very minimal [7].

CeO$_2$ nanoparticles induced oxidative stress and apoptosis in the lungs is associated with MAPK and caspase activation

CeO$_2$ nanoparticles have been shown to induce oxidative stress and apoptosis in cultured lung cells[16]. However, little is known about the effects of these nanomaterials on the intact lung. In addition, the cell signaling events associated with the CeO$_2$ nanoparticle toxicity are not currently clear. Here we evaluated the role of MAPKs and caspases in the oxidative stress and apoptosis induced by CeO$_2$ nanoparticles in the lungs following intratracheal instillation. Similar to previous work [119], CeO$_2$ nanoparticle exposure is associated with the activation of MAPKs protein signaling and increased oxidative stress. Specifically, we observed that CeO$_2$ nanoparticles activate p38 MAPK and inhibit the activity of ERK 1/2-MAPK. In addition, our data also show that the p38 MAPK activation (phosphorylation) is paralleled by STAT-3 phosphorylation. Phosphorylated p38 MAPK has been shown to play an important role in the activation of inflammatory cell signaling pathway by activating different cell signaling events and STAT-3 protein signaling is one such pathway [174]. CeO$_2$ nanoparticle exposure is also associated with an elevation of serum biomarkers that have been shown to play very crucial roles as inflammatory mediators. Increased oxidative stress is associated with increased protein expression of proapoptotic Bax and reduced expression of anti-apoptotic Bcl-2. This proapoptotic protein signaling is associated with the activation of caspase-9 and caspase-3. Altogether, the data from the current study indicates that CeO$_2$ nanoparticle induced oxidative stress is mediated through activation of the stress responsive MAP kinase protein signaling pathway, phosphorylation of STAT-3 and activation of the intrinsic pathway of apoptosis.

CeO$_2$ nanoparticles produce toxic effects in the liver

Our next step was to examine if CeO$_2$ nanoparticles could translocate to other organs from the lungs through the circulation. For these experiments, we evaluated the histopathology, organ weights and cerium concentration in the liver, kidney, spleen and heart. Similar to that observed with other nanoparticles [26, 27], CeO$_2$ nanoparticle exposure was associated with increased liver ceria levels, elevations in serum alanine transaminase levels, reduced albumin levels, a diminished sodium-potassium ratio and decreased serum triglyceride levels. Consistent with these data, rats exposed to CeO$_2$ nanoparticles also exhibited reductions in liver weight and dose dependent hydropic degeneration, hepatocyte enlargement, sinusoidal dilatation and the accumulation of granular material in the hepatocytes. No histopathological alterations were observed in the kidney, spleen and heart. Analysis of the serum biomarkers suggested that there was an elevation of the acute phase reactants in the CeO$_2$ nanoparticles exposed rats. Taken together, these data suggest that intratracheal instillation of CeO$_2$ nanoparticles can result in liver accumulation and can damage the liver.

Hepatic toxicity induced by CeO$_2$ nanoparticles is associated with oxidative stress and apoptosis

There are several studies that show that nanoparticle toxicity is mediated through the activation of oxidative stress and apoptosis [2, 24]. To investigate this mechanism, rats were instilled with either CeO$_2$ nanoparticles or normal saline and sacrificed 1, 3, 14, 28, 56 or 90 days after exposure. Our data demonstrated an increase in the concentration of cerium with

day of the exposure indicating that cerium bioaccumulates in the liver. Lipid peroxidation assays and staining with dihydroethidium indicated increased oxidative stress 1, 3 and 90 days post exposure. Compared to saline control animals, the increased oxidative stress was associated with evidence of apoptosis in the livers at 1, 3 and 90 days exposure groups. Immunoblotting data indicated that these changes were associated with an increased proapoptotic Bax/Bcl-2 ratio, increased caspase-9 protein levels and increased caspase-3 protein levels. Taken together, these data suggest that CeO_2 nanoparticle exposure is associated with increased oxidative stress and apoptosis in the liver.

Summary

1. Intratracheal instillation of CeO_2 nanoparticles is associated with changes in the histological and gross appearance of the lungs.

2. CeO_2 nanoparticle instillation is associated with activation of MAP kinase and STAT-3 signaling in the lungs.

3. CeO_2 nanoparticle instillation is associated with oxidative stress in the lungs and activation of intrinsic pathway of apoptosis.

4. The CeO_2 nanoparticles can translocate to the liver and induce toxic effects on the liver but do not appear to induce any histological alterations in the kidney, spleen or heart.

5. Histological alterations induced by CeO_2 nanoparticles include hydropic degeneration, hepatocyte enlargement, sinusoidal dilatation and the accumulation of granular material inside the hepatocytes.

6. CeO_2 nanoparticles appear to bioaccumulate in the liver.

7. CeO_2 nanoparticle induced hepatic toxicity is associated with oxidative stress and apoptosis. The oxidative stress and apoptosis appear to follow a biphasic response.

8. CeO_2 nanoparticles exposure causes the generation of ROS and apoptosis of the hepatocytes. CeO_2 nanoparticles also appear to cause lipid peroxidation of the membranes.

Figure 4-1: Activation of MAP kinases and caspases in the lungs
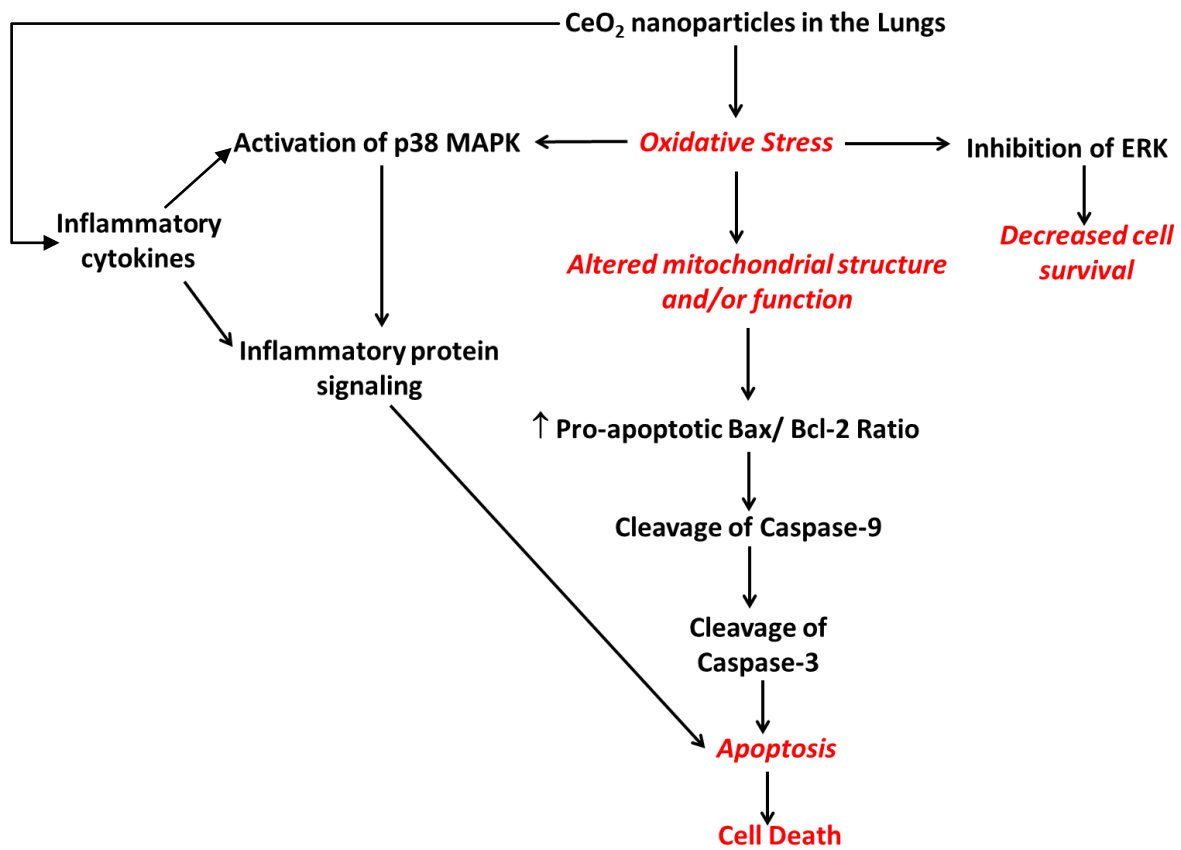
Note: In the above figure, black colored text indicates the results from our studies and the red colored text indicates what is already known or what can be implied from the previous studies.

Figure 4-2: Possible route of translocation of CeO_2 nanoparticles into the liver
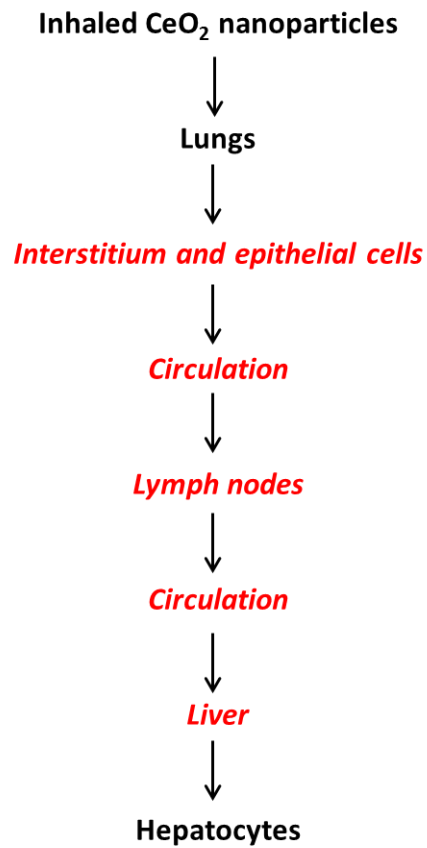
Inhaled CeO$_2$ nanoparticles

↓

Lungs

↓

Interstitium and epithelial cells

↓

Circulation

↓

Lymph nodes

↓

Circulation

↓

Liver

↓

Hepatocytes

Note: In the above figure, black colored text indicates the results from our studies and the red colored text indicates what is already known or what can be implied from the previous studies.

Figure 4-3: Possible role of oxidative stress and apoptosis in the hepatic toxicity induced by

CeO$_2$ nanoparticles

Bioaccumulation of CeO$_2$ nanoparticles in the Liver

↓

↑ **Generation of superoxide radicals**

↓

Oxidative Stress

↓

Altered mitochondrial structure and/or function

↓

↑ **pro-apoptotic Bax/ Bcl-2 Ratio**

↓

Cleavage of Caspase-9

↓

Cleavage of Caspase-3

↓

Apoptosis

↓

↑ **lipid peroxidation of the membranes**

Cell Death
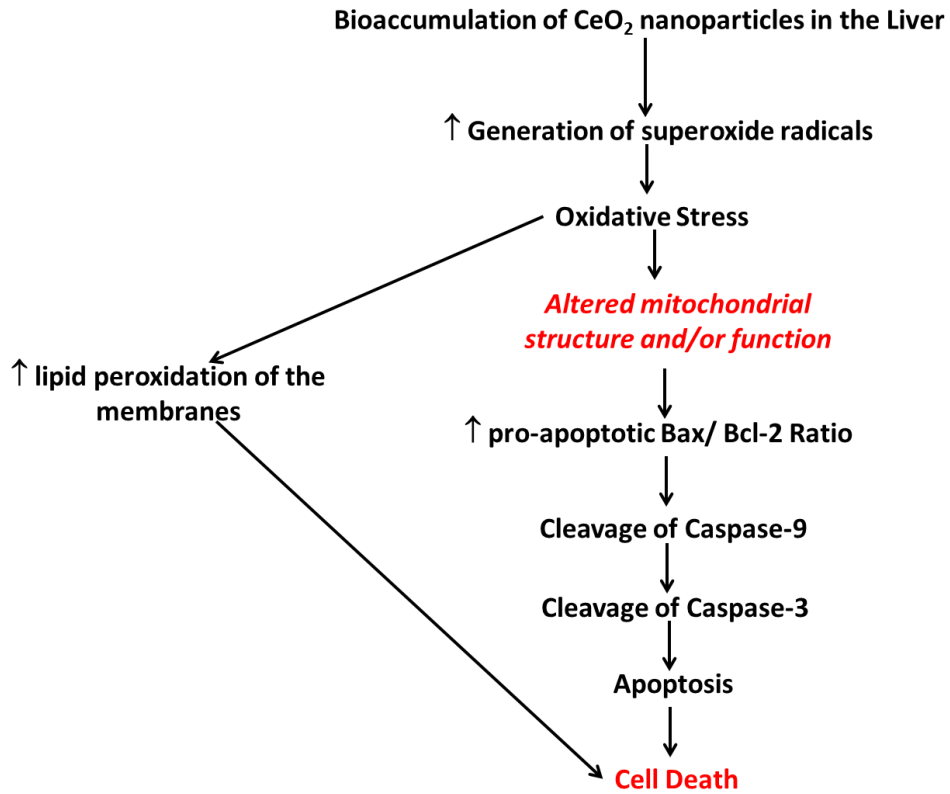
Note: In the above figure, black colored text indicates the results from our studies and the red

colored text indicates what is already known or what can be implied from the previous studies.

Future Directions

The current study evaluated the role of the oxidative stress and apoptosis in the toxicity induced by CeO_2 nanoparticles in the lungs and liver. We have shown that the CeO_2 nanoparticles can be translocated from the lungs to the liver and have shown that these materials induce oxidative stress and apoptosis. Previous work by others has shown that nanoparticles can be localized to subcellular organelles [21-23, 70]. Future work could determine if the mitochondria and nucleus take up CeO_2 nanoparticles. Although we have shown that CeO_2 nanoparticles can accumulate in the liver, it is not clear if they can be taken up by other organs or not. Additional studies examining other tissues or organs are needed. Potential aims for future studies could be:

Specific Aim I

To investigate the possible subcellular localization of the CeO_2 nanoparticles in the mitochondria and nucleus as well as to investigate the possible structural and functional alterations induced by CeO_2 nanoparticles following subcellular localization. Electron microscopy could be used to examine the structural alterations as well as the subcellular localization. Mitochondria or nuclei could be isolated to examine changes in protein signaling or for evidence of DNA damage. Mitochondrial function could be assessed by measuring the rate of mitochondrial ATP production and mitochondrial oxygen consumption using assay kits.

Specific Aim II:

To investigate the possible toxic effects of CeO_2 nanoparticles on the other vital organs such as brain. Studies have shown that the nanoparticles can enter brain and disturb the blood-brain barrier [1, 6, 96]. It is not clear if CeO_2 nanoparticles can induce any damage to the brain. We could investigate if cerium can accumulate in the brain and induce any structural alterations in the brain. We could also investigate if oxidative stress, inflammation and apoptosis have any role in the CeO_2 nanoparticles induced brain toxicity.

References

1. Buzea, C., Pacheco, II, and K. Robbie, *Nanomaterials and nanoparticles: sources and toxicity.* Biointerphases, 2007. **2**(4): p. MR17-71.
2. Oberdorster, G., E. Oberdorster, and J. Oberdorster, *Nanotoxicology: an emerging discipline evolving from studies of ultrafine particles.* Environ Health Perspect, 2005. **113**(7): p. 823-39.
3. Ju-Nam, Y. and J.R. Lead, *Manufactured nanoparticles: an overview of their chemistry, interactions and potential environmental implications.* Sci Total Environ, 2008. **400**(1-3): p. 396-414.
4. Jiao, P.F., et al., *Cancer-targeting multifunctionalized gold nanoparticles in imaging and therapy.* Curr Med Chem, 2011. **18**(14): p. 2086-102.
5. Fiorino, D.J., *Voluntary Initiatives, Regulation, and Nanotechnology Oversight Charting a Path. Woodrow Wilson International Center for Scholars;Project on Emerging Nanotechnologies.* 2010.
6. Hardas, S.S., et al., *Brain distribution and toxicological evaluation of a systemically delivered engineered nanoscale ceria.* Toxicol Sci, 2010. **116**(2): p. 562-76.
7. Cassee, F.R., et al., *Exposure, health and ecological effects review of engineered nanoscale cerium and cerium oxide associated with its use as a fuel additive.* Crit Rev Toxicol, 2011. **41**(3): p. 213-29.
8. Bumajdad, A., J. Eastoe, and A. Mathew, *Cerium oxide nanoparticles prepared in self-assembled systems.* Adv Colloid Interface Sci, 2009. **147-148**: p. 56-66.
9. Heckert, E.G., S. Seal, and W.T. Self, *Fenton-like reaction catalyzed by the rare earth inner transition metal cerium.* Environ Sci Technol, 2008. **42**(13): p. 5014-9.
10. Niu, J., et al., *Cardioprotective effects of cerium oxide nanoparticles in a transgenic murine model of cardiomyopathy.* Cardiovasc Res, 2007. **73**(3): p. 549-59.
11. Das, M., et al., *Auto-catalytic ceria nanoparticles offer neuroprotection to adult rat spinal cord neurons.* Biomaterials, 2007. **28**(10): p. 1918-25.
12. Colon, J., et al., *Protection from radiation-induced pneumonitis using cerium oxide nanoparticles.* Nanomedicine, 2009. **5**(2): p. 225-31.
13. Pirmohamed, T., et al., *Nanoceria exhibit redox state-dependent catalase mimetic activity.* Chem Commun (Camb), 2010. **46**(16): p. 2736-8.
14. Thill, A., et al., *Cytotoxicity of CeO2 nanoparticles for Escherichia coli. Physico-chemical insight of the cytotoxicity mechanism.* Environ Sci Technol, 2006. **40**(19): p. 6151-6.
15. Kim, I.S., M. Baek, and S.J. Choi, *Comparative cytotoxicity of Al2O3, CeO2, TiO2 and ZnO nanoparticles to human lung cells.* J Nanosci Nanotechnol, 2010. **10**(5): p. 3453-8.
16. Park, E.J., et al., *Oxidative stress induced by cerium oxide nanoparticles in cultured BEAS-2B cells.* Toxicology, 2008. **245**(1-2): p. 90-100.
17. Ma, J.Y., et al., *Cerium oxide nanoparticle-induced pulmonary inflammation and alveolar macrophage functional change in rats.* Nanotoxicology, 2010.
18. Lin, W., et al., *Toxicity of cerium oxide nanoparticles in human lung cancer cells.* Int J Toxicol, 2006. **25**(6): p. 451-7.
19. Eom, H.J. and J. Choi, *Oxidative stress of CeO2 nanoparticles via p38-Nrf-2 signaling pathway in human bronchial epithelial cell, Beas-2B.* Toxicol Lett, 2009. **187**(2): p. 77-83.
20. Kreyling, W.G., S. Hirn, and C. Schleh, *Nanoparticles in the lung.* Nat Biotechnol, 2010. **28**(12): p. 1275-6.
21. Xia, T., et al., *Comparison of the abilities of ambient and manufactured nanoparticles to induce cellular toxicity according to an oxidative stress paradigm.* Nano Lett, 2006. **6**(8): p. 1794-807.

22.   Berton, M., et al., *Uptake of oligonucleotide-loaded nanoparticles in prostatic cancer cells and their intracellular localization.* Eur J Pharm Biopharm, 1999. **47**(2): p. 119-23.

23.   Porter, A.E., et al., *Uptake of C60 by human monocyte macrophages, its localization and implications for toxicity: studied by high resolution electron microscopy and electron tomography.* Acta Biomater, 2006. **2**(4): p. 409-19.

24.   Li, N., T. Xia, and A.E. Nel, *The role of oxidative stress in ambient particulate matter-induced lung diseases and its implications in the toxicity of engineered nanoparticles.* Free Radic Biol Med, 2008. **44**(9): p. 1689-99.

25.   Hirst, S.M., et al., *Bio-distribution and in vivo antioxidant effects of cerium oxide nanoparticles in mice.* Environ Toxicol, 2011.

26.   Zhu, M.T., et al., *Particokinetics and extrapulmonary translocation of intratracheally instilled ferric oxide nanoparticles in rats and the potential health risk assessment.* Toxicol Sci, 2009. **107**(2): p. 342-51.

27.   Sung, J.H., et al., *Subchronic inhalation toxicity of silver nanoparticles.* Toxicol Sci, 2009. **108**(2): p. 452-61.

28.   Abdelhalim, M.A. and B.M. Jarrar, *Gold nanoparticles induced cloudy swelling to hydropic degeneration, cytoplasmic hyaline vacuolation, polymorphism, binucleation, karyopyknosis, karyolysis, karyorrhexis and necrosis in the liver.* Lipids Health Dis, 2011. **10**: p. 166.

29.   *NANOtechnology: untold promise, unknown risk.* Consum Rep, 2007. **72**(7): p. 40-5.

30.   Hobson, D.W., *Commercialization of nanotechnology.* Wiley Interdiscip Rev Nanomed Nanobiotechnol, 2009. **1**(2): p. 189-202.

31.   Kibble, A., *Pharma 2020--An Economist Conference Shaping the Future of the Pharmaceuticals Industry.* IDrugs, 2008. **11**(5): p. 331-3.

32.   Simonelli, F., et al., *Cyclotron production of radioactive CeO(2) nanoparticles and their application for in vitro uptake studies.* IEEE Trans Nanobioscience, 2011. **10**(1): p. 44-50.

33.   Environment Directorate, O., *WORKING PARTY ON MANUFACTURED NANOMATERIALS: LIST OF MANUFACTURED NANOMATERIALS AND LIST OF ENDPOINTS FOR PHASE ONE OF THE OECD TESTING PROGRAMME*, in *ENV/JM/MONO(2008)13/REV*. 2008.

34.   Singh, S. and H.S. Nalwa, *Nanotechnology and health safety--toxicity and risk assessments of nanostructured materials on human health.* J Nanosci Nanotechnol, 2007. **7**(9): p. 3048-70.

35.   Kumar, V., et al., *Evaluating the toxicity of selected types of nanochemicals.* Rev Environ Contam Toxicol, 2012. **215**: p. 39-121.

36.   Jennings, T. and G. Strouse, *Past, present, and future of gold nanoparticles.* Adv Exp Med Biol, 2007. **620**: p. 34-47.

37.   Dreaden, E.C., et al., *The golden age: gold nanoparticles for biomedicine.* Chem Soc Rev, 2011.

38.   Fiorino, D.J., *Voluntary Initiatives, Regulation, and Nanotechnology Oversight Charting a Path. Woodrow Wilson International Center for Scholars;Project on Emerging Nanotechnologies.* 2010.

39.   Malsch, D.H.a.I., *Hazards and Risks of Engineered Nanoparticles for the Environment and Human Health.* Sustainability, 2009. **1**(2071-1050): p. 1161-1194.

40.   Hofmann-Amtenbrink, M., H. Hofmann, and X. Montet, *Superparamagnetic nanoparticles - a tool for early diagnostics.* Swiss Med Wkly, 2010. **140**: p. w13081.

41.   Islam, T. and L. Josephson, *Current state and future applications of active targeting in malignancies using superparamagnetic iron oxide nanoparticles.* Cancer Biomark, 2009. **5**(2): p. 99-107.

42.   Bhaskar, S., et al., *Multifunctional Nanocarriers for diagnostics, drug delivery and targeted treatment across blood-brain barrier: perspectives on tracking and neuroimaging.* Part Fibre Toxicol, 2010. **7**: p. 3.

43. Tiede, K., et al., *Detection and characterization of engineered nanoparticles in food and the environment.* Food Addit Contam Part A Chem Anal Control Expo Risk Assess, 2008. **25**(7): p. 795-821.

44. Morris, V.J., *Emerging roles of engineered nanomaterials in the food industry.* Trends Biotechnol, 2011. **29**(10): p. 509-16.

45. Petosa, A.R., et al., *Aggregation and deposition of engineered nanomaterials in aquatic environments: role of physicochemical interactions.* Environ Sci Technol, 2010. **44**(17): p. 6532-49.

46. Gottschalk, F. and B. Nowack, *The release of engineered nanomaterials to the environment.* J Environ Monit, 2011. **13**(5): p. 1145-55.

47. Bernhardt, E.S., et al., *An ecological perspective on nanomaterial impacts in the environment.* J Environ Qual, 2010. **39**(6): p. 1954-65.

48. Woskie, S., *Workplace practices for engineered nanomaterial manufacturers.* Wiley Interdiscip Rev Nanomed Nanobiotechnol, 2010. **2**(6): p. 685-92.

49. Ren, H. and X. Huang, *Polyacrylate nanoparticles: toxicity or new nanomedicine?* Eur Respir J, 2010. **36**(1): p. 218-21.

50. Bystrzejewska-Piotrowska, G., J. Golimowski, and P.L. Urban, *Nanoparticles: their potential toxicity, waste and environmental management.* Waste Manag, 2009. **29**(9): p. 2587-95.

51. Khlebtsov, N. and L. Dykman, *Biodistribution and toxicity of engineered gold nanoparticles: a review of in vitro and in vivo studies.* Chem Soc Rev, 2011. **40**(3): p. 1647-71.

52. Trickler, W.J., et al., *Silver nanoparticle induced blood-brain barrier inflammation and increased permeability in primary rat brain microvessel endothelial cells.* Toxicol Sci, 2010. **118**(1): p. 160-70.

53. Yang, H., et al., *Comparative study of cytotoxicity, oxidative stress and genotoxicity induced by four typical nanomaterials: the role of particle size, shape and composition.* J Appl Toxicol, 2009. **29**(1): p. 69-78.

54. Simon-Deckers, A., et al., *Size-, composition- and shape-dependent toxicological impact of metal oxide nanoparticles and carbon nanotubes toward bacteria.* Environ Sci Technol, 2009. **43**(21): p. 8423-9.

55. Lam, C.W., et al., *A review of carbon nanotube toxicity and assessment of potential occupational and environmental health risks.* Crit Rev Toxicol, 2006. **36**(3): p. 189-217.

56. Jia, G., et al., *Cytotoxicity of carbon nanomaterials: single-wall nanotube, multi-wall nanotube, and fullerene.* Environ Sci Technol, 2005. **39**(5): p. 1378-83.

57. Warheit, D.B., et al., *Health effects related to nanoparticle exposures: environmental, health and safety considerations for assessing hazards and risks.* Pharmacol Ther, 2008. **120**(1): p. 35-42.

58. Monopoli, M.P., et al., *Physical-chemical aspects of protein corona: relevance to in vitro and in vivo biological impacts of nanoparticles.* J Am Chem Soc, 2011. **133**(8): p. 2525-34.

59. Geiser, M. and W.G. Kreyling, *Deposition and biokinetics of inhaled nanoparticles.* Part Fibre Toxicol, 2010. **7**: p. 2.

60. Sadauskas, E., et al., *Biodistribution of gold nanoparticles in mouse lung following intratracheal instillation.* Chem Cent J, 2009. **3**: p. 16.

61. Tjalve, H., et al., *Uptake of manganese and cadmium from the nasal mucosa into the central nervous system via olfactory pathways in rats.* Pharmacol Toxicol, 1996. **79**(6): p. 347-56.

62. Elder, A., et al., *Translocation of inhaled ultrafine manganese oxide particles to the central nervous system.* Environ Health Perspect, 2006. **114**(8): p. 1172-8.

63. Sharma, H.S. and A. Sharma, *Nanoparticles aggravate heat stress induced cognitive deficits, blood-brain barrier disruption, edema formation and brain pathology.* Prog Brain Res, 2007. **162**: p. 245-73.

64. Oberdorster, G., et al., *Translocation of inhaled ultrafine particles to the brain.* Inhal Toxicol, 2004. **16**(6-7): p. 437-45.

65. Tallkvist, J., et al., *Transport and subcellular distribution of nickel in the olfactory system of pikes and rats.* Toxicol Sci, 1998. **43**(2): p. 196-203.

66. Scheuch, G., et al., *Deposition, imaging, and clearance: what remains to be done?* J Aerosol Med Pulm Drug Deliv, 2010. **23 Suppl 2**: p. S39-57.

67. Henning, A., et al., *Influence of particle size and material properties on mucociliary clearance from the airways.* J Aerosol Med Pulm Drug Deliv, 2010. **23**(4): p. 233-41.

68. Geiser, M., *Update on macrophage clearance of inhaled micro- and nanoparticles.* J Aerosol Med Pulm Drug Deliv, 2010. **23**(4): p. 207-17.

69. Driscoll, K.E., et al., *Intratracheal instillation as an exposure technique for the evaluation of respiratory tract toxicity: uses and limitations.* Toxicol Sci, 2000. **55**(1): p. 24-35.

70. Stefani, D., D. Wardman, and T. Lambert, *The implosion of the Calgary General Hospital: ambient air quality issues.* J Air Waste Manag Assoc, 2005. **55**(1): p. 52-9.

71. Chawla, J.S. and M.M. Amiji, *Cellular uptake and concentrations of tamoxifen upon administration in poly(epsilon-caprolactone) nanoparticles.* AAPS PharmSci, 2003. **5**(1): p. E3.

72. Rouse, R.L., et al., *Soot nanoparticles promote biotransformation, oxidative stress, and inflammation in murine lungs.* Am J Respir Cell Mol Biol, 2008. **39**(2): p. 198-207.

73. Stone, V., H. Johnston, and M.J. Clift, *Air pollution, ultrafine and nanoparticle toxicology: cellular and molecular interactions.* IEEE Trans Nanobioscience, 2007. **6**(4): p. 331-40.

74. Johnston, H.J., et al., *A review of the in vivo and in vitro toxicity of silver and gold particulates: particle attributes and biological mechanisms responsible for the observed toxicity.* Crit Rev Toxicol, 2010. **40**(4): p. 328-46.

75. Mocan, T., et al., *Implications of oxidative stress mechanisms in toxicity of nanoparticles (review).* Acta Physiol Hung, 2010. **97**(3): p. 247-55.

76. Xiong, D., et al., *Effects of nano-scale TiO2, ZnO and their bulk counterparts on zebrafish: acute toxicity, oxidative stress and oxidative damage.* Sci Total Environ, 2011. **409**(8): p. 1444-52.

77. Clichici, S., et al., *Blood oxidative stress generation after intraperitoneal administration of functionalized single-walled carbon nanotubes in rats.* Acta Physiol Hung, 2011. **98**(2): p. 231-41.

78. Kumar, A., et al., *Engineered ZnO and TiO(2) nanoparticles induce oxidative stress and DNA damage leading to reduced viability of Escherichia coli.* Free Radic Biol Med, 2011. **51**(10): p. 1872-81.

79. Guyton, K.Z., et al., *Activation of mitogen-activated protein kinase by H2O2. Role in cell survival following oxidant injury.* J Biol Chem, 1996. **271**(8): p. 4138-42.

80. Tournier, C., et al., *Mediation by arachidonic acid metabolites of the H2O2-induced stimulation of mitogen-activated protein kinases (extracellular-signal-regulated kinase and c-Jun NH2-terminal kinase).* Eur J Biochem, 1997. **244**(2): p. 587-95.

81. Thomas, G., *MAP kinase by any other name smells just as sweet.* Cell, 1992. **68**(1): p. 3-6.

82. Boulton, T.G., et al., *ERKs: a family of protein-serine/threonine kinases that are activated and tyrosine phosphorylated in response to insulin and NGF.* Cell, 1991. **65**(4): p. 663-75.

83. Pages, G., et al., *Mitogen-activated protein kinases p42mapk and p44mapk are required for fibroblast proliferation.* Proc Natl Acad Sci U S A, 1993. **90**(18): p. 8319-23.

84. Kharbanda, S., et al., *Activation of the c-Abl tyrosine kinase in the stress response to DNA-damaging agents.* Nature, 1995. **376**(6543): p. 785-8.

85. Sluss, H.K., et al., *Signal transduction by tumor necrosis factor mediated by JNK protein kinases.* Mol Cell Biol, 1994. **14**(12): p. 8376-84.

86. Uchida, K., et al., *Activation of stress signaling pathways by the end product of lipid peroxidation. 4-hydroxy-2-nonenal is a potential inducer of intracellular peroxide production.* J Biol Chem, 1999. **274**(4): p. 2234-42.

87. Hsin, Y.H., et al., *The apoptotic effect of nanosilver is mediated by a ROS- and JNK-dependent mechanism involving the mitochondrial pathway in NIH3T3 cells.* Toxicol Lett, 2008. **179**(3): p. 130-9.

88. Yamakoshi, Y., et al., *Active oxygen species generated from photoexcited fullerene (C60) as potential medicines: O2-* versus 1O2.* J Am Chem Soc, 2003. **125**(42): p. 12803-9.

89. Hotze, E.M., et al., *Mechanisms of photochemistry and reactive oxygen production by fullerene suspensions in water.* Environ Sci Technol, 2008. **42**(11): p. 4175-80.

90. Zhang, Z., et al., *On the interactions of free radicals with gold nanoparticles.* J Am Chem Soc, 2003. **125**(26): p. 7959-63.

91. Lee, H.M., et al., *Nanoparticles up-regulate tumor necrosis factor-alpha and CXCL8 via reactive oxygen species and mitogen-activated protein kinase activation.* Toxicol Appl Pharmacol, 2009. **238**(2): p. 160-9.

92. Kennedy, I.M., D. Wilson, and A.I. Barakat, *Uptake and inflammatory effects of nanoparticles in a human vascular endothelial cell line.* Res Rep Health Eff Inst, 2009(136): p. 3-32.

93. Boonstra, J. and J.A. Post, *Molecular events associated with reactive oxygen species and cell cycle progression in mammalian cells.* Gene, 2004. **337**: p. 1-13.

94. Turrens, J.F., *Mitochondrial formation of reactive oxygen species.* J Physiol, 2003. **552**(Pt 2): p. 335-44.

95. Eom, H.J. and J. Choi, *p38 MAPK activation, DNA damage, cell cycle arrest and apoptosis as mechanisms of toxicity of silver nanoparticles in Jurkat T cells.* Environ Sci Technol, 2010. **44**(21): p. 8337-42.

96. Borm, P.J., et al., *The potential risks of nanomaterials: a review carried out for ECETOC.* Part Fibre Toxicol, 2006. **3**: p. 11.

97. Lenaz, G., *The mitochondrial production of reactive oxygen species: mechanisms and implications in human pathology.* IUBMB Life, 2001. **52**(3-5): p. 159-64.

98. Kakarla, S.K., et al., *Chronic acetaminophen attenuates age-associated increases in cardiac ROS and apoptosis in the Fischer Brown Norway rat.* Basic Res Cardiol, 2010. **105**(4): p. 535-44.

99. Asano, S., et al., *Aging influences multiple indices of oxidative stress in the heart of the Fischer 344/NNia x Brown Norway/BiNia rat.* Redox Rep, 2007. **12**(4): p. 167-80.

100. Morimoto, Y. and I. Tanaka, *[Effects of nanoparticles on humans].* Sangyo Eiseigaku Zasshi, 2008. **50**(2): p. 37-48.

101. Nielsen, G.D., et al., *In vivo biology and toxicology of fullerenes and their derivatives.* Basic Clin Pharmacol Toxicol, 2008. **103**(3): p. 197-208.

102. Marano, F., et al., *Nanoparticles: molecular targets and cell signalling.* Arch Toxicol, 2011. **85**(7): p. 733-41.

103. Park, E.J., et al., *Carbon fullerenes (C60s) can induce inflammatory responses in the lung of mice.* Toxicol Appl Pharmacol, 2010. **244**(2): p. 226-33.

104. Rawlings, J.S., K.M. Rosler, and D.A. Harrison, *The JAK/STAT signaling pathway.* J Cell Sci, 2004. **117**(Pt 8): p. 1281-3.

105. Brierley, M.M. and E.N. Fish, *Stats: multifaceted regulators of transcription.* J Interferon Cytokine Res, 2005. **25**(12): p. 733-44.

106. Blank, V.C., C. Pena, and L.P. Roguin, *STAT1, STAT3 and p38MAPK are involved in the apoptotic effect induced by a chimeric cyclic interferon-alpha2b peptide.* Exp Cell Res, 2010. **316**(4): p. 603-14.

107. A., T., *Catalysis by Ceria and Related Materials,.* Catalytic Science Series, 2002. **2**.

108. Nikolaou, K., *Emissions reduction of high and low polluting new technology vehicles equipped with a CeO2 catalytic system.* Sci Total Environ, 1999. **235**(1-3): p. 71-6.

109. Park, B., et al., *Hazard and risk assessment of a nanoparticulate cerium oxide-based diesel fuel additive - a case study.* Inhal Toxicol, 2008. **20**(6): p. 547-66.

110. Zholobak, N.M., et al., *UV-shielding property, photocatalytic activity and photocytotoxicity of ceria colloid solutions.* J Photochem Photobiol B, 2011. **102**(1): p. 32-8.

111. Karakoti, A.S., et al., *Nanoceria as Antioxidant: Synthesis and Biomedical Applications.* JOM (1989), 2008. **60**(3): p. 33-37.

112. Celardo, I., et al., *Ce(3)+ ions determine redox-dependent anti-apoptotic effect of cerium oxide nanoparticles.* ACS Nano, 2011. **5**(6): p. 4537-49.

113. He, X., et al., *Lung deposition and extrapulmonary translocation of nano-ceria after intratracheal instillation.* Nanotechnology, 2010. **21**(28): p. 285103.

114. Hirst, S.M., et al., *Anti-inflammatory properties of cerium oxide nanoparticles.* Small, 2009. **5**(24): p. 2848-56.

115. Asati, A., et al., *Surface-charge-dependent cell localization and cytotoxicity of cerium oxide nanoparticles.* ACS Nano, 2010. **4**(9): p. 5321-31.

116. Sharma, V., et al., *Induction of oxidative stress, DNA damage and apoptosis in mouse liver after sub-acute oral exposure to zinc oxide nanoparticles.* Mutat Res, 2011.

117. Piao, M.J., et al., *Silver nanoparticles down-regulate Nrf2-mediated 8-oxoguanine DNA glycosylase 1 through inactivation of extracellular regulated kinase and protein kinase B in human Chang liver cells.* Toxicol Lett, 2011. **207**(2): p. 143-8.

118. Park, B., et al., *Initial in vitro screening approach to investigate the potential health and environmental hazards of Enviroxtrade mark - a nanoparticulate cerium oxide diesel fuel additive.* Part Fibre Toxicol, 2007. **4**: p. 12.

119. Samet, J.M., et al., *Activation of MAPKs in human bronchial epithelial cells exposed to metals.* Am J Physiol, 1998. **275**(3 Pt 1): p. L551-8.

120. Wu, M., et al., *Acetaminophen improves protein translational signaling in aged skeletal muscle.* Rejuvenation Res, 2010. **13**(5): p. 571-9.

121. Nalabotu, S.K., et al., *Intratracheal instillation of cerium oxide nanoparticles induces hepatic toxicity in male Sprague-Dawley rats.* Int J Nanomedicine, 2011. **6**: p. 2327-35.

122. Donaldson, K., et al., *Carbon nanotubes: a review of their properties in relation to pulmonary toxicology and workplace safety.* Toxicol Sci, 2006. **92**(1): p. 5-22.

123. Park, E.J., et al., *Induction of chronic inflammation in mice treated with titanium dioxide nanoparticles by intratracheal instillation.* Toxicology, 2009. **260**(1-3): p. 37-46.

124. Bergamaschi, E., et al., *Nanomaterials and lung toxicity: interactions with airways cells and relevance for occupational health risk assessment.* Int J Immunopathol Pharmacol, 2006. **19**(4 Suppl): p. 3-10.

125. Folkmann, J.K., et al., *Oxidatively damaged DNA in rats exposed by oral gavage to C60 fullerenes and single-walled carbon nanotubes.* Environ Health Perspect, 2009. **117**(5): p. 703-8.

126. Jeong, Y.S., et al., *Cellular uptake, cytotoxicity, and ROS generation with silica/conducting polymer core/shell nanospheres.* Biomaterials, 2011. **32**(29): p. 7217-25.

127. Koike, E. and T. Kobayashi, *Chemical and biological oxidative effects of carbon black nanoparticles.* Chemosphere, 2006. **65**(6): p. 946-51.

128. Kuwano, K., *Epithelial cell apoptosis and lung remodeling.* Cell Mol Immunol, 2007. **4**(6): p. 419-29.

129. Kang, K.A., et al., *Myricetin Protects Cells against Oxidative Stress-Induced Apoptosis via Regulation of PI3K/Akt and MAPK Signaling Pathways.* Int J Mol Sci, 2010. **11**(11): p. 4348-60.

130.   Ruckerl, R., et al., *Ultrafine particles and platelet activation in patients with coronary heart disease--results from a prospective panel study.* Part Fibre Toxicol, 2007. **4**: p. 1.

131.   Chakrabarti, S., et al., *The role of CD40L and VEGF in the modulation of angiogenesis and inflammation.* Vascul Pharmacol, 2010. **53**(3-4): p. 130-7.

132.   Yazdi, A.S., et al., *Nanoparticles activate the NLR pyrin domain containing 3 (Nlrp3) inflammasome and cause pulmonary inflammation through release of IL-1alpha and IL-1beta.* Proc Natl Acad Sci U S A, 2010. **107**(45): p. 19449-54.

133.   Gojova, A., et al., *Effect of cerium oxide nanoparticles on inflammation in vascular endothelial cells.* Inhal Toxicol, 2009. **21 Suppl 1**: p. 123-30.

134.   Korsvik, C., et al., *Superoxide dismutase mimetic properties exhibited by vacancy engineered ceria nanoparticles.* Chem Commun (Camb), 2007(10): p. 1056-8.

135.   Salyer, D.C. and J.C. Eggleston, *Oat cell carcinoma of the bronchus and the carcinoid syndrome.* Arch Pathol, 1975. **99**(10): p. 513-5.

136.   Simonelli, F., et al., *Cyclotron Production of Radioactive Nanoparticles andTheir Application for UptakeStudies.* IEEE Trans Nanobioscience, 2011.

137.   Costelli, P., et al., *Ca(2+)-dependent proteolysis in muscle wasting.* Int J Biochem Cell Biol, 2005.

138.   Li, Y., et al., *Systematic influence induced by 3 nm titanium dioxide following intratracheal instillation of mice.* J Nanosci Nanotechnol, 2010. **10**(12): p. 8544-9.

139.   Jin, C., et al., *[Comparative study of the effect on oxidative damage in rats inhaled by nano-sized and micro-sized silicon dioxide].* Wei Sheng Yan Jiu, 2008. **37**(1): p. 16-8, 36.

140.   Yang, B., et al., *Systems toxicology used in nanotoxicology: mechanistic insights into the hepatotoxicity of nano-copper particles from toxicogenomics.* J Nanosci Nanotechnol, 2010. **10**(12): p. 8527-37.

141.   Yasuda, J., et al., *Lactate dehydrogenase isoenzyme patterns in bovine liver tissue.* Nihon Juigaku Zasshi, 1989. **51**(4): p. 733-9.

142.   Chen, J.W., D.Z. Chen, and G.Z. Lu, *Asymptomatic process of hepatic artery thrombosis in a patient after orthotopic liver transplantation.* Hepatobiliary Pancreat Dis Int, 2004. **3**(1): p. 149-51.

143.   Memis, D., et al., *Curcumin attenuates the organ dysfunction caused by endotoxemia in the rat.* Nutrition, 2008. **24**(11-12): p. 1133-8.

144.   Chaung, S.S., et al., *The hepatoprotective effects of Limonium sinense against carbon tetrachloride and beta-D-galactosamine intoxication in rats.* Phytother Res, 2003. **17**(7): p. 784-91.

145.   Liu, Y., et al., *Potential health impact on mice after nasal instillation of nano-sized copper particles and their translocation in mice.* J Nanosci Nanotechnol, 2009. **9**(11): p. 6335-43.

146.   Bogers, M., et al., *Effects of the exposure profile on the inhalation toxicity of carbon tetrachloride in male rats.* J Appl Toxicol, 1987. **7**(3): p. 185-91.

147.   Arslan, M., et al., *The age- and gender-dependent effects of desflurane and sevoflurane on rat liver.* Exp Toxicol Pathol, 2010. **62**(1): p. 35-43.

148.   Turkez, H., M.I. Yousef, and F. Geyikoglu, *Propolis prevents aluminium-induced genetic and hepatic damages in rat liver.* Food Chem Toxicol, 2010. **48**(10): p. 2741-6.

149.   Kamalakkannan, N., et al., *Comparative effects of curcumin and an analogue of curcumin in carbon tetrachloride-induced hepatotoxicity in rats.* Basic Clin Pharmacol Toxicol, 2005. **97**(1): p. 15-21.

150.   Baykara, B., et al., *The protective effects of carnosine and melatonin in ischemia-reperfusion injury in the rat liver.* Acta Histochem, 2009. **111**(1): p. 42-51.

151.   Sutcu, R., et al., *The effects of subchronic methidathion toxicity on rat liver: role of antioxidant vitamins C and E.* Cell Biol Toxicol, 2006. **22**(3): p. 221-7.

152.	Higashisaka, K., et al., *Acute phase proteins as biomarkers for predicting the exposure and toxicity of nanomaterials.* Biomaterials, 2011. **32**(1): p. 3-9.

153.	Gabay, C. and I. Kushner, *Acute-phase proteins and other systemic responses to inflammation.* N Engl J Med, 1999. **340**(6): p. 448-54.

154.	Schiodt, F.V., et al., *Thrombopoietin in acute liver failure.* Hepatology, 2003. **37**(3): p. 558-61.

155.	Abdelhalim, M.A. and B.M. Jarrar, *Histological alterations in the liver of rats induced by different gold nanoparticle sizes, doses and exposure duration.* J Nanobiotechnology, 2012. **10**: p. 5.

156.	Ahmad, J., et al., *Apoptosis induction by silica nanoparticles mediated through reactive oxygen species in human liver cell line HepG2.* Toxicol Appl Pharmacol, 2012. **259**(2): p. 160-8.

157.	Neuzil, J., et al., *Molecular mechanism of 'mitocan'-induced apoptosis in cancer cells epitomizes the multiple roles of reactive oxygen species and Bcl-2 family proteins.* FEBS Lett, 2006. **580**(22): p. 5125-9.

158.	Zhang, L., et al., *The dose-dependent toxicological effects and potential perturbation on the neurotransmitter secretion in brain following intranasal instillation of copper nanoparticles.* Nanotoxicology, 2011.

159.	Valentovic, M.A., et al., *Characterization of 2-amino-4,5-dichlorophenol (2A45CP) in vitro toxicity in renal cortical slices from male Fischer 344 rats.* Toxicology, 2002. **172**(2): p. 113-23.

160.	Sun, B. and M. Karin, *NF-kappaB signaling, liver disease and hepatoprotective agents.* Oncogene, 2008. **27**(48): p. 6228-44.

161.	Llacuna, L., et al., *Reactive oxygen species mediate liver injury through parenchymal nuclear factor-kappaB inactivation in prolonged ischemia/reperfusion.* Am J Pathol, 2009. **174**(5): p. 1776-85.

162.	Aroor, A.R. and S.D. Shukla, *MAP kinase signaling in diverse effects of ethanol.* Life Sci, 2004. **74**(19): p. 2339-64.

163.	Valentovic, M., et al., *S-Adenosylmethionine (SAMe) attenuates acetaminophen hepatotoxicity in C57BL/6 mice.* Toxicol Lett, 2004. **154**(3): p. 165-74.

164.	Toblli, J.E., et al., *Assessment of the extent of oxidative stress induced by intravenous ferumoxytol, ferric carboxymaltose, iron sucrose and iron dextran in a nonclinical model.* Arzneimittelforschung, 2011. **61**(7): p. 399-410.

165.	Shukla, R.K., et al., *Titanium dioxide nanoparticles induce oxidative stress-mediated apoptosis in human keratinocyte cells.* J Biomed Nanotechnol, 2011. **7**(1): p. 100-1.

166.	Iida, A., et al., *Hepatocyte nuclear factor-kappa beta (NF-kappaB) activation is protective but is decreased in the cholestatic liver with endotoxemia.* Surgery, 2010. **148**(3): p. 477-89.

167.	Kuboki, S., et al., *Hepatocyte NF-kappaB activation is hepatoprotective during ischemia-reperfusion injury and is augmented by ischemic hypothermia.* Am J Physiol Gastrointest Liver Physiol, 2007. **292**(1): p. G201-7.

168.	Zhao, G., et al., *[Protective effect of remifentanil preconditioning against hepatic ischemia-reperfusion injury in rats: role of p38 mitogen-activated protein kinases].* Nan Fang Yi Ke Da Xue Xue Bao, 2011. **31**(12): p. 2016-20.

169.	Harrington, P.M., et al., *Eotaxin and eotaxin receptor (CCR3) expression in Sephadex particle-induced rat lung inflammation.* Int J Exp Pathol, 1999. **80**(3): p. 177-85.

170.	Ishihara, Y., et al., *Acute biological effects of intratracheally instilled titanium dioxide whiskers compared with nonfibrous titanium dioxide and amosite in rats.* Inhal Toxicol, 1999. **11**(2): p. 131-49.

171.	Underwood, S.L., et al., *Functional characterization and biomarker identification in the Brown Norway model of allergic airway inflammation.* Br J Pharmacol, 2002. **137**(2): p. 263-75.

172.	Inoue, K., et al., *Effects of nano particles on antigen-related airway inflammation in mice.* Respir Res, 2005. **6**: p. 106.

173. Lima, C., et al., *Eosinophilic inflammation and airway hyper-responsiveness are profoundly inhibited by a helminth (Ascaris suum) extract in a murine model of asthma.* Clin Exp Allergy, 2002. **32**(11): p. 1659-66.
174. Park, E.J., et al., *Oxidative stress and apoptosis induced by titanium dioxide nanoparticles in cultured BEAS-2B cells.* Toxicol Lett, 2008. **180**(3): p. 222-9.

Siva Krishna Nalabotu DVM, MS
6129, Country Club Drive, Huntington, WV-25705
Phone – 304.638.3696
E-mail: sivaknalabotu@gmail.com

Career Objective

To obtain an assistant professor position in toxicology while utilizing my veterinary clinical skills and research experience for growth and development of the institution with excellent career growth perspective

Summary of Qualifications

➤ Over four years of post-graduate research experience in the design, implementation, conduct and management of research projects on efficacy of drugs to treat age and metabolic related medical conditions and to evaluate the toxicity effects of nanomaterials

➤ Licensed veterinarian to practice veterinary medicine in the USA with thorough knowledge in pharmacology, physiology, toxicology, and pathology of the laboratory and pet animals

➤ Highly motivated, hardworking, intelligent, enthusiastic and very successful graduate student with 15 publications; 6 published, 3 under review in peer-reviewed journals and another 6 publications in preparation.

➤ Ability to comprehend and understand complex research works with work experience in varied fields including toxicology, nanotechnology, histopathology, Immunoblotting, immunohistochemistry, biomarkers and microfluidics.

Professional Experience

<u>Graduate Research Assistant</u> - **2008-Present**

Center for Diagnostic Nano systems, Marshall University, Huntington, WV

➤ Devised and implemented research projects on efficacy of drugs to treat age and metabolic related conditions and toxicological evaluation of nanomaterials
➤ Developed standard operating animal protocols to get approval with IACUC
➤ Designed and implemented academic research project to investigate the toxicity potential and the mechanisms of the toxicity of CeO_2 nanoparticles
➤ Led project team of four graduate students for a toxicity evaluation study on the laboratory rats that includes dosing with nanomaterials, physiological and biochemical monitoring of animals after dosing with the nanomaterial, euthanizing and collecting the tissues from the animals
➤ Investigated the toxicological effects of nanomaterials on lungs, liver, kidney, heart and brain
➤ Identification of serum biomarkers and microRNAs to predict hepatic toxicity of nanoparticles

- Critical analysis and interpretation of the scientific data; developed and published the manuscripts in peer reviewed journals
- Gave training for graduate and undergraduate students on various laboratory techniques such as western blotting and immunohistochemistry
- Made successful collaborations with senior scientists at National Institute of Occupational Health Sciences and Hazards and Veterans Affairs Medical Center to work on research studies

<u>Intern Veterinary Doctor</u> **Feb 2007-Oct 2007**

Veterinary Poly Clinic, Ongole, AP, India

- Responsible to manage the veterinary hospital facility along with other senior doctors to treat the patients
- Addressed the client questions and instructed clients on how to take care of the patient
- Scheduled and performed surgeries
- Managed, led and motivated the paramedical staff of the facility to get the best performance
- Public outreach to make farmers and clients aware of the zoonotic diseases and vaccinated the animal population to reduce mortality and morbidity

Dissertation Project
Objectives:

i. To evaluate the systemic toxicological effects of Cerium Oxide nanoparticles following intratracheal instillation in male Sprague-Dawley rats
ii. To investigate the role of oxidative stress and apoptosis in the toxicity induced by Cerium Oxide nanoparticles following intratracheal instillation in male Sprague-Dawley rats.

Results:

i. Intratracheal instillation of Cerium Oxide nanoparticles induces hepatic toxicity but do not appear to cause any toxic effects on kidney, spleen and heart. (**Published in Int. J Nanomedicine**)
ii. Hepatic toxicity induced by Cerium Oxide nanoparticles is associated with bioaccumulation of cerium in the liver and this accumulation results oxidative stress that in turn causes apoptosis of hepatocytes in male Sprague-Dawley rats. (Manuscript in preparation)

Education

July 2009-Present   Ph.D., Biomedical Sciences (Toxicology) Joan C Edwards School of Medicine, Marshall University, Huntington, WV

Jan 2008-Jun 2009   MS, Biological Sciences (Bionanotechnology) College of Science, Marshall University, Huntington, WV-25755

Aug 2002-Oct 2007   B.V.Sc & A.H **(DVM)** College of Veterinary Science, Sri Venkateswara Veterinary University, Tirupati, Andhra Pradesh, INDIA

Board Certification Educational Commission for Foreign Veterinary Graduates (ECFVG) Certification

Licensure   Pennsylvania State Board of Veterinary Medicine License #: **BV012989**
Kentucky Board of Veterinary Examiners License #: **NS-KY-4653**

Skills and Techniques

- Lab animal husbandry and maintenance
- Lab animal medicine and surgery
- Small animal (dog and cat) internal medicine and surgery
- Biochemical and physiological monitoring of lab animals
- Cell cultures
- Histopathology
- Immunohistochemistry
- Immunoblotting
- Fluorescent microscopy
- Working with nanomaterials and intratracheal instillation of nanomaterials
- Microarray
- Identification of MicroRNAs and serum biomarkers to predict hepatic toxicity
- Fabrication of microfluidic devices
- Photolithography

Familiarity of Techniques

- HPLC
- FTIR Spectrometry
- Electron microscopy
- Interpretation and data analysis of ICP-MS
- Echocardiography and electrocardiography of rodents
- RT-PCR

Computer Skills

- Excellent hands-on experience with MS Office. (MS Word, Excel, PowerPoint, Outlook and Access)
- Excellent experience with statistical software – Sigma Stat
- Excellent experience with imaging software – Alpha Ease, Image J
- Excellent experience with Adobe software (Acrobat, Photoshop), and Endnote

Awards & Honors

1. Mar 2011: Marshall University Biomedical Sciences travel grant for poster presentation at Society of Toxicology Annual Meeting held at Washington D.C.

2. <u>Jan 2008-June2009</u>: Marshall University, NSFEPSCoR #9871948 graduate assistantship with stipend.

3. <u>Oct 2007</u>: Best volunteer for National Social Service program during veterinary internship program.

Professional Memberships

1. Society of Toxicology

2. American Association for Advancement of Sciences

3. Veterinary Council of India (Eligible to practice Veterinary medicine in India)

4. A.P Veterinary Council (Eligible to practice Veterinary medicine in Andhra Pradesh, India)

5. West Virginia e-mentoring service

Publications in Peer-Reviewed Journals

1. **Siva K Nalabotu**, Hideyo Takatsuki, Madhukar Kolli, Leslie Frost, Benjamin Crowder, Shinji Yoshiyama , Murali K Gadde, Sunil K Kakarla, Kazuhiro Kohama, Arun Kumar and Eric R. Blough. *Control of myosin motor activity by the reversible alteration of protein structure for applications in the development of a bio nano device*. <u>(Accepted for publication in Advanced Science Letters. Jan-2012)</u>

2. **Siva K Nalabotu**, Madhukar B. Kolli, William E. Triest, Jane Y. Ma, Nandini D.P.K. Manne, Anjaiah Katta, Hari S. Addagarla, Kevin M. Rice, and Eric R. Blough. *Intratracheal instillation of cerium oxide nanoparticles induces hepatic toxicity in male Sprague dawley rats*. <u>Int J Nanomedicine. 2011; 6:2327-35.</u>

3. Hideyo Takatsuki, Hideyuki Tanaka, Kevin M Rice, Madhukar B Kolli, **Siva K Nalabotu**, Kazuhiro Kohama, Parviz Famouri and Eric R Blough. *Transport of single cells using an actin bundle-myosin bionanomotor transport system*. <u>Nanotechnology 22 (2011) 245101.</u>

4. Madhukar B. Kolli, B. Scott Day, Hideyo Takatsuki, **Siva K Nalabotu**, Kevin M. Rice, Kazuhiro Kohama, Murali K. Gadde, Sunil K. Kakarla, Anjaiah Katta, and Eric R. Blough. *Application of Poly (amidoamine) Dendrimers for Use in Bionanomotor Systems*. <u>Langmuir 2010, 26(9)</u>

5. Satyanarayana Paturi, Anil K. Gutta, Anjaiah Katta, Sunil K. Kakarla, Ravi K. Arvapalli, Murali K. Gadde, **Siva K Nalabotu**, Kevin M. Rice, Miaozong Wu, Eric Blough. *Effects of aging and gender on muscle mass and regulation of Akt-mTOR-p70s6k related signaling in the F344BN rat model*. <u>Mechanisms of Ageing and Development 131 (2010) 202–209</u>

6. Sunil K. Kakarla, Jacqueline C. Fannin, Saba Keshavarzian, Anjaiah Katta, Satyanarayana Paturi, **Siva K Nalabotu**, Miaozong Wu, Kevin M. Rice, Kamran Manzoor, Ernest M. Walker Jr., Eric R. Blough. *Chronic acetaminophen attenuates age-associated increases in cardiac ROS and apoptosis in the Fischer Brown Norway rat*. <u>Basic Res Cardiol (2010) 105:535–544</u>

Manuscripts in Review in Peer-Reviewed Journals

1. Anjaiah Katta, Sunil Kakarla, Nandini Manne, **Siva K Nalabotu**, Miaozong Wu, Sudarsanam Kundla, Madhukar Kolli, and Eric Blough. *Attenuation of load-induced muscle hypertrophy in the obese Zucker rat is associated with alterations in AMPK and dsRNA-dependent protein kinase activation.* (Journal of Applied Physiology)

2. Anjaiah Katta, Srinivas Thulluri, Murali Gadde, Nandini D.P.K. Manne, **Siva K Nalabotu**, Kevin M. Rice, and Eric R. Blough. *Overload induced heat shock proteins (HSPs), MAPK and miRNA (miR-1 and miR133a) response in insulin-resistant skeletal muscle.* (The American Journal of Physiology- Cell Physiology

3. Sunil K. Kakarla, Sudarsanam Kundla, Madhukar Kolli, Anjaiah Katta, **Siva K Nalabotu**, Emily Whitt, Kevin M. Rice and Eric R. Blough. *Mechanisms of age-related cardiac hypertrophy in the F344XBN rat model* (Mechanisms of Ageing and Development)

Manuscripts in Preparation

1. **Siva K. Nalabotu**, Nandini D.P.K. Manne, Madhukar B. Kolli, Geeta Nandyala, Radha K. Para, Jane Y. Ma, and Eric R. Blough. *Role of Oxidative Stress and Apoptosis in the hepatic Toxicity induced by Cerium Oxide Nanoparticles Following Intratracheal Instillation in Male Sprague-Dawley Rats.*

2. **Siva K. Nalabotu**, Nandini D.P.K. Manne, Madhukar B. Kolli, Geeta Nandyala, Radha K. Para, Jane Y. Ma, and Eric R. Blough. *Exposure to cerium oxide nanoparticles is associated with activation of MAPK signaling and apoptosis in the rat lungs.*

3. **Siva K. Nalabotu**, Niraj Nepal, Srinivas Thulluri, Madhukar B. Kolli, Nandini D.P.K. Manne, Robert Harris and Eric R. Blough. *Cerium oxide nanoparticles induce genotoxic effects in the liver of male Sprague-Dawley rats following intratracheal instillation.*

4. Radha K. Para, **Siva K. Nalabotu**, Nandini D.P.K. Manne, Madhukar B. Kolli, Geeta Nandyala, Jane Y. Ma, and Eric R. Blough. *Investigating the role of oxidative stress, autophagy and apoptosis in the toxicity induced by CeO2 nanoparticles on the heart of male Sprague-Dawley rats following intratracheal instillation.*

5. Madhukar B. Kolli, Radha K. Para, **Siva K. Nalabotu**, Nandini D.P.K. Manne, and Eric R. Blough. *Cerium oxide nanoparticles treatment attenuates Monocrotaline induced pulmonary arterial hypertension and associated right ventricular hypertrophy in rats.*

6. Nandini D.P.K. Manne, **Siva K. Nalabotu**, Madhukar B. Kolli, and Eric R. Blough. *Cancer Cachexia in the heart of APC Min/+ mice model of colon cancer is associated with activation of Akt and inhibition of mTOR dependent signaling.*

Abstracts & Presentations

1. **Siva K. Nalabotu**, Nandini Manne, Madhukar Kolli, Geeta Nandyala, Radha K Para, Valentovic Monica, Jane Ma and Eric R. Blough. Evaluation of oxidative stress and apoptosis in the liver following a single intratracheal instillation of cerium oxide nanoparticles in male Sprague dawley rats. (Society of Toxicology Annual Meeting, San Francisco 2012)

2. Guest speaker at University of Charleston School of Pharmacy as a part of Brown bag lunch seminar series on **"Nanomaterials and Nanotoxicity: Should we be scared?"**(Oct 2011)

3. **Siva K. Nalabotu**[†], Ashu Dhanjal[†], Lucy Dornon, Nandini Manne, Madhukar B. Kolli, Paulette Wehner, and Eric R. Blough. *Intratracheal instillation of the cerium oxide nanoparticles may induce cardiac alterations in the male Sprague-Dawley rats.* (West Virginia-ACC Annual Meeting 2011**)**

4. **Siva K. Nalabotu**, Jane Ma, William E. Triest, Madhukar Kolli, Paulette Wehner, and Eric R. Blough. *Intratracheal instillation of nano ceria induces systemic toxicity in rats.* (Society of Toxicology Annual Meeting, Washington D. C. 2011).

5. **Siva K. Nalabotu**, Jane Ma, William E. Triest, Madhukar Kolli, Paulette Wehner, Nandini Manne and Eric R. Blough. *Systemic toxicological effects of nanoceria following intratracheal instillation.* (Marshall University Research day 2011).

6. Hideyo Takatsuki, Kevin Rice, Madhukar B. Kolli, **Siva K. Nalabotu**, Kazuhiro Kohama, Famouri, Micheal Norton and Eric R. Blough. *Autonomous nanocargo transport system using actin bundle-myosin bionanomotor.* (ACS CERM Meeting 2011)

7. Madhukar B Kolli, Arun Kumar, Feras Elbash, Radha Para, **Siva K. Nalabotu**, Nandini D Manne, Geeta Nandyala, Paulette Wehner, Eric R. Blough. *Efficacy Of Curcumin Nanoparticles On Monocrotaline Induced Pulmonary Arterial Hypertension And Right Ventricular Hypertrophy.* (American Heart Association HPBL, 2011).

8. Katta, A, Kundla S, Kakarla S, Wu M, Paturi S, Gadde M.K., Arvapalli R, Kolli M, **Siva K. Nalabotu**. Rice, Kevin M., Blough, R., *Impaired Overload-induced Hypertrophy Is Associated With Diminished mTOR Signaling In Insulin Resistant Obese Zucker Rat* (American College of Sports & Medicine, Baltimore 2010).

9. Murali K. Gadde, Hideyo Takatsuki, Madhukar Kolli, Kevin M. Rice, **Siva K Nalabotu**, Kazuhiro Kohama, Eric Blough. *Disassembly of fascin bundled actin filaments induced by myosin II motors in an in-vitro motility assay and its applications to nanotechnology.* (Sigma Xi Research day, April 2008)

Media Reports about Publication (Selected from more than 30 reports))

1. Nanoparticles Used as Additives in Diesel Fuels Can Travel from Lungs to Liver ScienceDaily (Nov. 17, 2011)

2. In vivo study reveals toxic effects of cerium oxide nanoparticles in liver Safenano; Europe Center of excellence on nanotechnology hazard and risk (21/11/2011)

3. Marshall Study: Efficiency Additive Linked to Liver Damage West Virginia State Journal (Nov 17, 2011)

References

1. **Dr. Eric R Blough**
   (Thesis Advisor for MS and PhD)
   Room # 241 R BBSC Building
   Marshall University
   Huntington, WV 25755
   Phone: (304) 696 2708
   blough@marshall.edu

2. **Dr. Monica A Valentovic**
   Room # 406 BBSC Building
   Marshall University
   Huntington, WV 25755
   Phone: (304) 696-7332
   valentovic@marshall.edu

3. **Dr. Gary O Rankin**
   Room # 435-F BBSC Building
   Marshall University
   Huntington, WV 25755
   Phone: (304) 696-7319
   rankin@marshall.edu